POWER SYSTEMS DEVELOPMENT FACILITY

TOPICAL REPORT

GASIFICATION TEST CAMPAIGN TC19

NOVEMBER 5 – DECEMBER 1, 2005

DOE Cooperative Agreement
DE-FC21-90MC25140

Prepared by:
Southern Company Services, Inc.
Power Systems Development Facility
P.O. Box 1069
Wilsonville, AL 35186
Tel: 205-670-5840
Fax: 205-670-5843
http://psdf.southernco.com

May 2008

DISCLAIMER

This report was prepared as an account of work sponsored by an agency of the United States Government. Neither the United States Government nor any agency thereof, nor any of their employees, nor Southern Company Services, Inc., nor any of its employees, nor any of its subcontractors, nor any of its sponsors or cofunders, makes any warranty, expressed or implied, or assumes any legal liability or responsibility for the accuracy, completeness, or usefulness of any information, apparatus, product, or process disclosed, or represents that its use would not infringe privately owned rights. Reference herein to any specific commercial product, process, or service by trade name, trademark, manufacturer or otherwise, does not necessarily constitute or imply its endorsement, recommendation, or favoring by the United States Government or any agency thereof. The views and opinions of authors expressed herein do not necessarily state or reflect those of the United States Government or any agency thereof.

This report is available to the public from the National Technical Information Service, U.S. Department of Commerce, 5285 Port Royal Road, Springfield, VA 22161. Phone orders are accepted at (703) 487-4650.

ABSTRACT

In support of technology development to utilize coal for efficient, affordable, and environmentally clean power generation, the Power Systems Development Facility (PSDF), located in Wilsonville, Alabama, routinely demonstrates gasification technologies using various types of coals. The PSDF is an engineering scale demonstration of key features of advanced coal-fired power systems, including a KBR Transport Gasifier, a hot gas particulate control device (PCD), advanced syngas cleanup systems, and high-pressure solids handling systems.

This report summarizes the results of test campaign TC19 of the PSDF gasification process. TC19 occurred from November 5 to December 1, 2005, with the gasifier train accumulating 518 hours of operation using Powder River Basin (PRB) subbituminous coal. The test campaign included the commissioning and operation of a newly installed gasification ash removal process, the continuous coarse ash depressurization (CCAD) system. A new on-line particulate monitor, the Process Particle Counter (PPC), was also commissioned and operated. PCD testing featured a new type of on-line failsafe tester, which operated reliably to simulate filter element failure and characterize failsafe performance. The test campaign also provided the opportunity for additional testing in various areas of gasification technology.

ACKNOWLEDGEMENT

The authors wish to acknowledge the contributions and support provided by various project managers, including Morgan Mosser, Elaine Everitt, and Ron Breault of the Department of Energy, and Neville Holt of the Electric Power Research Institute. The project is sponsored by the U.S. Department of Energy National Energy Technology Laboratory under contract DE-FC21-90MC25140.

TABLE OF CONTENTS

Section.....Page

Inside Cover
Disclaimer
Abstract
Acknowledgement

List of Tables iii
List of Figures iv

1.0 EXECUTIVE SUMMARY 1-1
1.1 Background 1-1
1.1.1 PSDF Gasification Technology Overview 1-1
1.1.2 Process Description 1-1
1.2 Test Campaign Summary 1-4
1.2.1 Major Objectives 1-4
1.2.2 Secondary Objectives 1-5
1.3 Report Structure 1-6

2.0 COAL FEED 2-1
2.1 Coal Feed Operation 2-1
2.2 Coal Analyses 2-1

3.0 TRANSPORT GASIFIER 3-1
3.1 Gasifier Performance 3-1
3.1.1 Gas Analyses 3-1
3.1.2 Solids Analyses 3-3
3.1.3 Carbon Conversion 3-5
3.1.4 Gasification Efficiencies 3-5
3.1.5 Automation 3-6
3.1.6 CCAD Commissioning 3-6
3.1.7 Gas Analysis Modifications 3-7
3.2 Gasifier Inspections 3-7

4.0 PARTICULATE CONTROL DEVICE 4-1
4.1 Overview 4-1
4.2 Particle Collection Performance 4-2
4.2.1 PCD Inlet Mass Loadings 4-2
4.2.2 PCD Outlet Mass Loadings 4-2
4.2.3 Failsafe Performance Tests 4-3
4.2.4 Filter Element Sealing Issues 4-4
4.3 Real-Time Particulate Monitoring 4-4

4.3.1 PCME Particulate Monitor 4-4
4.3.2 PPC Particulate Monitor 4-5
4.4 PCD Solids Analyses 4-6
4.4.1 Particle Size Distributions 4-6
4.4.2 Dustcake Observations and Thickness Measurements 4-6
4.4.3 Dust Physical Properties and Chemical Compositions 4-7
4.5 PCD Pressure Drop Performance 4-8
4.6 Prediction of PCD Drag and Pressure Drop 4-9
4.7 Analysis of PCD Filter Element Condition 4-10

5.0 ADVANCED SYNGAS CLEANUP 5-1
5.1 Desulfurization and COS Hydrolysis 5-1
5.2 Ammonia Cracking and Hydrocarbon Reforming 5-1

6.0 CONCLUSIONS 6-1

APPENDICES
Appendix A Operating History A-1
Appendix B Operating Trends B-1
Appendix C Material and Energy Balances C-1

LIST OF TABLES

Table ..... Page

1-1 Steady State Operating Periods 1-7
1-2 Major Operating Parameters for the Steady State Operating Periods 1-8

2-1 PRB As-Fed Coal Characteristics 2-3

3-1 Gasifier Circulating Solids Analysis 3-9
3-2 Gasifier Loop Seal Solids Analysis 3-9
3-3 PCD Solids Analysis 3-9

4-1 In-Situ Particulate Measurements 4-12
4-2 Residual Dustcake Thickness Measurements 4-13
4-3 Physical Properties of In-Situ and Hopper Samples 4-14
4-4 Chemical Composition of In-Situ and Hopper Samples 4-15
4-5 Physical Properties of Residual Dustcake 4-16
4-6 Chemical Composition of Residual Dustcake 4-16
4-7 Transient Drag Determined from PCD Pressure Drop and from Lab Measurements 4-17
4-8 Comparison of Average Drag Values Determined from PCD Pressure Drop and from Lab Measurements 4-18

5-1 Nominal Properties of Sulfur Sorbents and COS Hydrolysis Catalyst and Operating Parameters 5-2
5-1 Nominal Properties of Ammonia Cracking and Hydrocarbon Reforming Catalyst and Operating Parameters 5-2

A-1 Gasification Operating History A-2

LIST OF FIGURES

Figure ..... Page

1-1 PSDF Gasification Process Flow Diagram 1-9

2-1 Coal Particle Sizes 2-4
2-2 Coal Fines and Oversize Particles 2-4

3-1 Syngas Moisture Concentrations 3-10
3-2 Syngas Lower Heating Value and Carbon Dioxide, Hydrogen, Carbon Monoxide, and Methane Concentrations 3-10
3-3 Projected Syngas Lower Heating Value 3-11
3-4 Gasifier and PCD Solids Silicon Dioxide Contents 3-11
3-5 Gasifier and PCD Solids Calcium Contents 3-12
3-6 Gasifier and PCD Solids Particle Sizes 3-12
3-7 Gasifier and PCD Solids Bulk Densities 3-13
3-8 Carbon Conversion 3-13
3-9 Hot and Cold Gasification Efficiencies 3-14
3-10 Gas Analysis Reflux Probes 3-14
3-10 Gasifier Cyclone Inspection 3-15

4-1 PCD Inlet Particulate Concentration as a Function of Coal Feed Rate 4-19
4-2 PCD Outlet Particulate Concentrations for TC18 and TC19 4-20
4-3 Photomicrograph of Particles on PCD Outlet Filter Number 5 4-21
4-4 Valve-Activated Failsafe Tester 4-22
4-5 PCME Particulate Monitor Response to Dust Injection 4-23
4-6 PCME Response to Dust Injection for Several Test Campaigns 4-24
4-7 PPC Particulate Monitor Response to Dust Injection 4-25
4-8 Comparison of TC18 and TC19 Particle Size Distributions from In-Situ Samples 4-26
4-9 Comparison of Particle Size Distributions for In-Situ and Hopper Samples 4-27
4-10 Effect of Non-Carbonate Carbon on Specific Surface Area 4-28
4-11 PCD Transient Drag versus Carbon Content of In-Situ Samples 4-29
4-12 Normalized PCD Pressure Drop 4-30
4-13 Comparison of Normalized PCD Pressure Drop from TC14 to TC19 4-30
4-14 Lab-Measured Drag as a Function of Particle Size 4-31
4-15 Comparison of PCD Transient Drag with Lab Measurements 4-32
4-16 Pressure Drop versus Face Velocity of Top Plenum Filter Elements Before Cleaning 4-33
4-17 Pressure Drop versus Exposure Hours of Top Plenum Filter Elements Before and After Cleaning 4-34
4-18 Pressure Drop versus Exposure Hours of Bottom Plenum Filter Elements Before and After Cleaning 4-35

4-19 Photograph of Filter Elements from TC19 Arranged by Age 4-36
4-20 Photograph of Iron Aluminide Filter Media Showing Corrosion Progression with Age 4-37

B-1 Gasifier Mixing Zone, Riser, and Outlet Temperatures B-2
B-2 Standpipe and Loop Seal Temperatures B-2
B-3 Gasifier Pressures B-3
B-4 Gasifier Differential Pressures B-3
B-5 PCD Temperatures B-4
B-6 PCD Baseline Pressure Drop and Face Velocity B-4
B-7 System Temperature Profile B-5
B-8 System Gas Flows B-5
B-9 Main Air Compressor Operation B-6
B-10 Original Coal Feeder Operation B-6
B-11 Developmental Coal Feeder Operation B-7
B-12 Syngas Analyzers B-7
B-13 Atmospheric Syngas Combustor Operation B-8

C-1 Mass Balance C-2
C-2 Energy Balance C-2
C-3 Carbon Balance C-3

1.0 EXECUTIVE SUMMARY

Test campaign TC19 at the Power Systems Development Facility (PSDF) occurred from November 5 to December 1, 2005, with the gasifier train accumulating 518 hours of operation using Powder River Basin (PRB) subbituminous coal. New features of the process included a unique gasification ash removal process, the continuous coarse ash depressurization (CCAD) system; a real-time particulate monitor, the Process Particle Counter (PPC), designed to measure low particulate concentrations and particle sizes; and a valve-activated failsafe tester for on-line testing in the particulate control device (PCD). The test campaign demonstrated steady state operation at various operating conditions. Data obtained during TC19 will be used to further develop various gasification technologies and to optimize operations at the PSDF.

1.1 Background

1.1.1 PSDF Gasification Technology Overview

The PSDF, located near Wilsonville, Alabama, began operation in 1996 to support the U.S. Department of Energy's effort to develop cost-competitive and environmentally acceptable coal-based power generation technologies. This effort promotes fuel diversity—a key component in maintaining national security—while meeting the highest environmental standards. The PSDF is developing environmentally friendly technologies that will allow the continued use of coal, the United States' most abundant and least expensive fuel resource.

The PSDF is operated by Southern Company Services. Other project participants currently include the Department of Energy National Energy Technology Laboratory, Electric Power Research Institute, Siemens Power Generation, KBR (formerly Kellogg Brown & Root), the Lignite Energy Council, Burlington Northern Santa Fe Railway, and Peabody Energy. The facility is a highly flexible test center where researchers can evaluate innovative power system components on a semi-commercial scale at a low cost. Development of advanced power systems at the PSDF is focused specifically on identifying ways to reduce capital cost, enhance equipment reliability, and increase efficiency while meeting strict environmental standards. Current testing involves pressurized solids handling systems, coal gasifier optimization using a variety of fuels, sensor development, hot gas particulate removal, and advanced syngas cleanup.

1.1.2 Process Description

The PSDF gasification process, shown in Figure 1-1, features high pressure solids feed systems; a KBR Transport Gasifier; syngas coolers; a hot gas filter vessel, the PCD; continuous ash depressurization systems developed at the PSDF for ash removal; a slipstream syngas cleanup unit to test various pollutant control technologies; and a novel piloted syngas burner.

The coal used as the gasifier feedstock is processed on site, first crushed and then pulverized to a nominal particle diameter between 250 and 400 microns. Coal may be fed to the gasifier using two systems, the original coal feed system and a secondary coal feed system. The original coal feed system is a lockhopper, vertical pocket feeder design with a "rotofeed" dispenser. It consists of two pressure vessels, with the coal pressurized in the upper lock vessel and then gravity fed into a dispense vessel, which is always pressurized. The material is fed out of the dispense vessel by the rotofeed dispenser, which is driven by a variable speed electric motor and delivers the material into the discharge line where it is conveyed by air or nitrogen into the gasifier. The secondary coal feeder is a developmental test unit designed to evaluate different feeder mechanisms. Types of mechanisms that can be tested with this system include auger-style, fluid bed, and a higher pressure rotary feeder.

A sorbent feeder is available to feed material into the gasifier for in-situ sulfur capture or to address ash chemistry issues. For sulfur capture, either limestone or dolomite is fed after being crushed and pulverized to a nominal particle diameter of 10 to 100 microns. The sorbent feeder utilizes the same design as the original coal feeder, but for a lower feed rate.

The start-up burner is a direct propane-fired burner operated to heat the gasifier to about 1,200^{o}F. The burner is typically started at a system pressure of 60 psig, and can operate at pressures up to 135 psig.

The Transport Gasifier, a pressurized, advanced circulating fluidized bed reactor, consists of a mixing zone, riser, disengager, cyclone, standpipe, loop seal, and J-leg. Steam and either air or oxygen are mixed together and introduced in the lower mixing zone while the fuel, sorbent, and additional air or oxygen and steam (if needed) are added in the upper mixing zone. The upper mixing zone, located below the riser, has a slightly larger diameter than that of the riser. The gas and solids move up the riser before entering the disengager, which removes larger particles by gravity separation. The majority of the solids flow from the disengager into the standpipe, and the remaining solids flow, along with the syngas, to the cyclone, which removes most of the particles not collected by the disengager. The solids collected by the disengager and cyclone are recycled back to the gasifier mixing zone through the standpipe and a J-leg. The standpipe level can be reduced by removing solids through the new CCAD system or via a screw cooler and lock hopper system. The nominal gasifier operating temperature is 1,800^{o}F, and the gasifier system is designed to have a maximum operating pressure of 294 psig with a thermal capacity of about 41 MBtu/hr.

The syngas exits the Transport Gasifier, passes through the primary gas cooler where the gas temperature is reduced to about 750°F, and enters the PCD for final particulate removal. The metal or ceramic filter elements used in the PCD remove essentially all the dust from the gas stream. The PCD utilizes a tube sheet holding up to 91 filter elements, which are attached to one of two plenums. Process gas flows into the PCD through a tangential entrance, around a shroud, and through the filter elements into the plenums.

Failsafe devices are located downstream of the filter elements to stop solids leakage by plugging in the event of element failures. High pressure nitrogen back-pulsing, typically lasting 0.2 seconds, is used to clean the filters periodically to remove the accumulated solids and control the pressure drop across the tube sheet. The solids fall to the bottom of the PCD and are removed through the continuous fine ash depressurization (CFAD) system.

After exiting the PCD, a small portion of the syngas, up to 100 lb/hr, can be directed to an advanced syngas cleanup system downstream of the PCD. The syngas cleanup system is a specialized, flexible unit, capable of operating at a range of temperatures, pressures, and flow rates, and provides a means to test various pollutant control technologies, including removal of sulfur, nitrogen, chlorine, and mercury compounds. The syngas cleanup slipstream can also be used to test other power technologies such as fuel cells.

A portion of the syngas can also be directed to the piloted syngas burner (PSB), a gas turbine combustor designed to burn coal-derived syngas with a lower heating value below 100 Btu/SCF. After combusting in the burner, the gas passes through a turbine before exiting the turbine stack. An associated generator can supply power from the turbine to the electric transmission grid.

The main stream of syngas is then cooled in a secondary gas cooler, which reduces the temperature to about 450°F. Some of this gas may be compressed and sent to the gasifier for aeration to aid in solids circulation. The recycle gas compressor is a vertically mounted centrifugal compressor which operates at high temperature, nominally 500 to 600°F, and was designed to have a throughput of about 2,000 to 3,000 lb/hr.

The remaining syngas is reduced to near atmospheric pressure through a pressure control valve. The gas is then sent to the atmospheric syngas combustor which burns the syngas components. The flue gas from the atmospheric syngas combustor flows to a heat recovery boiler, through a baghouse, and then is discharged out a stack. A flare is available to combust the syngas in the event of a system trip when the atmospheric syngas combustor is off-line.

A brief description of gasification test campaign history can be found in Appendix A.

1.2 Test Campaign Summary

The test campaign consisted of 22 periods of steady state operation. These periods are given in Table 1-1, and the major operating parameters for each period are shown in Table 1-2. The operating periods had a cumulative time of about 140 hours, which was about 27 percent of the total TC19 on-coal operation time. Air was the oxidant for the entire test campaign. Operating periods TC19-1, TC19-2, and TC19-7 used recycle gas for gasifier aeration, while all other periods used nitrogen. While nitrogen was used to convey the coal into the gasifier during the TC19-1 through TC19-15, air was the coal conveying gas during TC19-16 through TC19-22. Operating trends for the entire test campaign are shown in Appendix B.

1.2.1 Major Objectives

CCAD Commissioning. The CCAD system, a Southern Company proprietary design, operates to both cool and depressurize the coarse gasification ash removed from the gasifier. It was installed to replace a screw cooler and lock hopper system which operated unreliably and required a high level of maintenance. The fundamental principles on which the CCAD system was designed were essentially the same as those of the CFAD system, which had been successfully operated since its installation in early 2004. These ash removal systems depressurize solids in a continuous stream, filtering the entrained gas in a stationary bed of solids. To cool the gasifier solids, cooling coils were installed in the CCAD collection vessel.

Like CFAD, CCAD operated remarkably well since its commissioning. It reliably removed solids from the gasifier throughout the test campaign. The depressurization and cooling stages as well as the discharge rate control operated as designed. Normal discharge rates ranged from about 100 to 600 lb/hr, while the maximum rate tested was 1,600 lb/hr. The gasification ash was cooled from nominally 1,800 to 200°F.

PPC Particulate Monitor. The first attempt to collect real-time particulate measurements at the PCD outlet using the PPC made by Process Metrix was conducted. Although many problems were encountered, the instrument showed potential for reliably detecting low levels of particulate. The PPC showed marked response during a gasification ash injection test.

Failsafe Testing. During TC19, a new type of failsafe tester was introduced. Previous failsafe testers either simulated small leaks or were inconsistent in their operation. The new device consisted of a ball valve installed in the hopper of the PCD. When opened, the valve provided a 1.5 inch hole through which unfiltered syngas reached the failsafe being tested. The tester proved reliable and easy to control. Test results showed good performance of the failsafe tested, the iron aluminide fuse.

1.2.2 Secondary Objectives

Coal Feed Systems. Operation of the coal feed systems were evaluated to further optimize performance. For several operating periods, air was used in place of nitrogen to convey the coal to the gasifier. This testing showed a slight increase in the gas heating value during most of this testing due to decreased nitrogen dilution, although the affect was not apparent in all the operating periods due to changes in other process parameters. Short-term tests were planned incorporating a coal feed nozzle installed lower than the normally used injection point. However, flow restrictions prevented successful testing.

Transport Gasifier Optimization. Evaluating the gasifier performance continued with testing at high coal feed rates, circulation rates, and exit temperatures, and at various air flow distribution configurations. Automation efforts continued with the evaluation of enhancements to the automatic temperature controls, most of which showed improvement over previous control logic.

Sensor Development. Promecon probes were used to measure the solids velocity through the riser. The Promecon probes seemed to give accurate results during sand circulation at the TC19 start-up, but the probes stopped functioning after a short period of operation.

Gas Analysis Modifications. For the first time, continuous gas analysis samples for oxygen and carbon monoxide concentrations were taken upstream of the PCD to increase response time and to give measurements of oxygen levels prior to combustion (as in the case of filter cake combustion to clean the filter elements following system shutdown). The testing was successful, and gas analysis upstream of the PCD will be expanded in future test campaigns.

Advanced Syngas Cleanup. Testing of syngas desulfidation, ammonia cracking, and hydrocarbon reforming was conducted with catalysts supplied by Sud-Chemie. The testing showed high rates of conversion for the syngas contaminants.

1.3 Report Structure

The following report presents the operational data and results of gasification technology development at the PSDF during TC19, compiled in the sections listed below.

2.0 Coal Feed — Discusses operation of the coal feed systems and presents coal analyses.

3.0 Transport Gasifier — Includes the major gasifier operating parameters and the gasifier performance as indicated by gas and solids analyses. Also includes gasifier automation efforts, gas analysis modifications, and inspection data for the gasifier and related equipment, including gas coolers, the recycle gas system, and ash removal systems.

4.0 Particulate Control Device — Describes the hot gas filter particulate characteristics, performance, failsafe and filter element testing, and development of real-time particulate monitors.

5.0 Advanced Syngas Cleanup — Details various testing to support emissions control studies.

Conclusions of the test campaign and lessons learned are given in Section 6.0. A brief operating history is given in Appendix A, operating trends are shown in Appendix B, and Appendix C shows mass, energy, and carbon balances.

Table 1-1. Steady State Operating Periods.

Operating Period[1,2]	Start Time	End Time	Duration Hours	Operating Period Average Time	Operating Period Relative Hours
TC19-1	11/9/05 15:00	11/9/05 19:30	4.50	11/9/2005 17:15	22
TC19-2	11/10/05 3:30	11/10/05 7:45	4.25	11/10/2005 5:37	35
TC19-3	11/11/05 19:15	11/11/05 22:30	3.25	11/11/2005 20:52	74
TC19-4	11/12/05 2:45	11/12/05 8:45	6.00	11/12/2005 5:45	83
TC19-5	11/12/05 15:45	11/13/05 3:00	11.25	11/12/2005 21:22	98
TC19-6	11/13/05 15:15	11/13/05 20:45	5.50	11/13/2005 18:00	119
TC19-7	11/14/05 7:15	11/14/05 13:30	6.25	11/14/2005 10:22	135
TC19-8	11/15/05 4:15	11/15/05 13:30	9.25	11/15/2005 8:52	158
TC19-9	11/15/05 14:00	11/15/05 19:15	5.25	11/15/2005 16:37	166
TC19-10	11/15/05 23:30	11/16/05 7:30	8.00	11/16/2005 3:30	176
TC19-11	11/16/05 9:00	11/16/05 14:00	5.00	11/16/2005 11:30	185
TC19-12	11/17/05 21:30	11/18/05 1:30	4.00	11/17/2005 23:30	221
TC19-13	11/19/05 3:45	11/19/05 8:00	4.25	11/19/2005 5:52	251
TC19-14	11/22/05 8:15	11/22/05 12:15	4.00	11/22/2005 10:15	327
TC19-15	11/22/05 14:45	11/22/05 22:15	7.50	11/22/2005 18:30	336
TC19-16	11/24/05 3:00	11/24/05 19:45	16.75	11/24/2005 11:22	376
TC19-17	11/24/05 20:45	11/25/05 1:30	4.75	11/24/2005 23:07	388
TC19-18	11/27/05 2:15	11/27/05 7:30	5.25	11/27/2005 4:52	420
TC19-19	11/27/05 13:00	11/27/05 23:30	10.50	11/27/2005 18:15	433
TC19-20	11/28/05 1:15	11/28/05 5:45	4.50	11/28/2005 3:30	443
TC19-21	11/29/05 4:45	11/29/05 9:00	4.25	11/29/2005 6:52	470
TC19-22	11/30/05 2:00	11/30/05 7:30	5.50	11/30/2005 4:45	492

Notes:

1. Recycle gas was used as gasifier aeration except during TC19-1,TC19-2, and TC19-7.
2. Transport Air was used as coal conveying gas during TC19-16 to TC19-22.

Table 1-2. Major Operating Parameters for the Steady State Operating Periods.

Operating Period[1,2]	Average Relative Hours	Mixing Zone Temperature, °F	Pressure, psig	Coal Feed Rate[3], lb/hr	Air Feed Rate, lb/hr	Syngas Rate, lb/hr	Steam Feed Rate[4], lb/hr	Nitrogen Feed Rate, lb/hr	PCD Inlet Temperature, °F	PCD Solids Rate, lb/hr
TC19-1	22	1,690	210	2,100	10,300	19,400	1,400	4,850	790	220
TC19-2	35	1,690	216	2,400	10,900	20,000	1,500	5,200	780	230
TC19-3	74	1,670	230	3,900	12,700	23,600	1,500	6,300	780	260
TC19-4	83	1,700	230	3,900	13,400	23,800	1,500	4,600	800	270
TC19-5	98	1,710	230	3,500	13,200	23,900	1,600	4,700	800	280
TC19-6	119	1,710	230	3,800	13,200	23,300	1,500	4,800	790	310
TC19-7	135	1,700	230	3,200	12,800	23,200	1,600	6,100	790	330
TC19-8	158	1,690	230	4,300	13,900	24,300	1,500	4,800	790	370
TC19-9	166	1,680	230	4,200	13,400	23,900	1,600	4,900	780	360
TC19-10	176	1,690	238	3,600	14,200	27,100	3,000	4,900	810	340
TC19-11	185	1,690	238	3,600	13,800	26,500	2,300	4,800	810	320
TC19-12	221	1,700	232	3,400	12,800	23,600	1,500	5,200	780	250
TC19-13	251	1,690	232	3,600	13,300	24,400	1,600	5,200	780	270
TC19-14	327	1,680	198	2,000	9,400	17,500	1,400	4,600	730	350
TC19-15	336	1,680	198	2,000	9,300	17,500	1,400	5,000	730	350
TC19-16	376	1,690	226	3,600	12,600	21,500	1,700	3,500	760	350
TC19-17	388	1,690	226	4,300	12,900	22,100	1,600	3,500	760	350
TC19-18	420	1,720	216	3,700	13,500	23,300	1,600	4,300	800	210
TC19-19	433	1,700	214	3,600	12,800	22,200	1,600	4,600	770	210
TC19-20	443	1,700	214	3,500	12,600	21,800	1,500	4,600	770	210
TC19-21	470	1,700	214	3,600	12,400	21,600	1,500	4,000	760	290
TC19-22	492	1,700	232	1,700	8,500	15,500	1,200	4,100	730	310

Notes:

1. Recycle gas was used as gasifier aeration during TC19-1, TC19-2, and TC19-7.
2. Transport Air was used as coal conveying gas during TC19-16 through TC19-22.
3. Coal rates are calculated from weigh cell data.
4. All steam rates calculated from hydrogen balance.

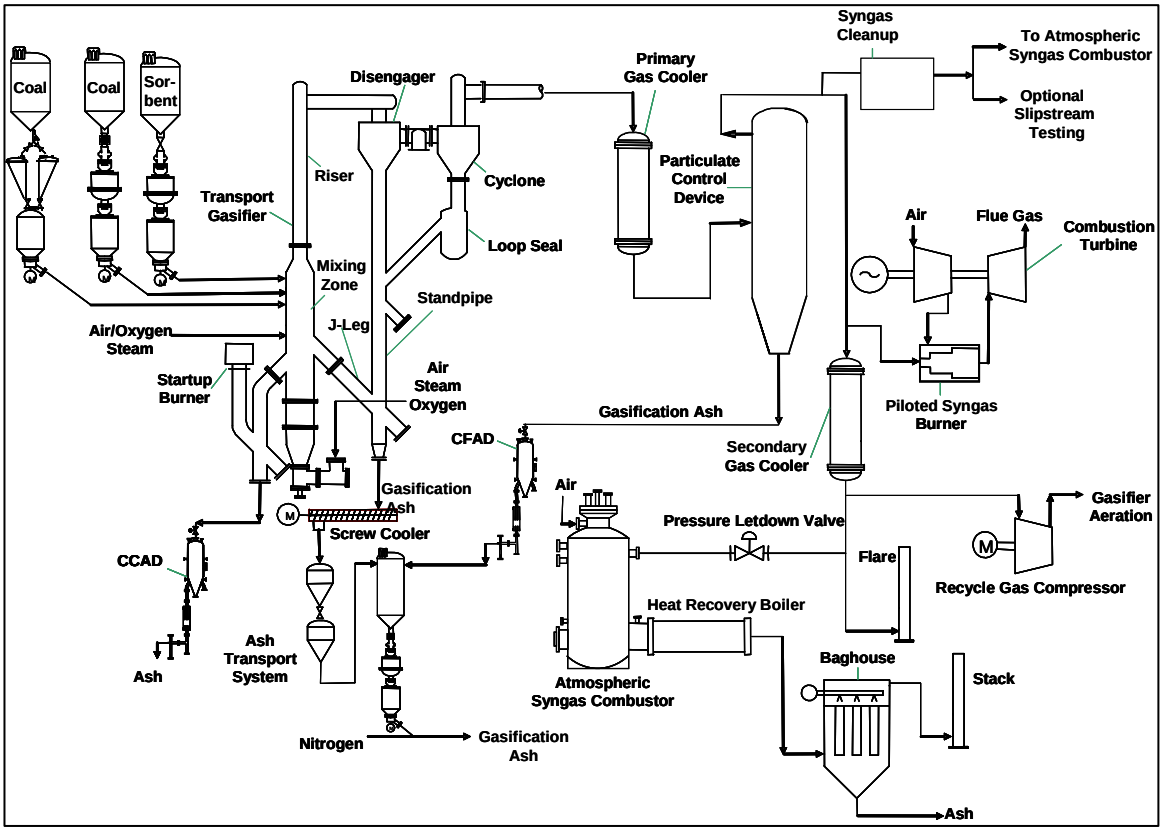

Figure 1-1. PSDF Gasification Process Flow Diagram.

2.0 COAL FEED

2.1 Coal Feed Operation

During TC19, both the original coal feeder and the secondary (or developmental) coal feeder were used. The original coal feeder operated well. The vent valves on the lock vessel were relocated prior to TC19 and operated with fewer problems than in previous test campaigns. The particle size distribution occasionally varied outside of the developed operating envelope, and at these times the coal feeder experienced problems with the dispense vessel vent lines plugging. Design modifications are planned to reduce the vent valves plugging.

The secondary coal feeder was operated for a total of 240 hours. At times, the particle size distribution varied outside of the developed operating envelope. As a result, the coal feeder experienced numerous plugs in the discharge line. Additional design limitations were identified that will be addressed before further testing to improve the feeder operation with fine coal particles.

Feeding coal with air as the conveying gas instead of nitrogen was tested during several periods of the TC19 (TC19-16 through TC19-22 steady state operating periods). The testing was completed using the original coal feeder, and began with a mixture of 50 percent air and 50 percent nitrogen. Later, the transition was made to a 100 percent air. The feed system and gasifier operated well with transport air. A higher heating value was observed for all these operating periods except for the last one, when other process variables obscured this trend.

Testing of coal feed through a nozzle located at a lower elevation than the normally used nozzle was attempted. Due to the numerous bends in the line to the lower coal feed nozzle, flow could not be maintained, so coal feed was resumed using the normally used nozzle, which is located just below the riser. This nozzle and the original coal feeder discharge line are approximately at the same elevation, and the major flow restrictions in this piping include only two 135-degree bends.

2.2 Coal Analyses

Table 2-1 shows the analysis of the PRB coal used during TC19 as sampled from the coal feeders. The analysis includes the coal heating values. The lower heating value (LHV) is not measured directly, but is calculated by subtracting the heat of vaporization of the coal moisture from the higher heating value (HHV). The coal HHV is determined using a bomb calorimeter. The calorimeter condenses all the coal combustion moisture as liquid water. The lower heating values for the PRB coal ranged from 8,900 to 9,600 Btu/lb during the test campaign.

The mass median diameter (MMD) and Sauter mean diameter (SMD) of the coal sampled from the coal feeders are shown in Figure 2-1. The average MMD for the coal sampled from the original feeder was 255 microns, and the average MMD for the coal sampled

from the developmental feeder was 198 microns. The coal sampled from the original feeder had an average SMD of 169 microns; the coal SMD of the coal sampled from the developmental feeder averaged 142 microns.

Figure 2-2 shows the weight percentage of fine coal, that below 45 microns, and the percentage of coal above 1,180 microns, considered oversize coal. The fines and oversize data became more scattered during the last half of the test campaign. After Hour 325, there was an increase in oversize particles for the original feeder. Prior to Hour 325, the original feeder had less than 5 percent oversize particles, while after Hour 325 the oversize particles contents were between 2 and 20 percent. The developmental coal feeder oversize particle contents were between 0 and 2 percent prior to Hour 325 and then increased to 5 percent by the end of TC19. The variability was likely caused by changes in mill operation (including the removal of a vibrating sieve screen on one of the mills) that were made to reduce the fines content, which had begun increasing.

Table 2-1. PRB As-Fed Coal Characteristics.

	Average Value	Standard Deviation
Moisture, wt %	15.7	1.2
Carbon, wt %	58.6	0.85
Hydrogen[1], wt %	3.8	0.05
Nitrogen, wt %	0.8	0.07
Oxygen, wt %	14.9	0.41
Sulfur, wt %	0.25	0.01
Ash, wt %	6.0	0.45
Volatiles, wt %	35.1	0.58
Fixed Carbon, wt %	42.9	0.80
Higher Heating Value, Btu/lb	9,800	135
Lower Heating Value, Btu/lb	9,300	116
CaO, wt %	1.3	0.10
SiO_2, wt %	2.3	0.32
Al_2O_3, wt %	1.0	0.13
MgO, wt %	0.2	0.02
Na_2O, wt %	<0.1	--
Ca/S, mole/mole	3.0	0.27

Notes:
1. Hydrogen in coal is reported separately from hydrogen in moisture.

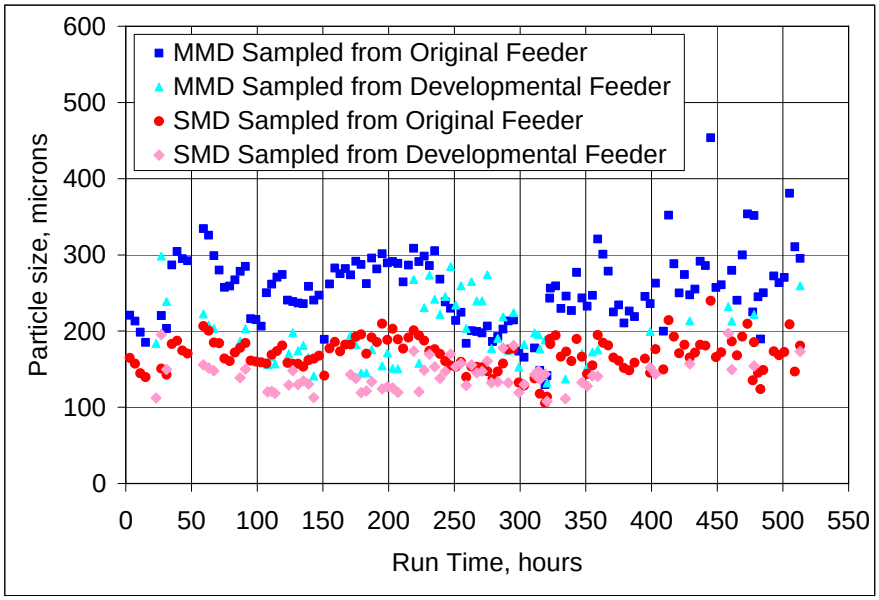

Figure 2-1. Coal Particle Sizes.

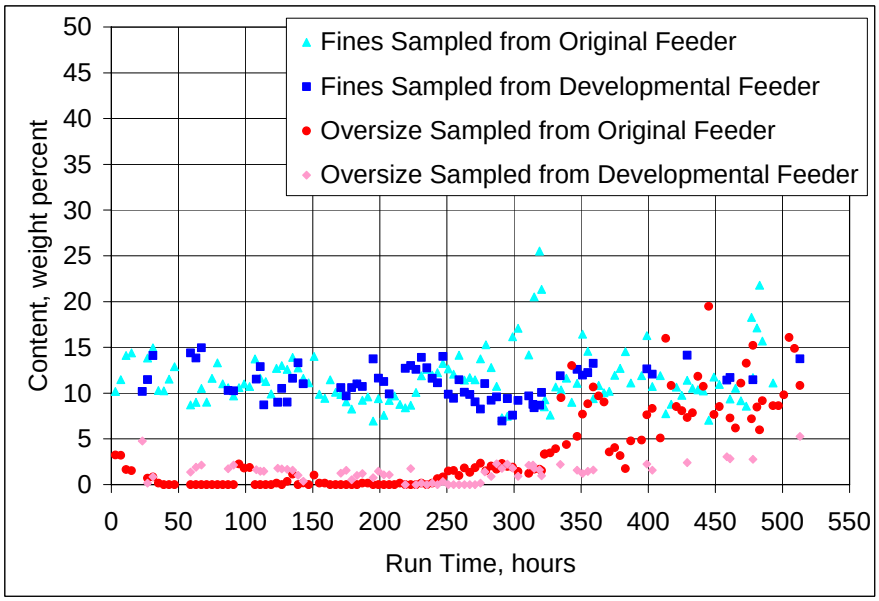

Figure 2-2. Coal Fines and Oversize Particles.

3.0 TRANSPORT GASIFIER

3.1 Gasifier Performance

3.1.1 Gas Analyses

During TC19, continuous syngas measurements were sampled at locations between the primary gas cooler and the PCD and between the secondary gas cooler and the atmospheric syngas combustor inlet. Periodic syngas measurements were sampled at the inlet of the advanced syngas cleanup system for analysis using a Fourier Transform Infrared (FTIR) instrument for determining ammonia (NH_3), water (H_2O), and hydrocarbon concentrations. In addition, syngas H_2O concentrations were measured by in-situ samples taken at the PCD outlet. Flue gas measurements were taken at the syngas combustor outlet.

Prior to TC19, all continuous syngas sampling was performed at the syngas combustor inlet, and this was the first test campaign during which syngas sampling was performed upstream of the PCD. Sampling was tested at this location to improve response time, since this was the first place in the process where the temperature was suitably low for sampling. It also provided a means of quickly measuring carbon monoxide (CO) and oxygen (O_2) levels prior to any combustion in the PCD (for example, when filter element are cleaned immediately following shutdown by adding vitiated air to combusted the filter dustcake). For this new application, reflux probes were successfully used to clean the syngas of particulate prior to analysis. More information on the modifications completed for this new application can be found in Section 3.1.7.

Only CO and O_2 were measured from the PCD inlet sampling during TC19, with additional gas analysis to be conducted at this location in future test campaigns after the success of this method experienced in TC19. For TC19, hydrogen (H_2), H_2O, nitrogen (N_2), carbon dioxide (CO_2), methane (CH_4), and redundant measurements of CO and O_2 were taken at the atmospheric syngas combustor inlet.

The syngas H_2O concentration is plotted in Figure 3-1. The values shown were taken from in-situ sampling, from water-gas shift calculations based on a correlation of temperature, from a continuous syngas moisture analyzer, and from an FTIR analyzer. The continuous moisture analyzer was not functioning properly after Hour 376, so data after that time was not included. The moisture content was generally between 10 and 15 percent, with the higher values obtained during periods of high steam flow rate.

The estimated wet syngas concentrations of the major syngas components (not including nitrogen) based on these moisture concentrations are shown in Figure 3-2. The affect on syngas composition of recycle gas use and the use of air for coal transport was not always apparent due to changes in other process variables such as the coal feed rate and the steam flow rate.

CO, H_2, and CH_4 compositions are important in that these compounds provide the heating value for the syngas. The H_2 concentration was between 5.6 and 7.7 percent during the periods without recycle gas and between 5.6 and 9.2 percent with recycle gas. The CO concentration ranged from 4.5 to 7.8 percent when recycle gas was not in use and was between 4.6 and 9.7 percent during the recycle gas periods. The CH_4 concentration was between 0.5 and 1.0 percent without recycle gas and between 0.6 and 1.9 percent with recycle gas.

The raw lower heating value is also shown in Figure 3-2.

The lower heating value was calculated using the formula:

$$LHV(Btu/SCF) = \frac{275 \times (H_2\%) + 322 \times (CO\%) + 913 \times (CH_4\%)}{100}$$

Without recycle gas, the LHV typically ranged from 35 to 55 Btu/SCF. The LHV ranged from 35 to 72 Btu/SCF during recycle gas use. The periods with recycle gas averaged 59 Btu/SCF, while the periods without recycle gas averaged 44 Btu/SCF. Some overlap between the two sets of data exists due to other variables influencing the LHV.

CO_2 and nitrogen represent a large portion of the syngas, though they do not contribute to the heating value. The CO_2 concentration ranged from 9.2 to 9.4 percent without recycle gas and from 9.8 to 12.5 percent with recycle gas. The nitrogen content ranged from 63.2 to 67.6 percent without recycle gas and from 56.7 to 64.8 percent with recycle gas.

Minor constituents in the syngas include reduced sulfur compounds such as hydrogen sulfide (H_2S), carbonyl sulfide (COS), and carbon disulfide (CS_2), and reduced nitrogen compounds such as NH_3 and hydrogen cyanide (HCN). Most of the sulfur in the syngas is in the form of H_2S. The H_2S concentration ranged from about 200 to 330 ppm. A large portion of the coal-bound nitrogen is converted to NH_3. Due to the limited availability of the FTIR ammonia analyzer, only a small number of ammonia measurements were available, and these indicated ammonia concentrations from about 720 to 2,460 ppm.

Projected Syngas Heating Values. A commercial Transport Gasifier will produce syngas of a higher quality than the PSDF gasifier because of these commercial features:

- The more extensive use of recycle gas rather than nitrogen for aeration and PCD backpulsing.
- A lower heat loss per pound of coal gasified because of a lower gasifier surface area-to-volume ratio.
- A smaller number of instruments and thus less instrument purge.
- A cold gas cleanup train that removes moisture from the syngas.

The commercially projected LHVs at the gas turbine inlet for each operating period, shown in Figure 3-3, ranged from 80 to 121 Btu/SCF. Details on the projected LHV calculation are discussed in previous reports (e.g. TC18 Topical Report).

3.1.2 Solids Analyses

During TC19, the gasifier solid samples were taken from the following locations:

- Gasifier standpipe (circulating solids)
- Gasifier loop seal
- CFAD system (PCD solids).

During gasification, some of the gasification ash produced in the gasifier is removed from the standpipe via the CCAD system, while the remainder is collected in the PCD and removed via the CFAD system. Chemical analyses of these solids are based on the following assumptions:

- All carbon dioxide measured is from calcium carbonate ($CaCO_3$), hence moles of CO_2 measured equals moles of $CaCO_3$.
- All sulfide sulfur measured is from calcium sulfide (CaS).
- All calcium not taken by CaS and $CaCO_3$ is from calcium oxide (CaO).
- All magnesium is in the form of magnesium oxide (MgO).
- Total carbon is measured, which is the sum of organic and inorganic carbonate carbon. The organic carbon is the total carbon minus the inorganic carbonate carbon.

Both elemental sulfur (ultimate analysis) and ash inerts sulfur contents were measured. Assumedly, no iron sulfide (FeO) forms in the gasifier, and all of the sulfur in the standpipe and PCD solids is present as CaS. Thermodynamically, some iron sulfide (FeS) formation is possible, but most of the captured sulfur should be in the form of CaS due to the higher concentration of calcium than of iron in the system.

Table 3-1 gives the analysis of solids sampled from the standpipe. The standpipe solids re-circulate through the mixing zone, riser, and standpipe. Table 3-2 lists the solids analysis for the loop seal samples. The solids from the loop seal are the solids that pass through the disengager with the syngas, but are separated from the syngas in the cyclone. Samples from both gasifier locations showed a start-up silicon dioxide (SiO_2) content near 90 percent, and both locations declined in SiO_2 content over time, with an average of about 56 percent after the gasifier bed material reached a steady state composition (about Hour 350). These values were typical, since sand is the start-up gasifier bed material. After Hour 350, the aluminum oxide (Al_2O_3) content averaged about 17 percent for the circulating solids and averaged about 15 percent for the loop seal solids. The solids CaS and organic carbon contents were negligible in all of the standpipe and loop seal samples.

The PCD solids analysis is given in Table 3-3. The silicon dioxide (SiO_2) in the PCD solids is derived from the coal ash SiO_2, start-up sand that is being lost from the gasifier, and additional sand that is added to the gasifier. The SiO_2 PCD solids concentration was between 21.6 and 40.3 percent. Since only a minimal amount of Al_2O_3 is in the start-up sand, the PCD solids Al_2O_3 content comes predominantly from the coal ash. The PCD solids Al_2O_3 concentration remained low, ranging from 8.9 to 14.2 percent. The carbon content ranged from 12.4 to 45.3 percent. Since no sorbent feed occurred during the test campaign, all of the PCD solids calcium came from the PRB coal ash. The PCD solids concentration of $CaCO_3$ fluctuated from 4.1 to 1.4 percent. The PCD solids CaS concentration was 0.9 percent or less for the entire test campaign, indicating very low solids sulfur capture.

Solids Sample Comparison. The following comparisons of the gasifier solids and the PCD solids show how the solids compositions change throughout the process.

The SiO_2 from the sand entering the process as start-up bed material remains in the gasifier for several days, since the sand particle size is greater than that of the loop seal and standpipe solids. Figure 3-4 shows that the gasifier solids from the two sample locations had similar SiO_2 contents and were considerably higher than the SiO_2 contents of the PCD solids. Some of the gasifier material was removed via CCAD, and some sand eventually passed through the cyclone before being collected by the PCD, causing the replacement of sand in the gasifier with gasification ash bed material.

Figure 3-5 compares the calcium concentration from the gasifier and PCD solids samples. The calcium content was highest for the PCD solids, and it remained in the same range for the entire test campaign. The calcium contents of the standpipe and loop seal solids tracked each other. Each began the test campaign in the 2 to 4 percent range, but increased to around 10 percent as operation progressed. Note that the figure refers to the total calcium, which is distributed between the compounds $CaCO_3$, CaS, and CaO.

Solids Particle Size. The particle sizes (SMD) for the circulating solids, loop seal solids, and PCD solids are given in Figure 3-6. The average particle size of the standpipe solids was 156 microns SMD and 134 microns MMD, values close to that of sand at 150 microns. The circulating solids particle sizes quickly reached steady values between 150 and 165 microns SMD, even though the circulating solids SiO_2 concentration did not level out until about Hour 350. After the first 30 hours, the particle sizes of the loop seal solids tracked those of the circulating solids well and were relatively consistent, compared with previous test campaigns. The loop seal solids size ranged from 70 to 171 microns SMD and from 98 to 166 microns MMD.

The PCD fines SMD started around 12 microns, and averaged 7.8 microns. The MMD was about 5 microns larger than the SMD for most of the samples and followed the same trends as the SMD particle size, although changes were more pronounced for the MMD particle sizes. The TC19 PCD fines particle size was consistent with the particle size of previous PRB test campaigns.

Gasifier and PCD Solids Bulk Densities. The gasifier circulating solids and loop seal solids and the PCD solids bulk densities are given in Figure 3-7. The average bulk density of the standpipe solids was 80 lb/ft^3, a value slightly lower than that of sand. The density of the loop seal solids averaged 82 lb/ft^3. The bulk densities of the gasifier solids tracked each other closely. The PCD solids density averaged about 17 lb/ft^3.

3.1.3 Carbon Conversion

Carbon conversion is defined as the percent of fuel carbon that is gasified to CO, CO_2, CH_4, and higher hydrocarbons versus the amount of carbon that exits the gasifier in the PCD and gasifier solids. While the carbon conversion can be calculated several different ways, the most accurate method divides the carbon content in the syngas by the total carbon exiting the gasifier (from both solid and gas streams). Figure 3-8 gives the carbon conversions for the operating periods. The carbon conversion ranged from 91.1 to 97.6 percent and averaged 95.4 percent.

3.1.4 Gasification Efficiencies

Gasification efficiency is defined as the percentage of the entering energy that is converted to potentially useful syngas energy. Two types of gasification efficiencies have been defined, the cold gasification efficiency and the hot gasification efficiency. The cold gasification efficiency is the percentage of total energy fed that is available to a gas turbine as syngas latent heat. The hot gasification efficiency is the percentage of total energy fed that is available to produce electricity. The total energy to produce electricity includes the syngas latent heat recovered in a gas turbine plus the sensible heat recovered in a steam turbine.

Both the hot and cold gasification efficiencies are shown in Figure 3-9. The cold gasification efficiency ranged from 44.0 to 62.5 percent. Since less ambient-temperature nitrogen had to be heated to the gasifier temperature during recycle gas use, the efficiencies were expected to be higher during these periods. However, this trend was not clear due to changes in other process parameters.

The hot gasification efficiency assumes that the sensible heat of the syngas can be recovered in a heat recovery steam generator, so the hot gasification efficiency is always higher than the cold gasification efficiency. The hot gasification efficiency is the latent and the sensible heat of the syngas exiting the gasifier divided by the total amount of energy entering the gasifier, including the latent heat of the coal and the sensible heats of the air and steam. The hot gasification efficiencies ranged from 84.8 to 93.4 percent, with the periods of lowest efficiency occurring during the periods of low coal feed rate. The efficiency boundary for the calculated values is the gasifier itself, not including any downstream equipment.

The two main sources of efficiency losses are the gasifier heat loss and the latent heat of the PCD solids. The gasifier heat loss of 1.5 million Btu/hr was about 5 percent of the feed energy, while the total energy of the PCD solids was from 2 to 9 percent of the feed

energy (the higher numbers occurring during the periods of high PCD carryover rate). A commercial Transport Gasifier will be more efficient than the PSDF gasifier due to the more extensive use of recycle gas and lower heat losses.

3.1.5 Automation

Several automation tests were performed during TC19. The original automatic temperature control scheme was simplified by removing the secondary control and only using one controlling parameter. This design worked as well as the previous scheme in TC18 and was less complicated. However, the temperature control was less stable due to more air flow being directed to the lower mixing zone, forcing one of the control valves to operate in the lower control range of its stroke. Another automatic temperature control scheme was also implemented. This scheme used the coal feed rate as a feed-forward signal instead of a temperature indication. While the new control scheme showed promise at steady coal feed rates, it often caused the temperature deviation to increase when the coal flow was erratic. The planned load simulation controller testing did not occur in TC19, since the piloted syngas burner did not operate on syngas during the test campaign.

3.1.6 CCAD Commissioning

The CCAD system consists of gasifier ash removal, cooling, depressurization and conveying equipment. Coarse ash is taken from the start-up burner leg bottom into a refractory-lined pipe, which serves as a surge volume. The ash is initially cooled by heat transfer fluid (down to below 600°F) and then depressurized to an appropriate pressure (from about 5 to 30 psig), which is necessary to transport the ash to the ash silo or to a feeder surge bin to feed to the gasifier as make-up or start-up bed material. A low pressure fluidized bed cooler, located downstream of depressurization device, further cools the gasification ash to around 200°F. When sand is first added to the gasifier for start-up bed material, the CCAD system is filled with solids. During steady state gasifier operation, the CCAD system automatically controls the gasifier standpipe level by varying the gasification discharge rate.

The CCAD system was successfully commissioned on-line with circulating solids in the gasifier during an extended gasifier start-up period. All basic logic and controls were tested. In order to test higher discharge rates, an external circulation loop was established using the sorbent feeder to add solids back to gasifier. During this commissioning period, the CCAD system discharged solids to the sorbent feeder surge bin.

For the remainder of TC19, the CCAD system was fully available for service. Gasification ash depressurization and cooling, as well as gasifier standpipe level control performed as expected. Normal discharge rates were in the range of 100 to 600 lb/hr, while the peak rate was about 1,600 lb/hr.

The gasifier solids level was fairly constant during the test campaign. Sand was only added during start-up. Solids were removed from the gasifier about once a day via the CCAD system to maintain a constant standpipe level.

3.1.7 Gas Analysis Modifications

For the special application of taking continuous samples from particulate-laden syngas at the PCD inlet, reflux probes were installed. This type of probe was adapted from the petrochemical industry. Reflux probes have been used previously at the PSDF at other gas sampling points to condense moisture and hydrocarbons out of the gas stream. The gasification ash present in the syngas at the PCD inlet was an additional factor that the new configuration proved capable of processing. The rugged construction of the reflux probes (each weighs close to 200 pounds) and simple design (no moving parts) made these dependable pieces of equipment. The reflux probes are shown in Figure 3-10, with a disassembled probe shown on the left, and the two probes installed at the PCD inlet (demarked with blue dots) shown on the right.

The gasification ash and the condensed liquid from the syngas combined into a muddy mixture inside the probe. However, this did not affect the cooling efficiency, as the probes proved effective in processing the mixture. The probes dried the gas, and some dry ash passed through the probes. High pressure, large capacity cartridge filters were used on the probe outlets to prevent the ash from passing through to the analyzers. During gasifier operation, the probes are steam-cleaned twice every week to avoid any unscheduled down time. The filter element is also changed during one of these cleaning cycles. The use of redundant probes allowed continued gas sampling while one probe was being cleaned and cooled. Cleaning and filter changes required about one man hour every week. To cool the reflux probes, rugged vortex chillers manufactured by AirTX were used, and they have performed well, with no tube disintegration like that seen in chillers previously used at the PSDF.

The reflux probes used at the PSDF are ready for commercial applications. All probes in use have a pressure rating of 500 psig, and higher ratings are available. The temperature control loops were designed and built at the PSDF, and involve only typical equipment, such as thermocouples and control valves. Most commercial gasifier analyses will employ reflux probes, and the current setup using manual steam cleaning is acceptable for commercial application. Automated steam cleaning could be added, but would involve significant safety measures to avoid analyzer damage in the event of a leak.

3.2 Gasifier Inspections

The post-test campaign gasifier inspections were typical. The mixing zone, riser, and standpipe were relatively clean. The riser crossover and secondary crossover were removed in preparation for the upcoming gasifier modifications.

A portion of refractory was missing from the burner leg. This weakness in refractory could be attributed to a combination of high temperature and solids circulating aggressively in the leg. Portions of the hot and cold faced refractory were cracked.

In the mixing zone, a portion of hot faced refractory was cracked throughout and was missing in some areas where the burner leg enters the mixing zone. There was a small portion of insulating refractory that was also cracked in this area. The area of the J-leg that enters the mixing zone was clean. There were a few small areas with missing refractory. However, this was probably due to refractory age, and there was no noticeable effect on the process operation. The lower portion of the mixing zone refractory was also in relatively good condition. There was no change in the inner diameter.

The cyclone was in good condition, although a notch at the cyclone inlet, seen in previous inspections, had re-formed. A small amount of refractory was missing, which could be seen when looking into the top of the cyclone, as shown in Figure 3-11.

The primary and secondary gas coolers were also inspected. All of the tubes in the coolers were clear, and there was negligible accumulation of condensed organic material at the outlet of the secondary gas cooler.

All main components of the CCAD system were inspected. In addition, instrumentation and all solids handling systems associated with CCAD such as conveying lines, bends, and receiving systems were inspected. All this equipment appeared normal. The design concepts of the main depressurization unit were confirmed through inspection.

Upon completion of TC19, the recycle gas compressor and piping were inspected. Inspections following the TC18 had revealed water accumulation in the aeration lines. As a result, the steam purge that occurred on a recycle gas compressor trip was disabled. The TC19 inspections showed that no tar or crystal accumulation occurred during operation without the steam purge. Therefore, the decision was made to permanently disable the steam purge following a trip. The inspections also revealed the piping and compressor itself were both in very good condition.

Table 3-1. Gasifier Circulating Solids Analysis.

	Average	Standard Deviation	Minimum Value	Maximum Value
SiO_2, wt%	65.7	11.5	55.5	90.1
Al_2O_3, wt%	14.1	5.1	3.7	20.4
Other Inerts (Fe_2O_3, P_2O_5, Na_2O, K_2O, & TiO_2), wt%	7.8	2.7	2.3	10.4
$CaCO_3$, wt%	0.6	0.1	0.4	0.8
CaO, wt%	9.1	3.3	2.6	13.6
MgO, wt%	2.2	0.7	0.7	3.0

Table 3-2. Gasifier Loop Seal Solids Analysis.

	Average	Standard Deviation	Minimum Value	Maximum Value
SiO_2, wt%	64.7	10.7	54.5	89.8
Al_2O_3, wt%	12.1	4.6	2.3	17.1
Other Inerts (Fe_2O_3, P_2O_5, Na_2O, K_2O, & TiO_2), wt%	7.9	2.6	2.0	13.4
$CaCO_3$, wt%	0.5	0.1	0.3	0.7
CaO, wt%	11.4	3.8	3.3	16.2
MgO, wt%	2.4	0.8	0.8	3.3

Table 3-3. PCD Solids Analysis.

	Average	Standard Deviation	Minimum Value	Maximum Value
SiO_2, wt%	29.6	4.1	21.6	40.3
Al_2O_3, wt%	11.3	1.1	8.9	14.2
Other Inerts (Fe_2O_3, P_2O_5, Na_2O, K_2O, & TiO_2), wt%	6.6	0.6	5.1	7.9
$CaCO_3$, wt%	3.2	0.9	1.4	4.1
CaS, wt%	0.5	0.2	0.2	0.9
CaO, wt%	12.9	2.2	8.8	18.0
MgO, wt%	3.6	0.3	2.6	4.2
Organic Carbon, wt%	30.1	7.0	12.4	45.3
HHV, Btu/lb	4,529	1,113	1,781	6,964
LHV, Btu/lb	4,480	1,104	1,756	6,888

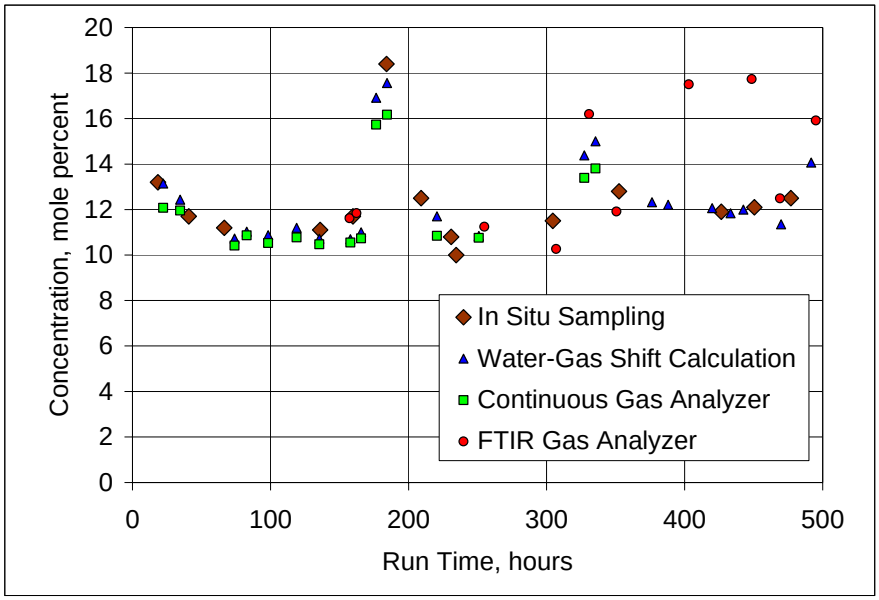

Figure 3-1. Syngas Moisture Concentrations.

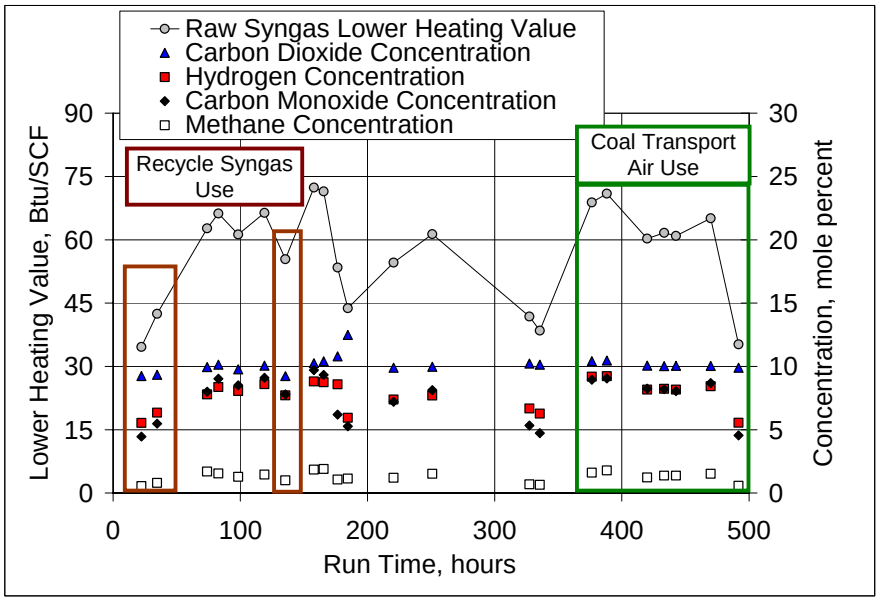

Figure 3-2. Raw Syngas Lower Heating Value and Carbon Dioxide, Hydrogen, Carbon Monoxide, and Methane Concentrations.

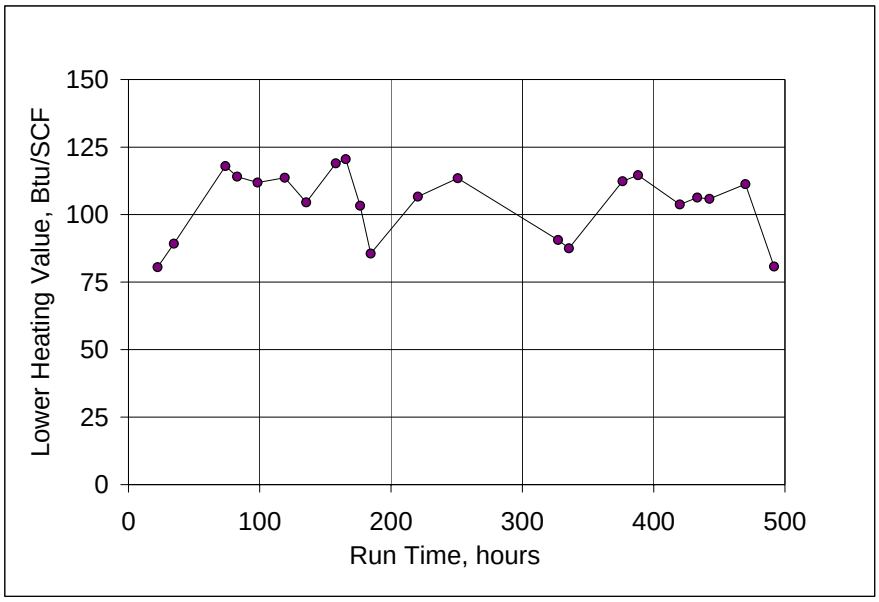

Figure 3-3. Projected Syngas Lower Heating Value.

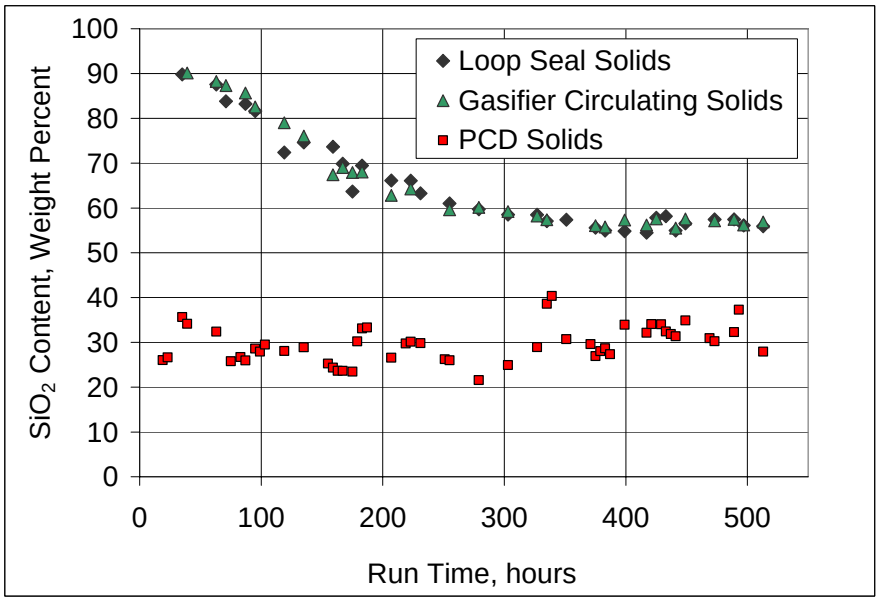

Figure 3-4. Gasifier and PCD Solids Silicon Dioxide Contents.

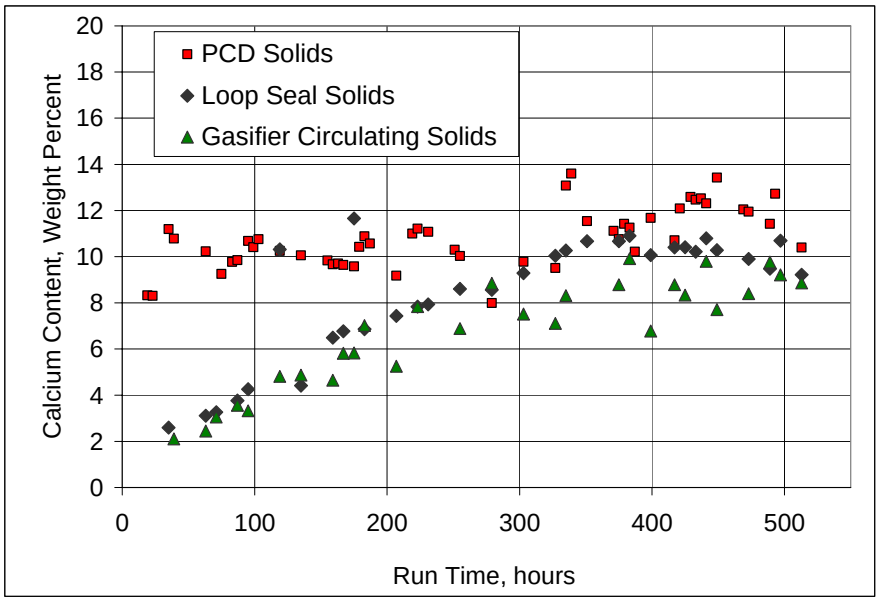

Figure 3-5. Gasifier and PCD Solids Calcium Contents.

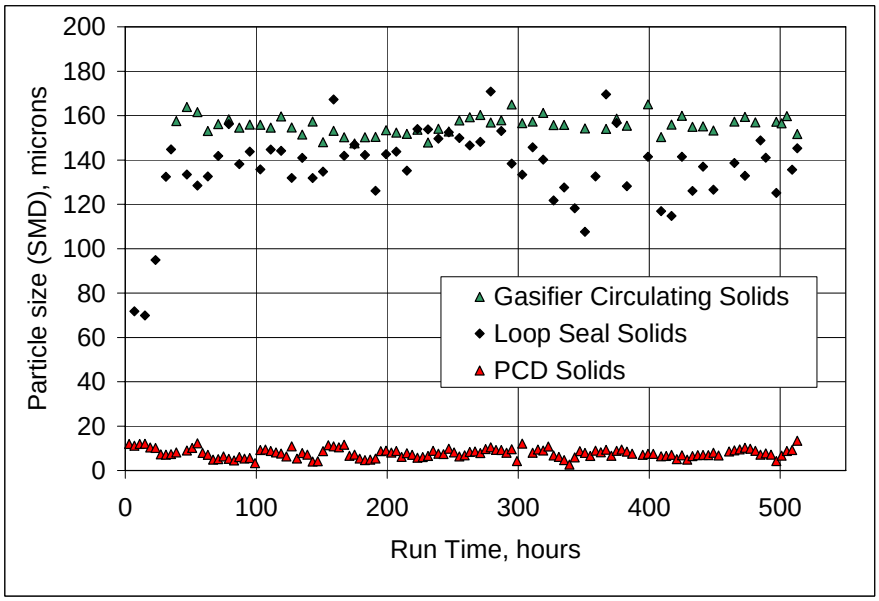

Figure 3-6. Gasifier and PCD Solids Particle Sizes.

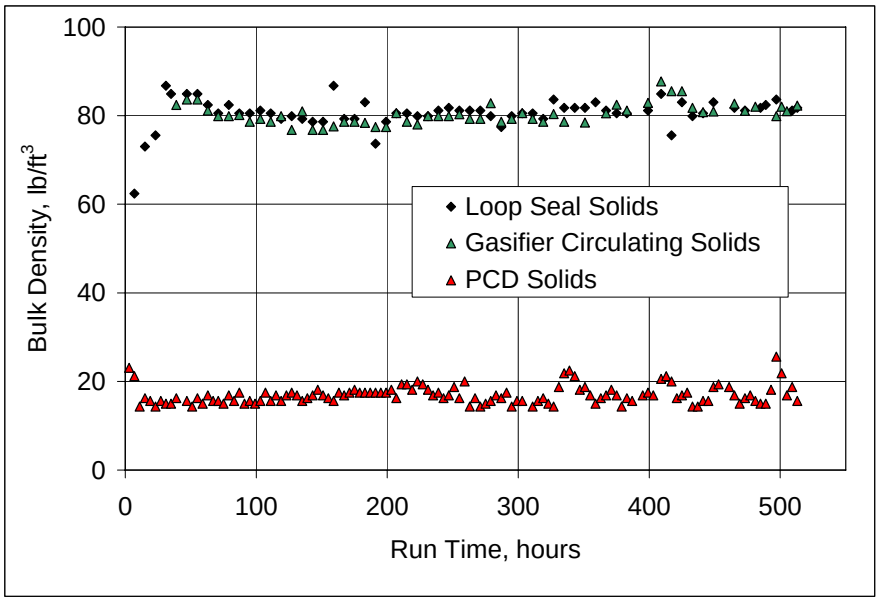

Figure 3-7. Gasifier and PCD Solids Bulk Densities.

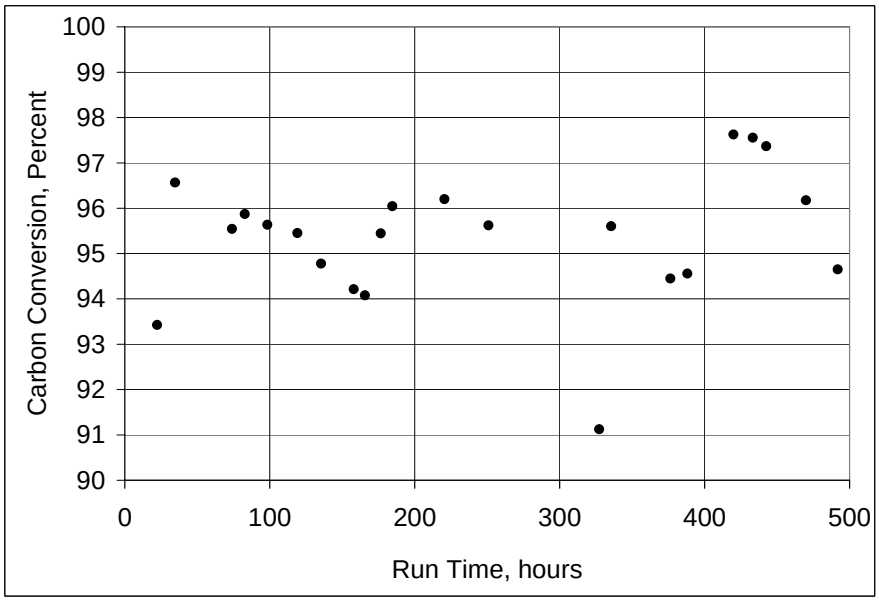

Figure 3-8. Carbon Conversion.

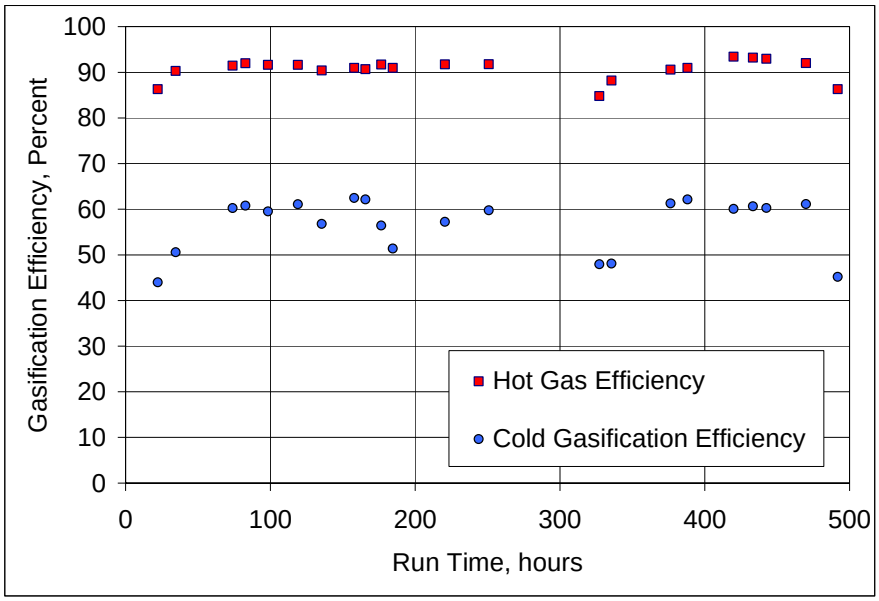

Figure 3-9. Hot and Cold Gasification Efficiencies.

Figure 3-10. Gas Analysis Reflux Probes.

Figure 3-11. Gasifier Cyclone Inspection.

4.0 PARTICULATE CONTROL DEVICE

4.1 Overview

TC19 was conducted with PRB coal and with a PCD installed almost entirely with Pall iron aluminide filter elements. Generally, the results of the test campaign were consistent with past successful tests conducted under these conditions. This is fortunate since TC19 was the last test campaign conducted with the original gasifier solids collection devices. The data from TC19 will be most readily compared data with the new solids collection devices used in TC20.

The next section (4.2) describes the results of in-situ particulate sampling at the inlet and outlet of the PCD and discusses particulate penetration issues with the PCD. Inlet measurements indicated values typical of PRB coal in past tests when the cyclone system was working properly. Outlet measurements showed overall low outlet particle penetration after an initial seasoning period. However, there were a number of large particles noted on the outlet sample filters that may cause a problem with downstream equipment. Filter element sealing issues related to gaskets and fasteners were improved.

The first attempt to collect near real-time PCD outlet particulate concentration data with the Process Metrix Process Particle Counter (PPC) is described in Section 4.3. Although many problems were encountered, the monitor showed potential for reliable real-time particulate monitoring.

Understanding the factors that affect PCD performance will come through analysis of the solid particles collected in the PCD. Section 4.4 presents these analyses with discussions of particle size distributions, PCD dustcake measurements, physical and chemical properties of the particulate, and dust flow resistance measurements. A modification to the lab drag measurement techniques is introduced for the TC19 data which improves the correlation between lab and field data. This technique will be evaluated for effectiveness in subsequent test campaigns.

The pressure drop performance of the PCD is analyzed in Section 4.5. Although transient pressure drop was reasonable and controllable, the baseline pressure drop did not stabilize during the test period. That is, baseline pressure drop was still continuing to increase with time until the outage.

Laboratory measurements of dustcake flow resistance are used to analyze the pressure drop performance of the PCD in Section 4.6. The regression analysis technique used to compare field and lab data was modified for TC19, producing much better predictions of pressure drop from dust characteristics.

Finally, Section 4.7 provides the results of measurements and observations made on the PCD filter elements after the end of the test campaign. The corrosion of the iron aluminide filter elements that was first noted in the TC17 report continued in TC19 and appeared to be contributing to increasing pressure drop of the elements with exposure time.

4.2 Particle Collection Performance

In-situ particulate sampling was performed at the PCD inlet and outlet using the SRI in-situ batch sampling systems described in previous reports. The inlet particle measurements are used to help understand the pressure drop characteristics of the PCD and will be used in a later section to calculate transient drag. The outlet measurements indicate the collection performance of the PCD with the installed filter elements and are critical to assessing the effect of particle leakage on downstream equipment. This section will also discuss failsafe tests conducted during TC19. Failsafe devices that work correctly are critical to prevent damage to downstream components and to allow continued operation when filter element failures occur. Progress that has been made in gasket sealing issues is also discussed.

4.2.1 PCD Inlet Mass Loadings

Particle mass concentrations and mass rates measured at the PCD inlet are given in Table 4-1, and the mass rates are plotted as a function of coal feed rate in Figure 4-1 along with similar data from other gasification test campaigns with PRB coal. The solid line is a linear regression to the TC19 data while the dashed lines are for past test campaigns. The average inlet concentration was 12,700 ppmw (282 lb/hr) with a range of values from 10,300 to 16,100 ppmw. When plotted as a function of coal feed rate, the TC19 loadings fall well within the range of other PRB data when the gasifier cyclone was functioning well. The solid triangles and steep dashed regression line are from TC14 when the cyclone system was not working correctly because of erosion of the refractory walls. The physical and chemical characteristics of these particle samples will be discussed in a later section.

4.2.2 PCD Outlet Mass Loadings

Particle concentrations measured at the PCD outlet are included in Table 4-1 and are plotted as a function of time in Figure 4-2. The graph also contains values measured during the previous test campaign (TC18). Bars in the graph that are below the “Minimum Measurement Resolution” line are not actually measured values but merely placeholders to indicate the numbers of tests that had immeasurably low concentrations.

As discussed in the TC18 report, on the last day of that test campaign there was a complete failure of three filter elements along with failure of a failsafe installed above one of those elements. This combination of failures produced a 1.25 inch hole through the tube sheet that resulted in an extremely high particle concentration (1773 ppmw) at the outlet of the PCD. Prior to the start of TC19 extraordinary efforts were made to clean up as much of the particulate contaminating the clean side of the PCD as possible. A vacuum truck was used to evacuate particulate that was resuspended using air lances from the inside of the PCD plenums, PCD head, and outlet ducts. A significant amount of particulate was removed by this process.

As discussed in previous reports, it is common to see an elevated particle concentration at the outlet of the PCD during the first few days of a test campaign. This may be due to seasoning of filter elements and plugging of gasket pores. However, at the start of TC19 the particulate loadings measured during sand circulation were higher than observed previously. Some of this

mass may have been material that penetrated through the PCD during TC18 or even due to old particulate that was disturbed in the cleaning process and not completely removed. Microscopic examination suggested that most of this was black material consistent with coal gasification ash and not corrosion product or sand.

Once coal feed was established, the PCD outlet loading dropped rapidly below the lower limit of measurement resolution (0.1 ppmw) and stayed there for the rest of the test campaign. The elevated levels in the table that are not shown in the graph are related to failsafe tests and particulate injection for evaluating the response of real-time particle monitors that will be discussed later in this report. The filter elements installed for TC19 included 69 Pall FEAL sintered powder filter elements with three Schumacher N10-20 ceramic filter elements. All of these elements have excellent collection efficiency as illustrated by the rapid drop in emission rate and very low outlet concentrations throughout the test campaign.

Despite the high overall collection efficiency and low total particle penetration, microscopic examination of sample filters from the PCD outlet indicated that there were significant numbers of large particles present. Figure 4-3 is an optical microscope picture of particles on the filter used for PCD outlet test Number 5, which had an overall particle loading below 0.1 ppmw. This is not an isolated particle but one of many that exceed 10 microns, which fall under more stringent turbine inlet specifications. Quantifying these large particles is a significant undertaking because of the small overall number present. This issue with the large-particle penetration will be addressed as discussed in a subsequent section.

4.2.3 Failsafe Performance Tests

During TC19 a new type of failsafe tester was introduced. Previous failsafe testers either simulated small leaks or were inconsistent in their operation. The new device is shown in Figure 4-4 and consists of a 1.5 inch inner diameter ball valve installed in the hopper of the PCD. The valve is actuated by a long handle that exits the pressure boundary through a packing gland. The valve is connected by flexible metal hose to a housing that contains a failsafe installed in the PCD tube sheet. When the valve is opened, it provides a 1.5 inch hole that has the entire pressure drop of the tube sheet across it. This should simulate a catastrophic and total failure of a filter element and subject the failsafe to instantaneous high particle loading. Measurement of particulate concentrations at the outlet of the PCD with and without the valve open should indicate the collection performance of the failsafe under these conditions.

Outlet Runs 10 and 11 in Table 4-1 were made during testing of the collection performance of a Pall iron aluminide “fuse” failsafe device. As the expected collection efficiencies of these devices improves with time, Run 10 was collected during the first hour of exposure and Run 11 covered a 3 hour period after reactivation the next day. Unfortunately, tar contamination of the sample filter during Run 10 raised the lower limit of resolution for that test to 0.15 ppmw. Microscopic examination of the sample filter indicated that little of the mass was particulate. The second test was not contaminated and indicated a concentration below 0.10 ppmw. Since this test simulated the failure of only one of 73 filter elements, the actual leakage of the failsafe could have been as high as 7.3 ppmw and would not have been detected by this measurement. However, measurements from the cold flow PCD model indicate that the Pall fuse is capable of limiting particulate penetration to less than 0.10 ppmw by itself without dilution from parallel

filter streams. This test is taken as confirmation that acceptable particulate collection can be obtained from this type of failsafe with a complete filter element failure.

Although collection performance of the Pall FEAL fuse is quite good, these units have broken at a disturbing rate. The common failure is breaking in the heat-affected zone of the porous metal near the weld to the mounting flange. Although many have broken during installation and removal, there have been instances where fuses have separated from the flange during operation and fallen down inside the filter element. If the element below a broken failsafe fails, it will result in a major leak necessitating immediate shutdown of the gasifier. A stronger failsafe or an improved welding system for the Pall fuse is needed. During TC20, a new prototype failsafe from Pall constructed of HR-160 fiber will be tested.

4.2.4 Filter Element Sealing Issues

The testing of bolt torques after TC18 showed that the use of the Belleville conical washers allowed retention of at least 92 percent of the original bolt torque, with most bolts retaining 100 percent of the original torque. Bolts without the conical washers had final torque values that were 30 to 75 percent of the original torque. Based on these torque measurements and supporting lab tests, conical washers were used on all of the bolts in TC19. For the TC19 installation, the stacked sets of three thin conical washers were replaced with thicker, one-piece conical washers with similar load deflection characteristics. Lab tests showed that the one-piece washers actually reduced the leakage in test fixtures that were baked in a muffle furnace, and the one-piece washers were much easier to work with during the installation.

In conjunction with the conical washers, rolled construction gaskets were used exclusively in the TC19 installation to eliminate any issues with gasket deterioration. (As discussed in previous reports, the old style gaskets with the chopped fiber filler material had shown severe degradation of the filler when heated to 800°F in laboratory testing.) Using the rolled construction gaskets with no filler in combination with the conical washers would hopefully completely eliminate the gaskets as a potential pathway for particle leakage. To further increase confidence in the installation, all bolts were torqued to specifications and then retorqued the next day.

After TC19, filter nut bolt torques were checked on 10 different elements (five on top plenum and five on bottom plenum). On all 40 bolts, the measured torque values were still at the original applied torque (either 100 in-lbs or 120 in-lbs depending on the bolting configuration). This result confirmed that the use of the conical washers in conjunction with the rolled construction gaskets had completely eliminated the problems with loss of bolt torque.

4.3 Real-Time Particulate Monitoring

4.3.1 PCME Particulate Monitor

The PCME DustAlert-90 (referred to as the PCME) particulate monitor was operational throughout TC19 although the data it collected were generally unremarkable since particle loadings were low throughout most of the test campaign. However, this instrument continues with a disturbing trend of producing false-positive indications. Typically, several times during each test campaign the PCME will indicate a particle increase that cannot be confirmed by in-

situ measurements. Since this instrument works by measuring tiny amounts of electrical charge flowing through the duct there are a number of interferences that could occur in a complex plant with many types of electrical devices. Regardless, the PCME does do a reasonably good job of detecting large actual particle leaks as discussed below. A new version of the PCME instrument is available that reportedly has greater sensitivity and better noise suppression. This instrument will be evaluated in the future.

Dust injection to the PCD outlet was conducted late in the test campaign using a fluidized bed dust injection system designed and built expressly for this purpose. The injection period corresponded to in-situ outlet Run 15 from Table 4-1, where an actual particulate concentration of 2.0 ppmw was measured. The real-time response and five minute average of the PCME is shown in Figure 4-5. The PCME gave a clear response to the start and stop of the dust injection and returned an average value of 3.9 percent over the period that comparative measurements were made. Figure 4-6 shows the TC19 result for actual particle concentration versus PCME output compared to previous tests. Since the PCME measures particles per second rather than concentration, the results in the figure have been normalized to a syngas flow of 25,000 lb/hr. The normalized TC19 result (1.56 ppmw) falls right on the linear regression line to all previous data. However close to the regression line the most recent result, the PCME data are quite scattered.

4.3.2 PPC Particulate Monitor

A new particle measuring instrument was installed and operated for the first time during TC19. The system consists of a sample extraction system designed by SRI and GTI (Gas Technology Institute) and a light scattering optical particle counter designed by Process Metrix, LLC. The instrument is generally known as the High Pressure Process Particle Counter and is abbreviated HPPPC or just PPC.

The PPC system was initially started up by representatives of GTI and Process Metrix. After the first few days of operation, the system was turned over to SRI employees at the PSDF for validation, operation, and maintenance. PPC operation was attempted for all of TC19 with limited results.

A number of problems were encountered with the PPC system during TC19. Although there were some minor hardware problems (sticking valves, heater failures, etc), the most significant technical issues related to condensation and contamination of optical windows with water and organic compounds from the syngas. Contamination of windows limited acceptable operation to only a few minutes after the unit was cleaned and started up, although it was not initially clear how quickly this occurred. Following the TC19 test campaign the system will be modified to add heaters to the optical window purge and to the optical cell cooling water. The window purge will have the capability for heating between 200 and 400°F while the water will be heated to the range of 150 to 212°F. Plans are underway to modify the cooling water passages in the high pressure cell to move the coolant away from the syngas stream, as well as to incorporate minor changes to some electronic components to reduce electrical noise problems. These changes should produce more reliable and accurate operation in the future.

Despite the problems, there was one period of apparently useful operation of the PPC during TC19. Figure 4-7 shows a trace generated from the output of the PPC during the injection of 2.0 ppmw of gasification ash into the PCD outlet duct that was previously discussed. This test was conducted just after starting the PPC with clean windows. Clearly there was a dramatic response to the increased particulate loading. The PPC returned an average particle concentration of 0.83 ppmw compared to the 2.0 ppmw measured with the in-situ sampler. This was considered reasonable agreement.

4.4 PCD Solids Analyses

PCD pressure drop, cleaning requirements, and bridging tendency can be influenced by changes in the characteristics of the solids being collected in the PCD. Important characteristics of the solids include particle size distribution, bulk density, true density, porosity, surface area, composition, and flow resistance. The effect of all these parameters must be considered in analyzing the performance of the PCD.

4.4.1 Particle Size Distributions

A Microtrac X-100 particle size analyzer was used to measure the particle size distributions of the in-situ particulate samples collected at the PCD inlet and the PCD hopper samples collected from the CFAD system used for the laboratory drag measurements.

In-Situ Samples. Figure 4-8 shows the average differential mass particle size distribution measured on the TC19 PCD inlet in-situ samples and compares these data to a similar distribution from TC18. As was seen in Figure 4-1, the total mass concentration during TC19 was somewhat lower than the PCD inlet concentration measured during TC18, even for the same coal feed rate. The particle size distribution shows that the reason for the high mass loading was primarily due to fewer large particles above 10 microns in TC19. Since the distributions were similar below that size, the lower mass loadings may have been attributable to operation of the gasifier cyclone. Regardless, the changes seen were minor and likely to be observable in the operation of the PCD.

Hopper Samples. Figure 4-9 compares the differential mass percentage distributions for the average of all in-situ samples with the raw hopper samples used for the TC19 lab drag measurements. (Although the in-situ samples are a more accurate representation of the particulate entering the PCD at a given time, they are far too small of be useful for drag measurements.) One of the hopper samples was almost a perfect match to the average PCD inlet distribution while the other was only slightly different. However, the November 21 sample was well within the range of data that went into the average in-situ distribution. Based on these data, the hopper samples chosen for the laboratory measurements seem reasonably representative in terms of particle size distribution.

4.4.2 Dustcake Observations and Thickness Measurements

The PCD dustcake was inspected and dustcake thickness measurements were made after the PCD internals were removed from the vessel following TC19 operation. The shutdown process at the end of TC19 was a “clean shutdown,” meaning that back pulsing of the filter elements was continued for several hours after coal feed ended. Thus, the dustcakes that remain on the

elements should be typical of residual cakes but provide no information on the transient dustcake. The thickness measurements are summarized in Table 4-2. Most of the measurements on the TC19 dustcake were in line with data from previous tests, which have shown a residual dustcake thickness typically on the order of 0.01 inches. However, some of the bottom plenum dustcakes were thicker by a factor of two at the top of the elements. There was no evidence of any tendency for the particulate to bridge between elements.

An "orange-peel" texture was noted on several of the bottom plenum elements, and it was later determined that these were older iron aluminide elements that showed signs of progressive corrosion. The lumpy dustcake structure on these elements may be related to the corrosion and localized plugging associated with the corrosion and sulfidation of the iron aluminide. After the elements were removed and pressure washed, a definite progression of the corrosion could be seen with increasing time of exposure. This will be discussed further in Section 4.6.

4.4.3 Dust Physical Properties and Chemical Compositions

This section discusses the physical properties and chemical compositions of the in-situ samples collected at the PCD inlet, the PCD hopper samples used for the laboratory drag measurements, and the dustcake samples.

In-Situ Samples. Tables 4-3 and 4-4 give the physical properties and chemical compositions, respectively, of the in-situ samples collected at the PCD inlet and the hopper samples selected for lab drag measurements. All of the in-situ samples were fairly consistent in physical properties and chemical compositions.

Previously, dust flow resistance has been related to particle surface area and, at the PSDF, to non-carbonate carbon in the dust particles. Non-carbonate carbon (NCC) is the carbon remaining from fuel gasification ash as opposed to alkaline carbonates in the ash. As in previous tests with PRB coal, the TC19 data showed a general increase in surface area with increasing NCC as shown in Figure 4-10. In general, the TC19 data fell somewhat above the previously established trend line for PRB coal without sorbent addition but still below the trend line for PRB coal with limestone addition. As noted in previous reports, the limestone addition produced an increase in the surface area at a given value of NCC due to the extensive pore structure that is created in the limestone during calcination at high temperatures in the gasifier. The graph also shows that the ash from the Illinois Basin coal had a much lower surface area than the ash from the PRB coal, even though it had a relatively high NCC content.

Hopper Samples. For lab drag measurements, two hopper samples with different carbon contents were selected, since previous studies have shown that drag increases with increasing carbon content. As shown in the tables, the sample with the lower NCC also had a lower surface area. All of the hopper samples appeared to be very similar to the corresponding in-situ samples collected under the same test conditions. Thus that the hopper samples selected were representative samples for the laboratory drag measurements.

Dustcake Samples. Tables 4-5 and 4-6 give the physical properties and chemical compositions, respectively, of the dustcake samples taken after TC19. Unlike TC18, where a substantial difference in mean particle size was found between the top and bottom plenums, the dustcakes

on the top and bottom plenums were very similar after TC19. This suggested that there was very little vertical segregation of particle sizes within the PCD in TC19. This was consistent with the finding of very little difference in dustcake thickness between the top and bottom plenums.

Compared to the in-situ particulate samples, the residual dustcakes from TC19 had higher bulk density, lower uncompacted bulk porosity, lower surface area, and finer particle size. These differences would be consistent with the fine particle enrichment theory. This theory asserts that with each backpulse, some very fine particles are re-entrained and recollected into the residual dustcake, resulting in gradual enrichment of the fine particle fraction of the dustcake.

4.5 PCD Pressure Drop Performance

Transient PCD Drag. The pressure rise within a backpulse cleaning cycle of the PCD is a direct measure of the characteristics of the particulate being collected at that time. Under stable operation, the vast majority of this particulate is removed from the filter elements during cleaning, so this is referred to as the transient pressure drop. Since pressure drop is a function of the gas velocity, temperature (gas viscosity), particulate loading, and the flow resistance of the particulate, using this parameter makes comparison of different conditions and particulate difficult. Therefore, a normalized drag is calculated, which is pressure drop that is normalized to 1 ft/min face velocity, 1 lb/ft^2 areal loading, and viscosity at 70°F. The result is a fundamental parameter that describes the flow resistance of the collected dustcake.

During each in-situ sampling run at the PCD inlet, the PCD transient drag was calculated using the measured particle concentration along with the pressure drop increase and face velocity during the period of the in-situ test. All of the particulate measured at the PCD inlet was assumed to be collected on the filter elements and to contribute to pressure drop. The inputs and results are shown in Table 4-7. The calculated transient drag at PCD conditions is listed under the column heading “PCD.” The corresponding normalized value of transient drag at room temperature is listed under the heading “PCD@RT” and is plotted as a function of non-carbonate carbon (NCC) content in Figure 4-11, along with data from recent PRB coal test campaigns and data from the Illinois Basin coal testing in TC17. There is considerable scatter in the TC19 data, but the data are generally scattered about the previously established trend line. This type of data scatter was to be expected given the variations in particle size of individual tests, equipment configuration, process conditions, coal composition, and limestone addition. Nevertheless, the data showed that there were definite distinctions between the data sets obtained with PRB coal, high sodium lignite, and Illinois basin coal. These distinctions were expected based on the morphological differences between the ashes produced from lignite, subbituminous, and bituminous coals. Overall, the data continued to show a definite trend toward increasing drag with increasing carbon content.

Baseline Pressure Drop Analysis. Figure 4-12 shows the peak and baseline PCD pressure drop measurements for the TC19 test campaign, and the data are compared to previous test campaigns in Figure 4-15. As noted in previous test campaigns, the baseline pressure drop did not stabilize over the course of the test campaign, although this is not obvious from Figure 4-12 because of coal feeder problems from November 17 through November 27 that caused a flat slope in the trend. Compressing this time period in Figure 4-13 shows that the upward trend continued until

shutdown. Longer test campaigns may be necessary to accurately determine the baseline pressure drop trend over long-term operation.

4.6 Prediction of PCD Drag and Pressure Drop

Lab Drag Measurements. Although the previous plot of PCD drag showed a relationship between drag and particulate carbon content, there was a great deal of scatter in the data. Another factor that has been found to be significant, particle size, was not included in that analysis. To investigate the characteristics of the TC19 particulate more completely, drag measurements were made in the laboratory flow resistance test device on the two hopper samples described previously. This apparatus used a series of cyclones between the dust generator and the dustcake collection surface to vary the particle size distribution of the dustcake. The results are illustrated in Figure 4-14 with normalized drag plotted against the mass median diameter (MMD) of the collected dustcake. The actual data points are indicated by the triangles and squares, while the solid lines are linear regressions to the data to illustrate the linearity of the results. The NCC contents of the two samples were different, with the high NCC sample containing 37.8 percent carbon in the bulk sample, while the low NCC sample contained 24.3 percent carbon. As expected, the dustcake drag values generally increased with increasing NCC and drag decreased with increasing particle size. The short-dash lines on the graph represent the range of PRB drag data measured previously and the TC19 lab data fall toward the middle of this range.

The solid circle symbols on the graph are the values of PCD transient drag calculated for each of the in-situ samples from Table 4-7. All of the PCD data points fall below the lab measurements despite similar values of bulk NCC. More complete analysis indicated that some of the carbon contents of the samples collected in the lab device were considerably higher (>10 percent higher in some cases) than the bulk samples they were derived from. The increased carbon content was greatest for the largest particle fractions, while the 2 to 3 micron fraction had about the same carbon as the bulk sample. This variation in carbon with size had not been noted to this extent in the past. Since drag increases with carbon content, it seemed reasonable to consider the actual properties of each of the lab drag samples at the different size ranges. A multiple linear regression was calculated between the drag, MMD, and NCC of each of the eight individual lab drag samples. This new technique produced the following equation:

$$\text{Drag} = 10^{(2.496 - (0.657 * \text{Log}(\text{MMD})) + 0.00599 * \text{NCC})}, \text{ with an } r^2 = 0.97.$$

In the past, the NCC of the bulk hopper sample loaded into the dust generator of the lab device was used to calculate a regression to the drag and MMD. That is, the carbon of the bulk sample was associated with all four particle size samples generated for a set of data. This technique applied to the TC19 samples produced the following:

$$\text{Drag} = 10^{(2.564 - (0.566 * \text{Log}(\text{MMD})) + 0.00396 * \text{NCC})}, \text{ with an } r^2 = 0.98.$$

The new technique indicated less effect from size and a somewhat greater effect from carbon content. Both showed good correlation to the data but the new procedure fit the actual PCD data much better. The regression with the new technique was used to calculate drag versus particle size with two different carbon contents that are equal to the minimum and average carbon contents of the in-situ samples, 17 percent and 28 percent NCC, respectively. These predictions

are shown on Figure 4-14 as the dash-dot and long-dash lines. Except for one outlier, the predictions made from the new regression technique matched the PCD data quite well.

The results of regression predictions for each individual value of PCD transient drag are shown in the rightmost two columns of Table 4-7. These calculations use the MMD and NCC of each in-situ sample to predict the transient drag of the PCD during that test. The column labeled as Lab(1) are drag predictions from the old technique while the Lab(2) column used the regression equation from the new technique. Based on each individual value and on the average of all the values, the new technique reduced the error in the lab measurements significantly.

Comparison of Lab Measurements with Transient Drag. Average lab and PCD drag values for all gasification test campaigns are summarized in Table 4-8 and plotted in Figure 4-15. The comparison showed excellent overall historical agreement (average difference of about 10 percent), even though the difference is much higher for certain test campaigns. For TC19, the difference was 12 percent or 40 percent depending on the prediction technique. The results for all gasification test campaigns are plotted in Figure 4-15 and continued to show scatter around the perfect agreement line. Both values for TC19 are shown on this graph with the new technique producing excellent agreement with past data for PRB coal and moving the point much closer to the perfect agreement line. As illustrated in the graph, the perfect agreement line falls within the 95 percent confidence interval on the regression line to the data, indicating good agreement between the data sets. The accuracy of these prediction techniques will continue to be monitored in subsequent test campaigns.

4.7 Analysis of PCD Filter Element Condition

Following TC19, the filter elements were inspected to analyze their condition. The filter elements installed were all Pall sintered powder filters iron aluminide (FEAL) filter elements, with the exception of three Schumacher ceramic elements. For several test campaigns, an apparent corrosion product was developing on the oldest FEAL elements. If the corrosion product contributed to increased pressure drop, perforation, or to weakening of the elements over relatively short periods of time, it would impact the viability of this type of filter element.

After the filter elements and plenums were blown off with high pressure air, all elements were removed from the PCD. All but one of the elements were intact and functional. One of the Schumacher ceramic elements was found to be cracked at the neck between the mounting flange and the main body of the element. Either the element cracked during shutdown, or the bottom support was holding the cracked element tightly together. If the filter cracked during operation, very little particulate penetrated through the crack, since outlet particulate concentrations were not elevated and flow test data indicated that the failsafe above the filter element was not plugged. Use of a filter neck sock between the filter element flange and the filter nut would probably have prevented this failure and will be used on future ceramic element installations.

Each of the filter elements were evaluated in the dirty condition in the PSDF filter element flow resistance testing facility. Although the filter elements had been air blown, this did not remove the particulate from the pore structure of the filter element and thus did not generally affect the dirty pressure drop greatly. The flow test device measures pressure drop for a whole filter element as a function of air flow over a range of filter face velocities from 2 to 8 ft/min.

Figure 4-16 shows the complete set of filter element flow resistance data for the dirty filter elements removed from the top plenum after TC19. The legend in the figure shows the PCD location (e.g., T1 designates an element on the top plenum at Location 1), the PSDF filter identification (ID) number, and the number of gasification hours in parentheses. While some of the filter elements have reasonably low pressure drop at the standard face velocity of 3 ft/min, some of the oldest filter elements did not reach 3 ft/min before the measuring device limit of 50 inH_2O was exceeded. (The pressure drop of a new FEAL filter element is 3 to 5 inH_2O at 3 ft/min.) The pressure drop for each filter element at 3 ft/min is plotted as a function of gasification exposure hours in Figure 4-17. The dirty filter element data from Figure 4-16 are shown as the solid symbols. (The filter elements with pressure drops over 50 inH_2O were manually extrapolated to 3 ft/min.) These dirty filter data show a trend of increasing pressure drop with time with a slope of over 7.5 inH_2O per 1,000 hours.

The open symbols on Figure 4-17 show the filter element pressure drop after pressure washing the filter elements with water. Cleaning the filter elements restored much of the pressure drop, although there was still an increasing trend with age that doubled the clean pressure drop. The large difference in pressure drop associated with the embedded particulate on young versus old filter elements may be a result of particle interaction with the very rough surface of the old filter elements as opposed to the smooth surface of the young filter elements.

Filter flow resistance data is plotted for the filter elements removed from the bottom plenum in Figure 4-18. These filter elements were generally younger than those from the top plenum because the oldest filter elements were generally installed in the top plenum. Regardless of the lower number of exposure hours, the trend of increasing pressure drop and increasing effect of embedded particulate with age was apparent in these data as well.

Figure 4-19 shows a photograph of all the filter elements removed after TC19 arranged by time of operation. The oldest filter elements were closest to the camera (7,677 hours of exposure) ranging to the filter elements that were new prior to TC19 with 518 accumulated hours at the far end. Figure 4-20 illustrates how the filter surface changes with age starting with isolated spots and growing to cover the entire filter element. After some test campaigns, the filter elements had a black tint as seen in the TC19 picture, while during other outages the filter elements had more of a rust red color as in the microscopic comparison. This may result from the specific conditions of shutdown that determine if the oxide or sulfide of iron remains after operation ends.

During the next test campaign, TC20, the collection efficiency of Pall Dynalloy sintered fiber filter elements constructed of Haynes HR-160 alloy will be evaluated. Some of these filter elements were used briefly in the past but were removed because of their lower particle collection efficiency relative to the FEAL filter elements. However, because of the corrosion problems with the FEAL filter elements, further study is planned to evaluate how the more corrosion resistant HR-160 filter elements will perform in the PCD. Several FEAL filter elements of varying age will remain in the PCD to continue the corrosion evaluation.

Table 4-1. In-Situ Particulate Measurements.

Test Date	PCD Inlet					PCD Outlet				
	Run No.	Start Time	End Time	Particle Loading, ppmw	Particle Loading, lb/hr	Run No.	Start Time	End Time	H_2O Vapor, vol %	Particle Loading, ppmw
Sand Circulation with Startup Burner										
11/7/05	--	--	--	--	--	1	13:00	14:00	--	1.30
11/8/05	--	--	--	--	--	2	13:00	15:00	--	0.85
PRB - Air Blown										
11/9/05	1	14:10	14:25	11600	224	3	12:30	14:30	13.2	0.16
11/10/05	2	8:45	9:00	11200	228	4	10:45	12:45	11.7	< 0.10
11/11/05	3	10:30	10:45	11200	244	5	12:35	14:35	11.2	< 0.10
11/14/05	4	10:00	10:15	13600	325	6	9:00	13:00	11.1	< 0.10
11/15/05	5	9:00	9:15	15100	370	7	8:45	12:45	11.7	< 0.10
11/16/05	6	9:15	9:30	12500	327	8	9:00	13:00	18.4	(1)
11/17/05	7	10:15	10:30	12500	281	9	10:10	14:08	12.5	< 0.10
11/18/05	8	10:00	10:20	10300	234	10	9:20	10:20	10.8	< 0.15 (2)
11/18/05	--	--	--	--	--	11	12:00	15:00	10.0	< 0.10 (3)
11/21/05	9	10:00	10:15	16100	348	12	9:30	13:30	11.5	< 0.10
11/23/05	--	--	--	--	--	13	9:30	13:30	12.8	< 0.10
11/27/05	--	--	--	--	--	14	9:30	11:30	11.9	< 0.10
11/28/05	10	10:20	10:35	10600	208	15	10:00	11:00	12.1	2.00 (4)
11/29/05	11	12:00	12:15	14700	310	16	11:30	14:15	12.5	< 0.10

Notes:
1. Value not reported due to disagreement between gravimetric and microscopic analyses.
2. Failsafe injection test. Some tar contamination of filter with very few particles.
3. Long-Term Failsafe injection test.
4. Dust injection for PPC and PCME evaluation.

Table 4-2. Residual Dustcake Thickness Measurements.

Element No.	Element Type	Failsafe Type	Thickness, in.	
			Top	Lower Middle
B-5	FEAL	Pall Ext Fuse SW Hollow Down	0.0136	0.0026
B-9	FEAL	PSDF	0.0113	0.0119
B-14	FEAL	Pall Ext Fuse SW Hollow Down	0.0216	0.0126
B-26	Schumacher 10-20 Ceramic	Pall Ext Fuse Holder Up	0.0207	0.0134
T-2	FEAL	Ceramem	0.0122	0.0122
T-7	FEAL	PSDF	0.0167	0.0171
T-14	FEAL	PSDF	0.0101	0.0108

Table 4-3. Physical Properties of In-Situ and Hopper Samples.

Sample ID	Run No.	Sample Date	Bulk Density, g/cc	True Density, g/cc	Bulk Porosity, %	Surface Area, m^2/g	Mass Median Particle Size, µm	Loss on Ignition, %
In-Situ Samples, Air-Blown								
AB20406	1	11/09/05	0.26	2.53	89.7	149	16.7	22.44
AB20407	2	11/10/05	0.26	2.45	89.4	160	15.0	30.88
AB20408	3	11/11/05	0.27	2.50	89.2	166	19.7	28.30
AB20409	4	11/14/05	0.25	2.45	89.8	197	17.3	32.57
AB20410	5	11/15/05	0.28	2.34	88.0	184	20.6	41.58
AB20411	6	11/16/05	0.27	2.49	89.2	191	16.0	28.02
AB20412	7	11/17/05	0.28	2.48	88.7	168	15.1	30.66
AB20413	8	11/18/05	0.30	2.54	88.2	140	13.7	25.14
AB20414	9	11/21/05	0.25	2.34	89.3	229	20.0	40.48
AB20415	10	11/28/05	0.30	2.61	88.5	112	13.6	18.59
AB20416	11	11/29/05	0.24	2.51	90.4	173	18.3	29.85
Composite Hopper Samples Used for Lab Drag Measurements								
AB19680	Low-Carbon	11/10/05	0.26	2.44	89.3	143	16.6	26.48
AB20136	High-Carbon	11/21/05	0.25	2.29	89.1	224	20.8	40.63

Table 4-4. Chemical Composition of In-Situ and Hopper Samples.

Sample ID	Run No.	Sample Date	$CaCO_3$ Wt %	CaS Wt %	CaO Wt %	Non-Carbonate Carbon Wt %	Inerts (Ash/Sand) Wt %	Loss on Ignition Wt %
In-Situ Samples - PRB Coal - Air-Blown								
AB20406	1	11/09/05	3.57	0.20	14.00	20.72	61.51	22.44
AB20407	2	11/10/05	3.84	0.27	13.01	28.28	54.61	30.88
AB20408	3	11/11/05	3.27	0.33	13.49	25.69	57.22	28.30
AB20409	4	11/14/05	3.98	0.38	12.38	29.91	53.35	32.57
AB20410	5	11/15/05	4.73	0.67	10.15	39.58	44.87	41.58
AB20411	6	11/16/05	3.64	0.20	12.55	25.89	57.72	28.02
AB20412	7	11/17/05	3.98	0.42	12.78	28.24	54.57	30.66
AB20413	8	11/18/05	3.93	0.29	13.94	23.03	58.81	25.14
AB20414	9	11/21/05	5.20	0.54	9.94	36.74	47.59	40.48
AB20415	10	11/28/05	3.07	0.22	16.80	17.12	62.78	18.59
AB20416	11	11/29/05	4.14	0.47	13.05	27.16	55.18	29.85
Composite Hopper Samples Used for Lab Drag Measurements								
AB19680	Low Carbon	11/10/05	3.77	0.20	12.83	24.26	58.94	26.48
AB20136	High Carbon	11/21/05	4.14	0.69	10.84	37.78	46.55	40.63

Table 4-5. Physical Properties of Residual Dustcake.

Sample ID	Sample Date	Bulk Density g/cc	True Density g/cc	Uncompacted Bulk Porosity %	Specific Surface Area m^2/g	Mass-Median Diameter mm	Loss on Ignition Wt %
TC19 Bulk Dustcake from Top Plenum							
AB20430	12/06/05	0.36	2.45	85.3	67	4.1	25.6
TC19 Bulk Dustcake from Bottom Plenum							
AB20431	12/06/05	0.35	2.49	85.9	68	5.1	25.0

Table 4-6. Chemical Composition of Residual Dustcake.

Sample ID	Sample Date	$CaCO_3$ Wt %	CaS Wt %	CaO Wt %	Non-Carbonate Carbon Wt %	Inerts (Ash/Sand) Wt %	Loss on Ignition Wt %
TC19 Bulk Dustcake from Top Plenum							
AB20430	12/6/05	3.68	1.60	14.55	22.87	57.29	25.56
TC19 Bulk Dustcake from Bottom Plenum							
AB20431	12/6/05	3.61	1.47	14.19	22.02	58.71	24.95

Table 4-7. Transient Drag Determined from PCD Pressure Drop and from Lab Measurements.

Run No.	ΔP/Δt, inwc/min	Δ(AL)/Δt, lb/ft^2/min	FV, ft/min	MMD, µm	NCC, %	Drag, inwc/(lb/ft^2)/(ft/min)			
						PCD	PCD@RT	Lab(1)	Lab(2)
1	1.64	0.017	3.33	16.7	20.7	95	56	90	66
2	1.17	0.018	3.42	15.0	28.3	67	40	102	78
3	2.38	0.019	3.51	19.7	25.7	126	74	86	63
4	3.10	0.025	3.86	17.3	29.9	124	73	96	73
5	3.43	0.029	3.98	20.6	39.6	120	71	95	74
6	3.62	0.025	4.17	16.0	25.9	143	85	97	72
7	2.27	0.022	3.53	15.1	28.2	105	62	102	78
8	2.06	0.018	3.61	13.7	23.0	115	68	103	77
9	2.76	0.027	3.38	20.0	36.7	103	62	94	73
10	1.73	0.016	3.31	13.6	17.1	108	64	98	71
11	2.14	0.024	3.57	18.3	27.2	89	53	91	68
Avg	2.39	0.022	3.61	16.9	27.5	109	64	96	72

Note 1. Lab drag data calculated from linear regression to MMD of lab drag sample and NCC of bulk sample
Note 2. Lab drag data calculated from linear regression to MMD and NCC of lab drag samples.

Nomenclature:

ΔP/Δt = rate of pressure drop rise during particulate sampling run, inH_2O/min.
Δ(AL)/Δt = rate of increase in areal loading during sampling run, lb/min/ft^2.
FV = average PCD face velocity during particulate sampling run, ft/min.
MMD = mass median diameter of in-situ particulate sample, µm.
NCC = non-carbonate carbon.
RT = room temperature, 77°F (25°C).

Table 4-8. Comparison of Average Drag Values Determined from PCD Pressure Drop and from Lab Measurements.

Run	Coal	Average Transient Drag Determined from PCD Performance, inwc/(lb/ft^2)/(ft/min)	Average Drag Determined from RAPTOR Lab Measurements, inwc/(lb/ft^2)/(ft/min)	Difference from Mean Value*, %
GCT2	PRB	29.3	20.9	-33.5
GCT3	PRB	80.2	92.7	14.5
GCT4	PRB	66.4	57	-15.2
TC06	PRB	89.4	81.2	-9.6
TC07	PRB	47.7	49.8	4.3
TC08	PRB	46.5	50	7.3
TC09	Hiawatha	29.0	23.3	-21.8
TC10	PRB	44.7	57.6	25.2
TC11	Falkirk Lignite	16.1	35.9	76.2
TC12	PRB	58.0	60.8	4.7
TC13	Freedom Lignite	34.4	39.4	13.6
TC14	PRB	47.4	41.6	-13.0
TC15	PRB	54.6	76.4	33.3
TC16	PRB + Limestone	49.3	51.7	4.8
TC16	Lignite + Dolomite	25.8	41.7	47.1
TC17	IL Basin	24.8	18.7	-27.8
TC18	PRB	59.0	82.0	32.6
TC19**	PRB	64.0	72.0	11.8
Average		48.1	52.9	8.6

* D = (R1-R2)/(R1+R2)/2*100
** Technique modified to use carbon content of lab drag sample

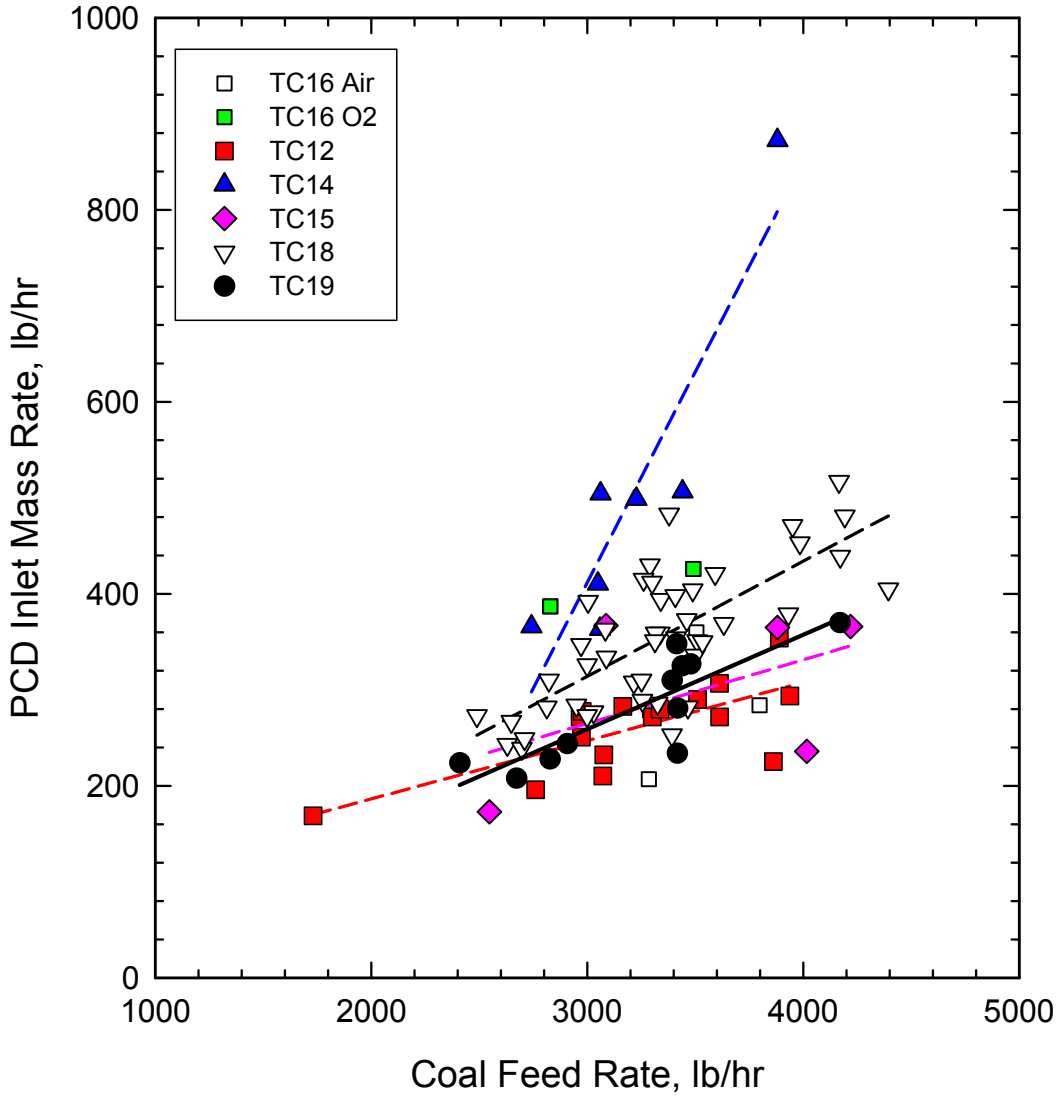

Figure 4-1. PCD Inlet Particulate Concentration as a Function of Coal Feed Rate.

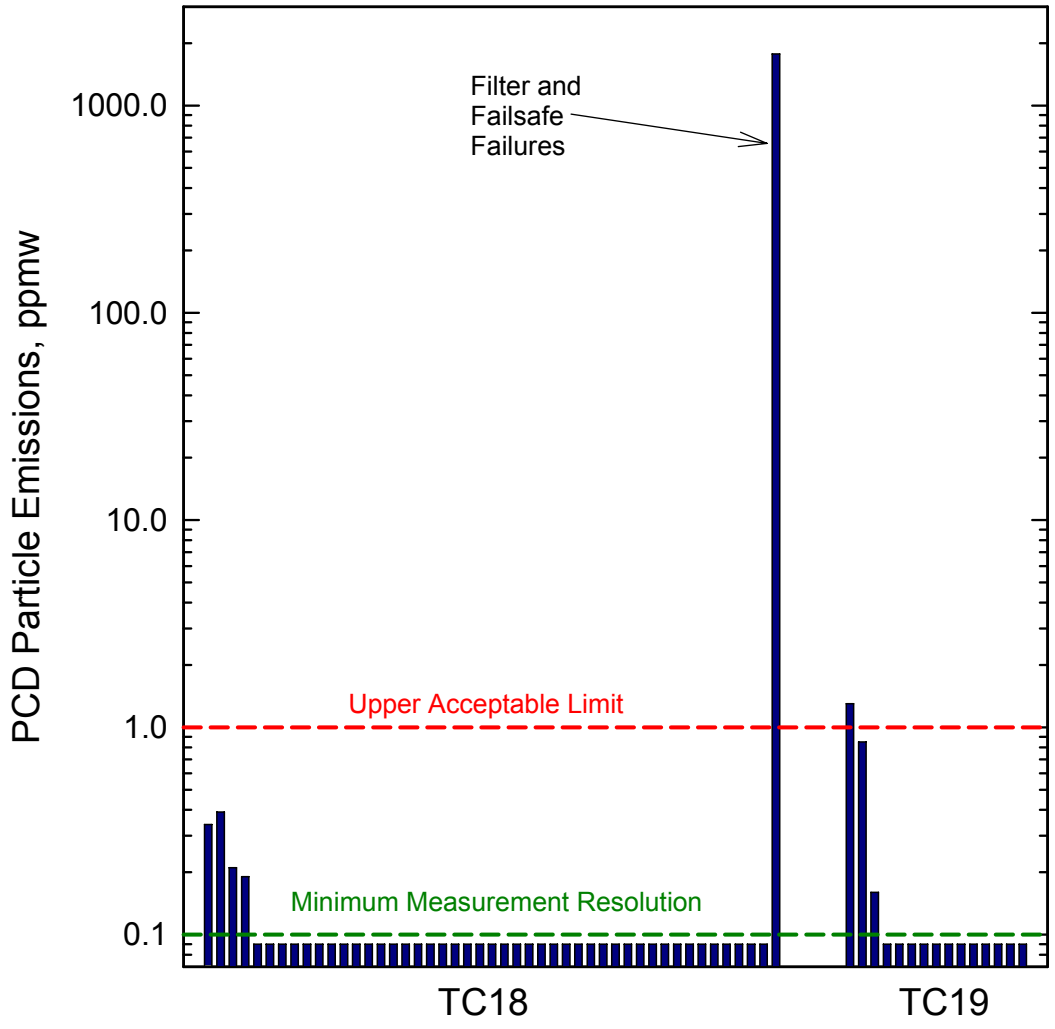

Figure 4-2. PCD Outlet Particulate Concentrations for TC18 and TC19.

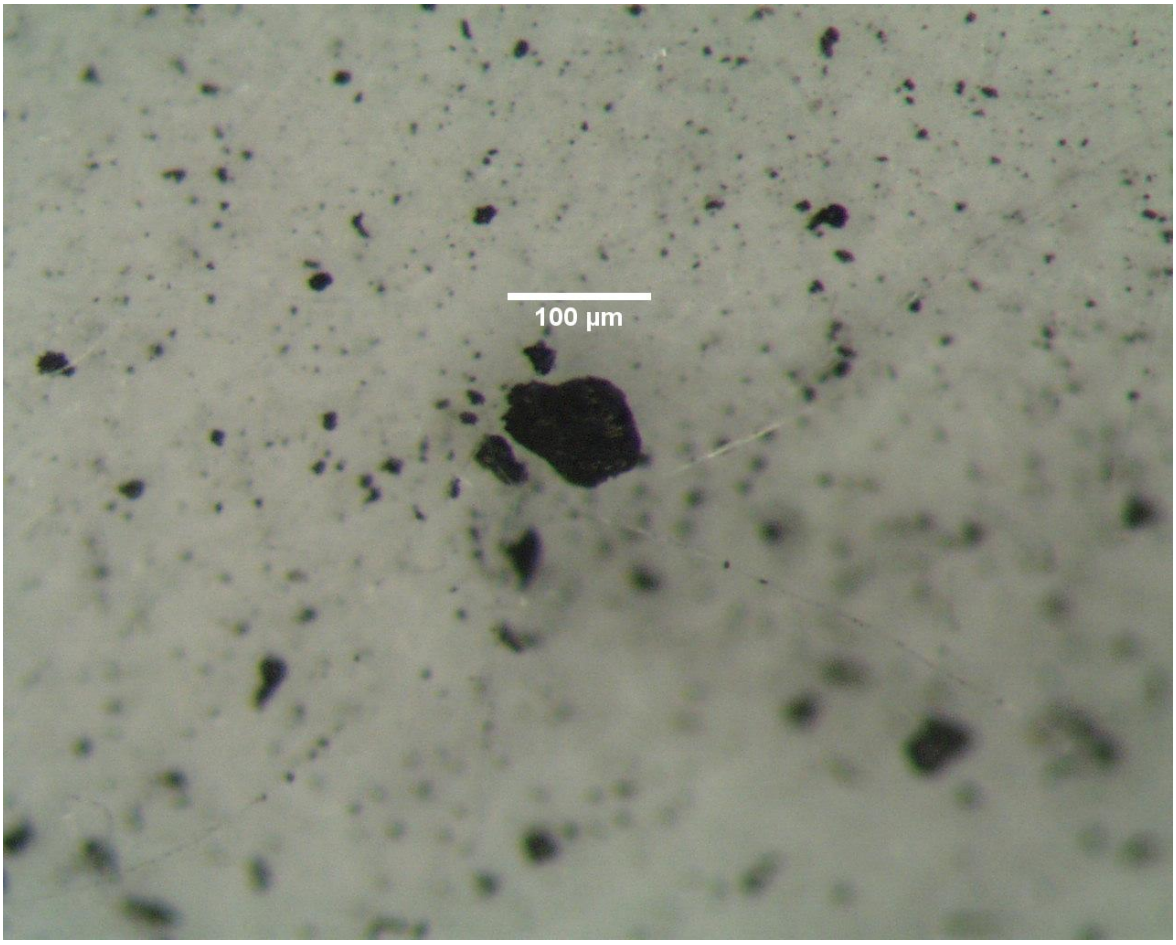

Figure 4-3. Photomicrograph of Particles on PCD Outlet Filter Number 5.

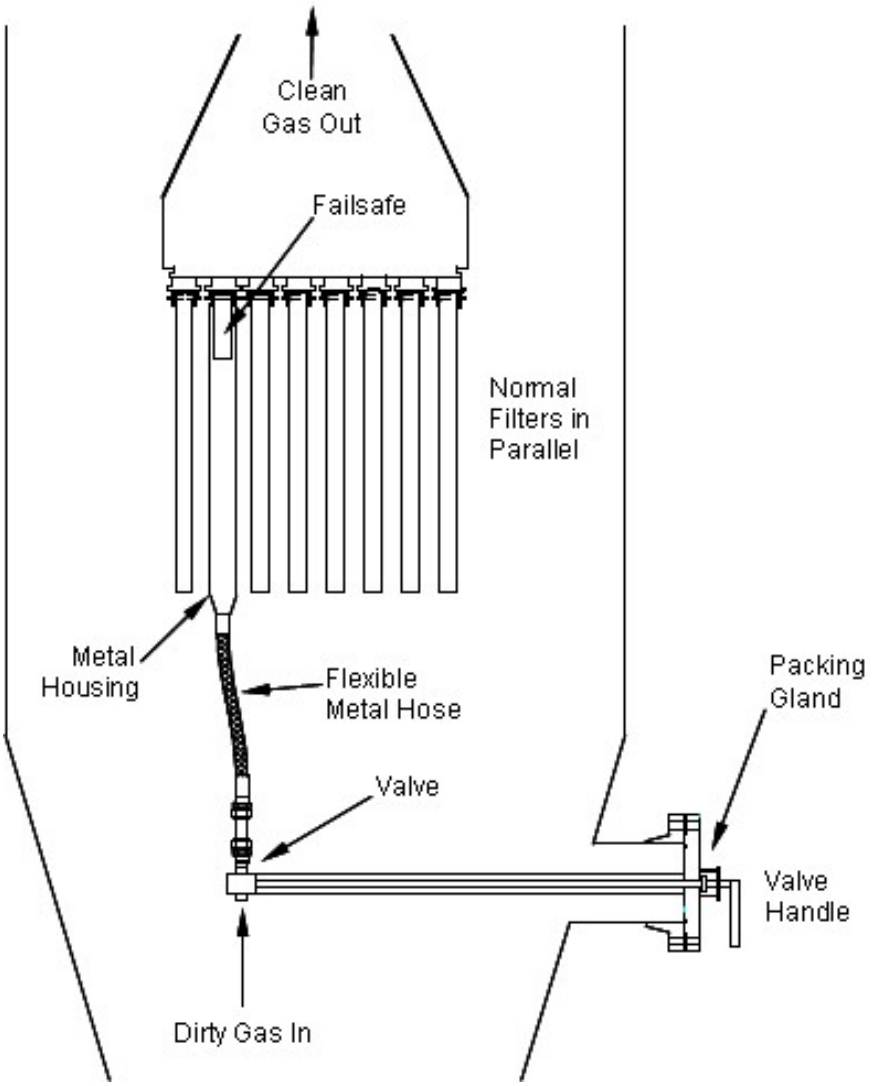

Figure 4-4. Valve-Activated Failsafe Tester.

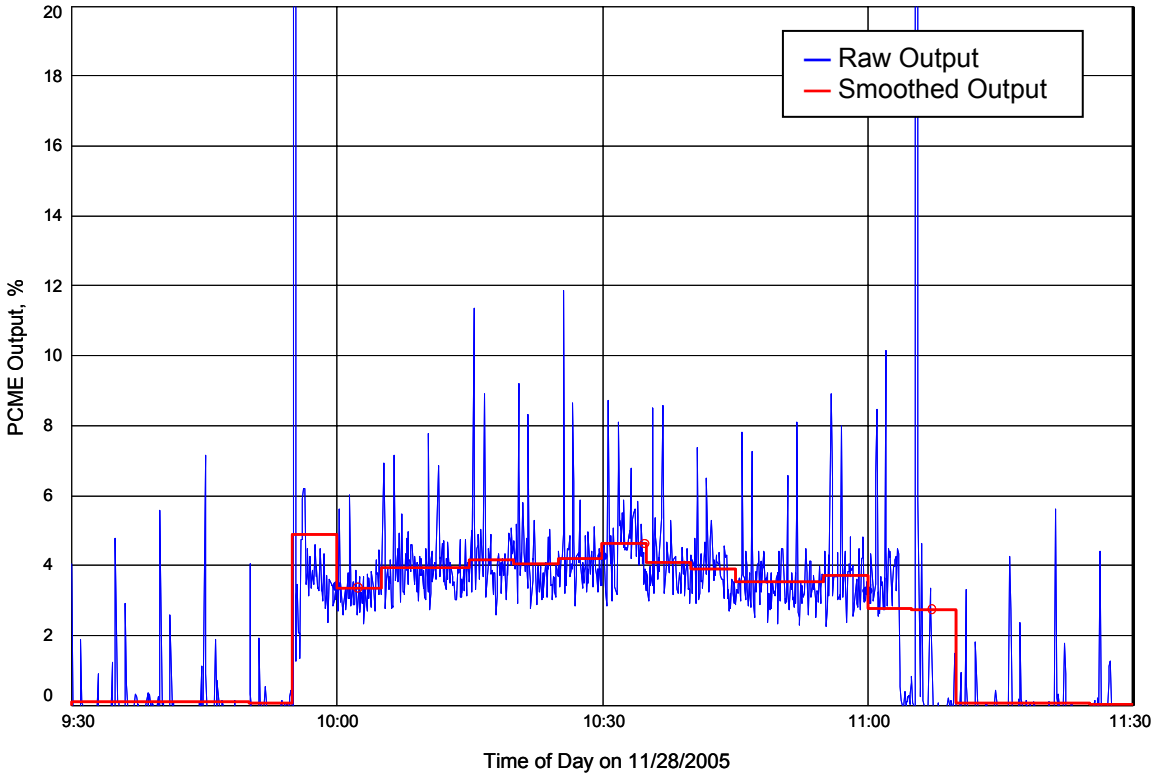

Figure 4-5. PCME Particulate Monitor Response to Dust Injection.

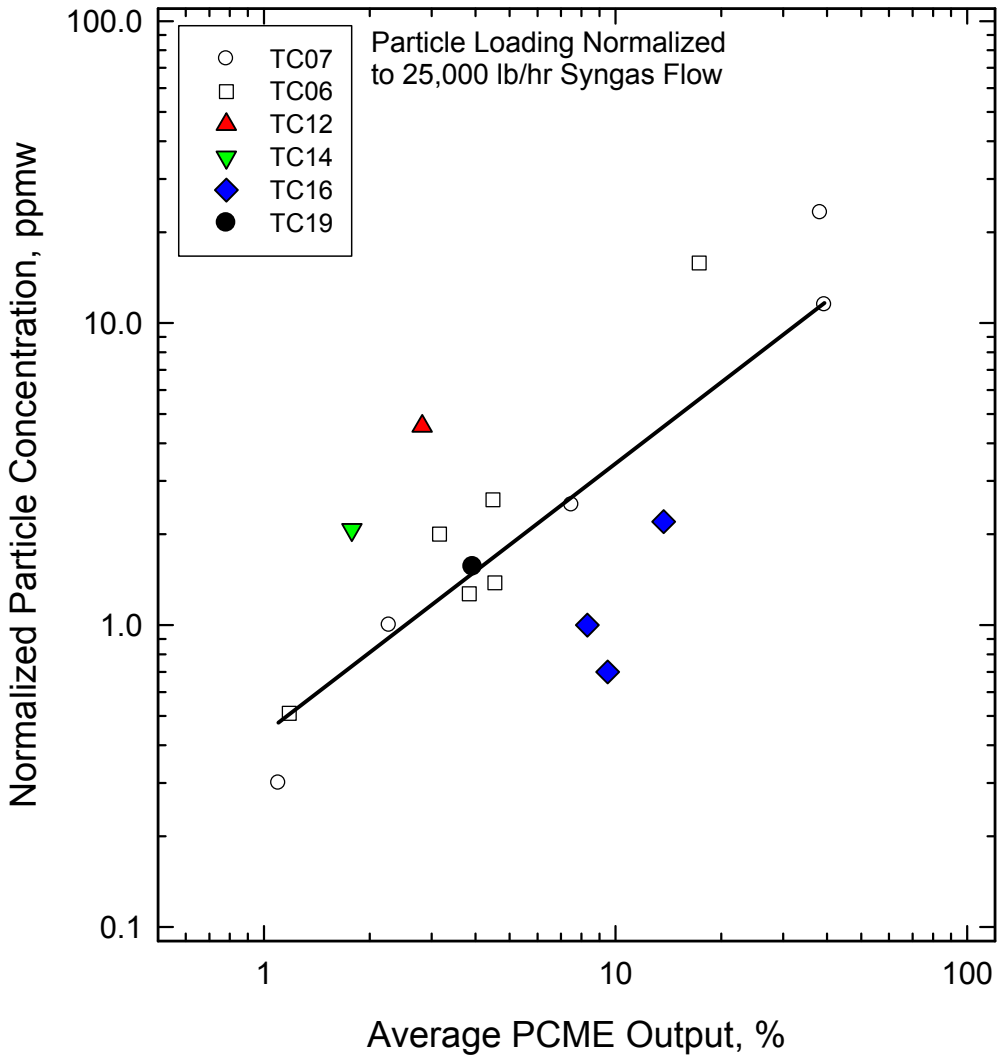

Figure 4-6. PCME Response to Dust Injection for Several Test Campaigns.

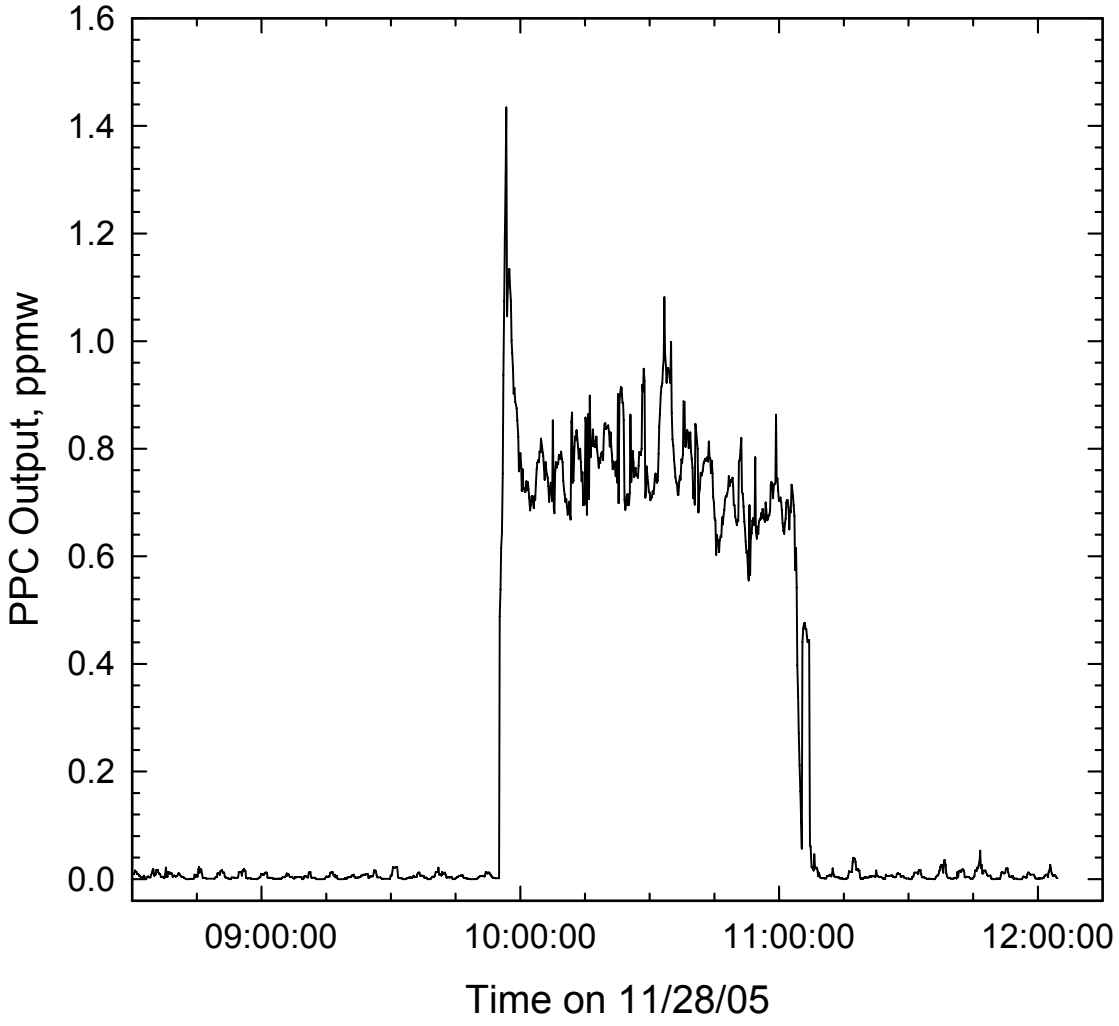

Figure 4-7. PPC Particulate Monitor Response to Dust Injection.

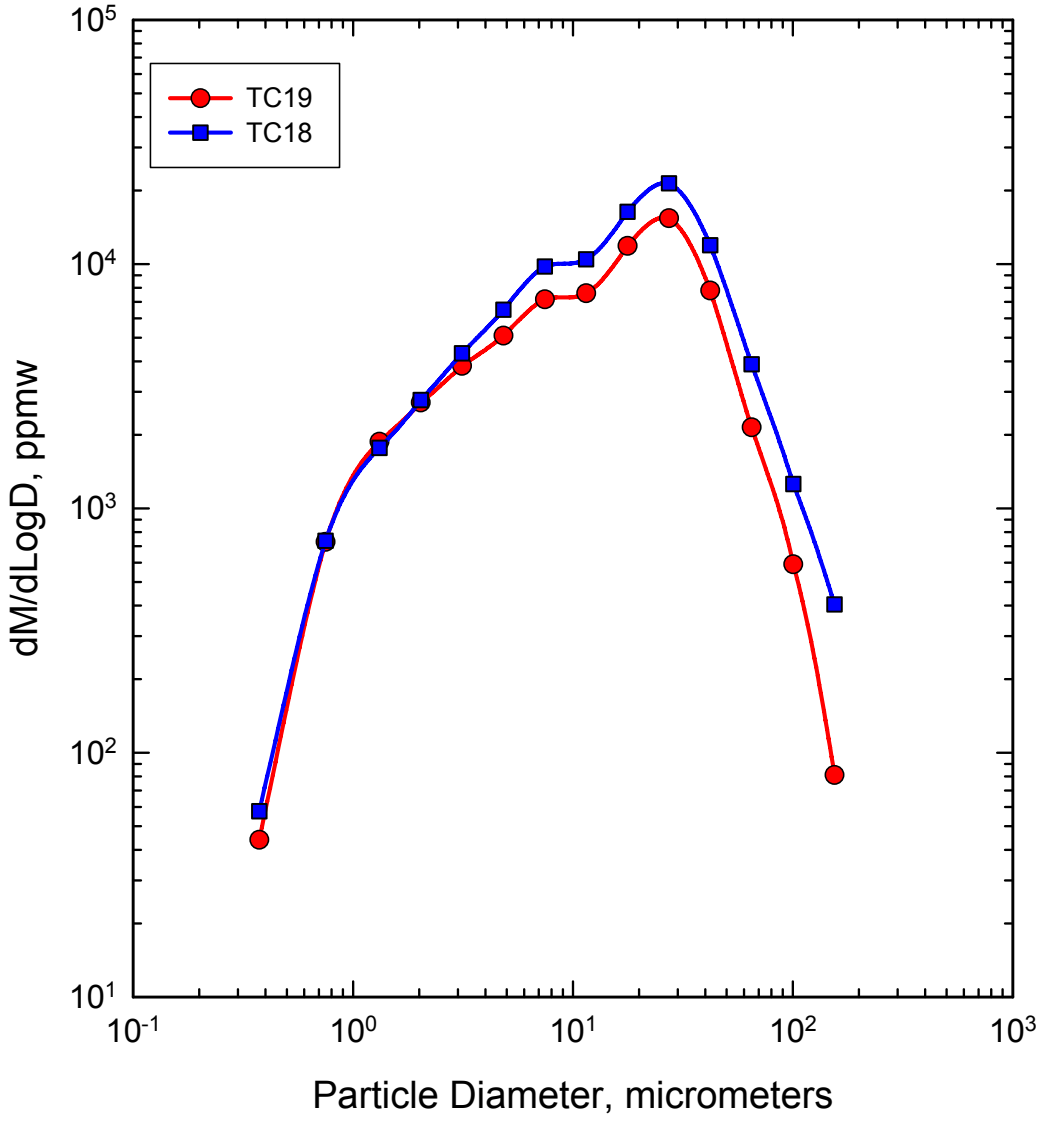

Figure 4-8. Comparison of Particle Size Distributions from In-Situ Samples.

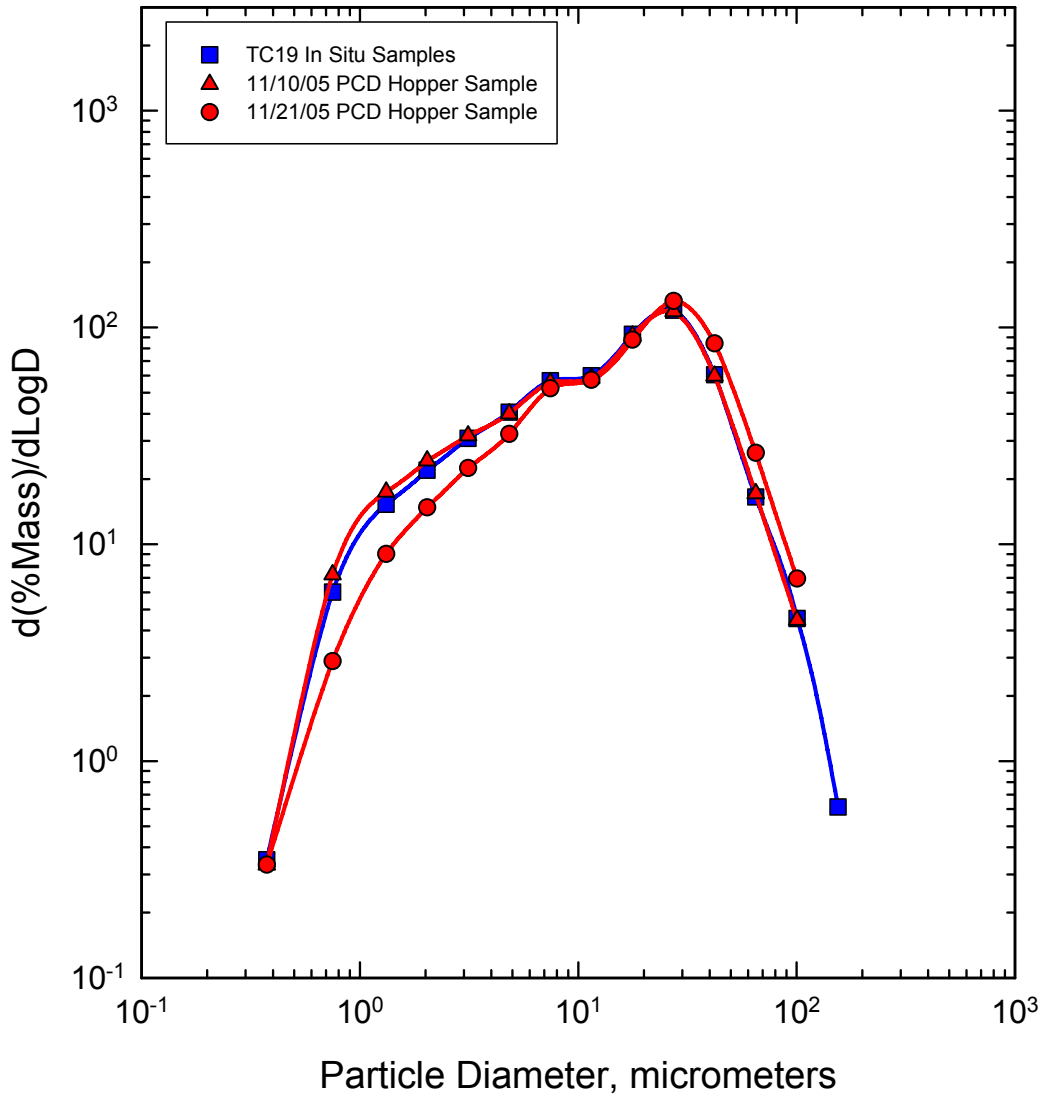

Figure 4-9. Comparison of Particle Size Distributions for In-Situ and Hopper Samples.

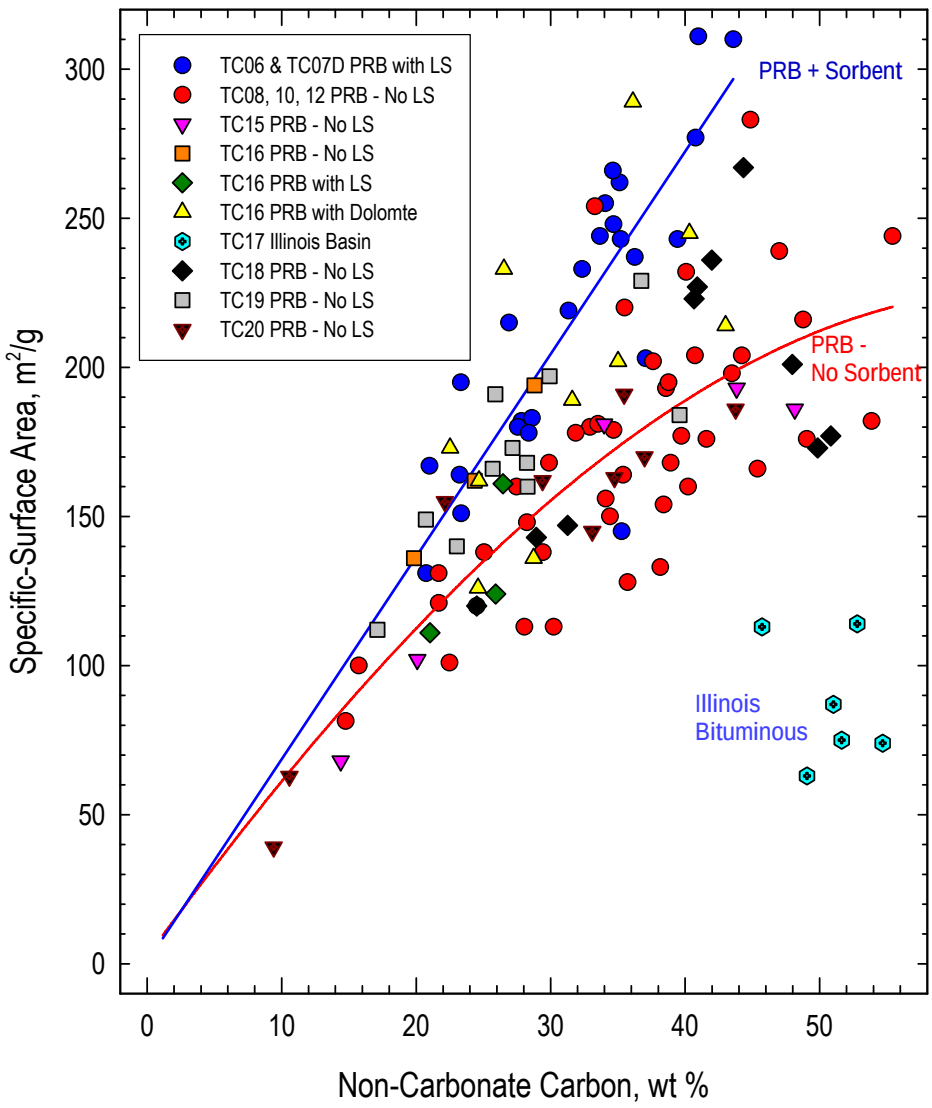

Figure 4-10. Effect of Non-Carbonate Carbon Content on Specific Surface Area.

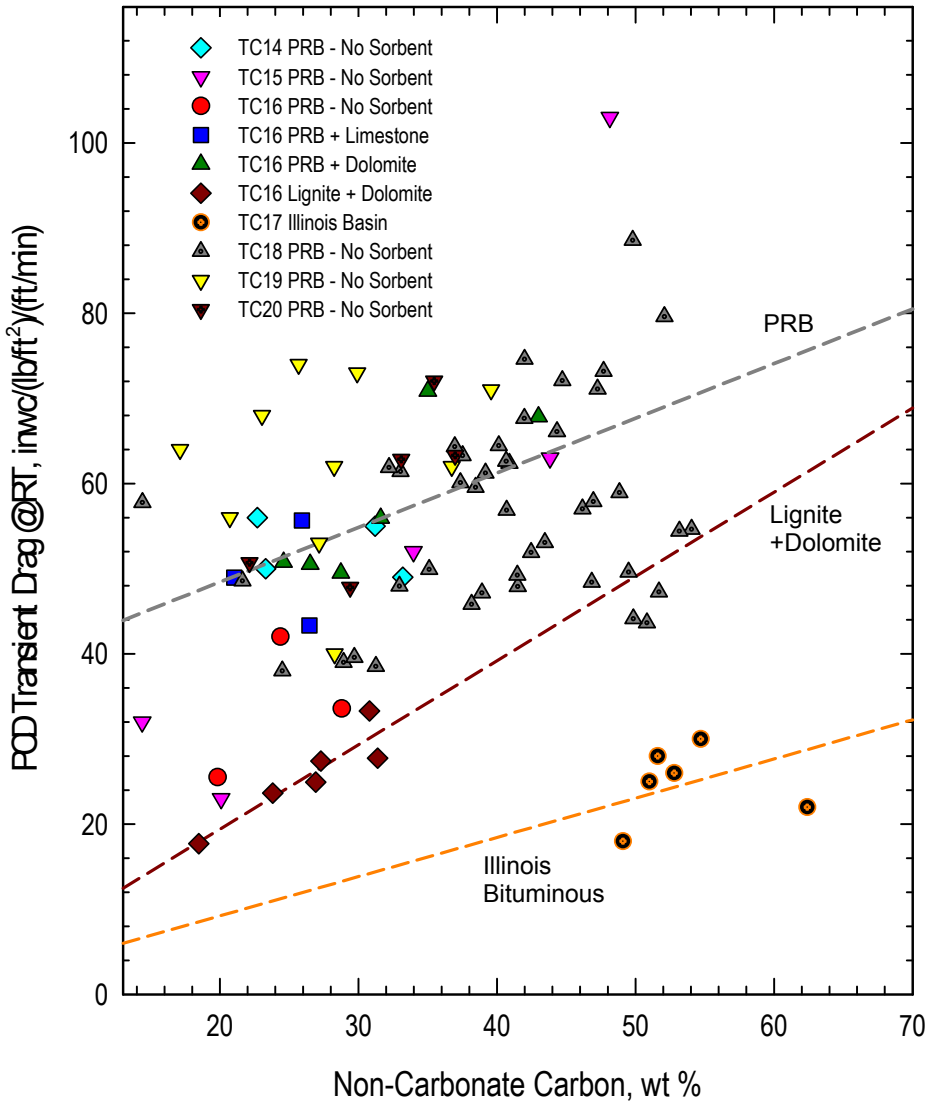

Figure 4-11. PCD Transient Drag Versus Carbon Content of In-Situ Samples.

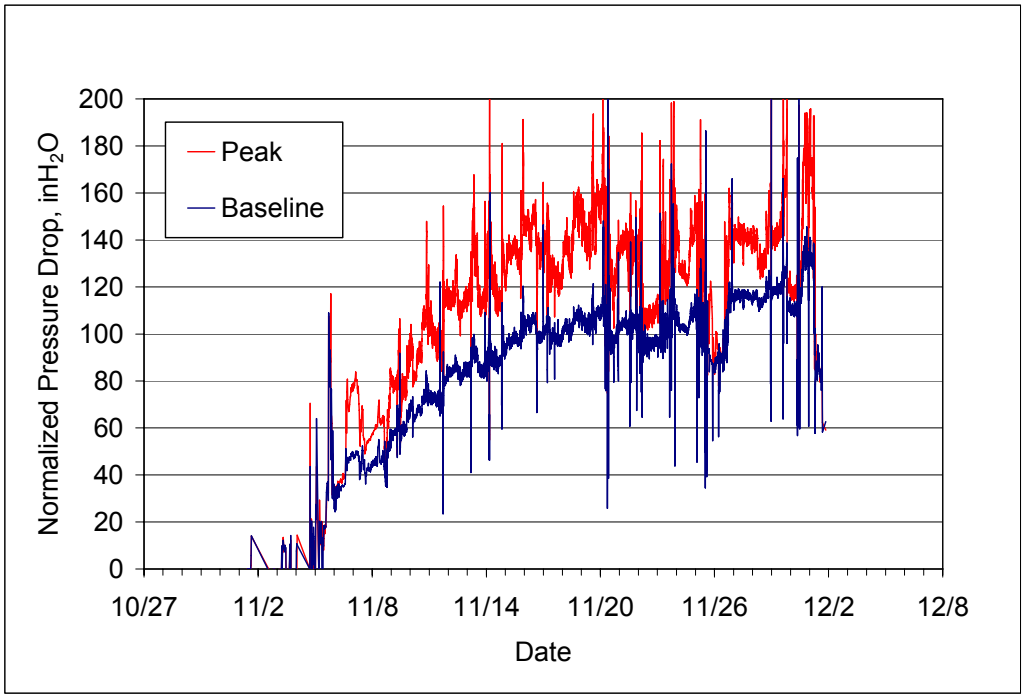

Figure 4-12. Normalized PCD Pressure Drop.

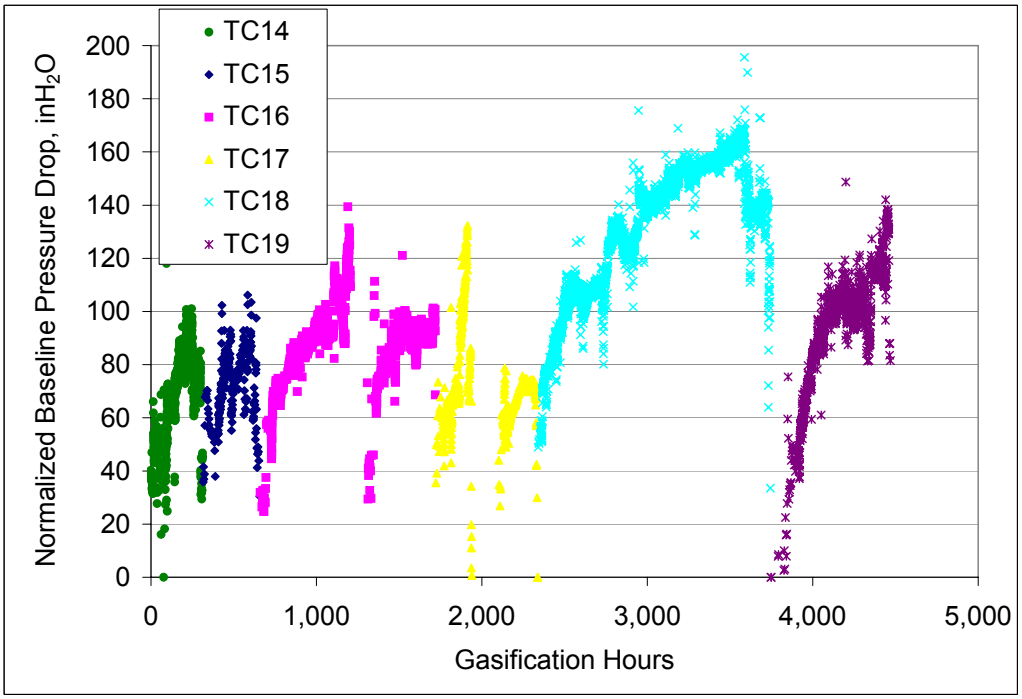

Figure 4-13. Comparison of Normalized PCD Pressure Drop from TC14 to TC19.

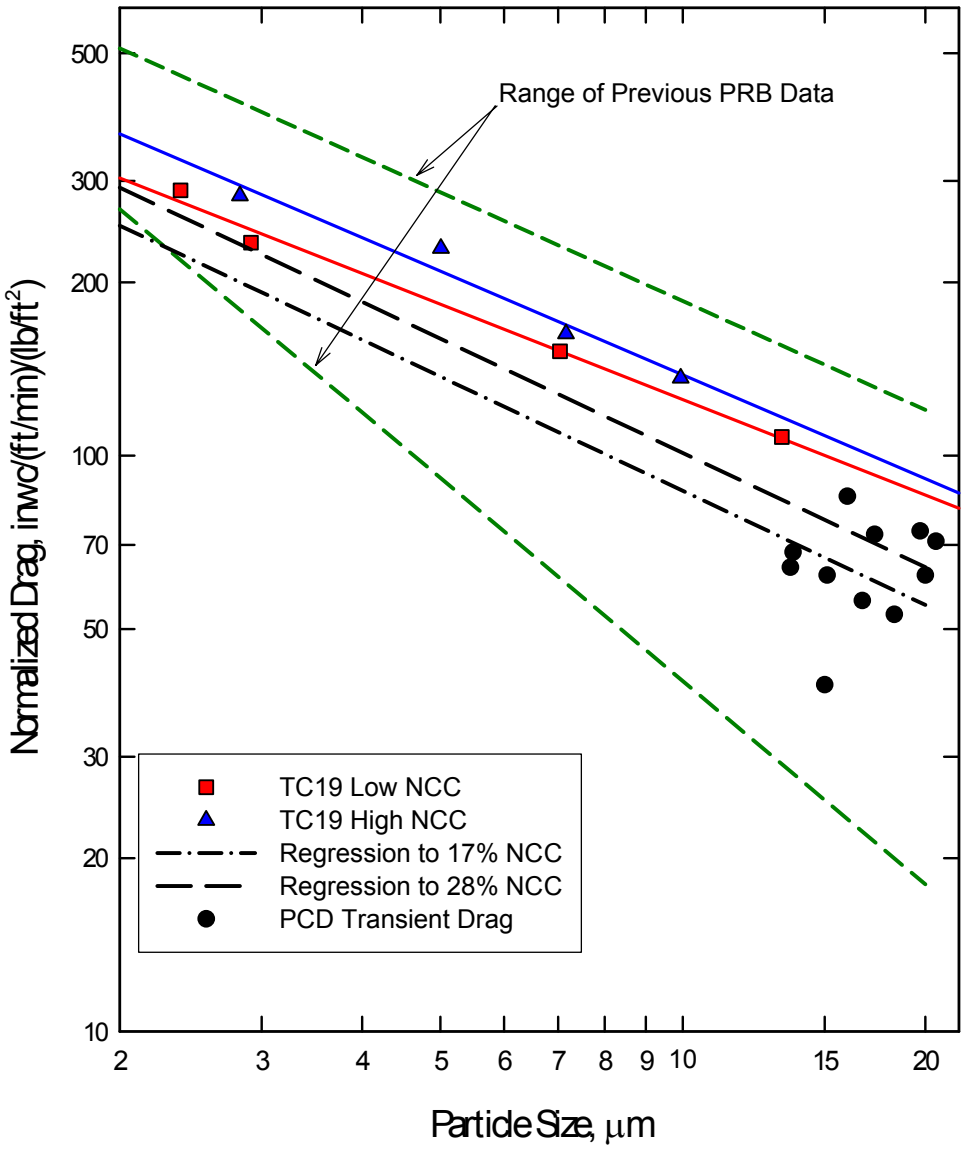

Figure 4-14. Lab-Measured Drag as a Function of Particle Size.

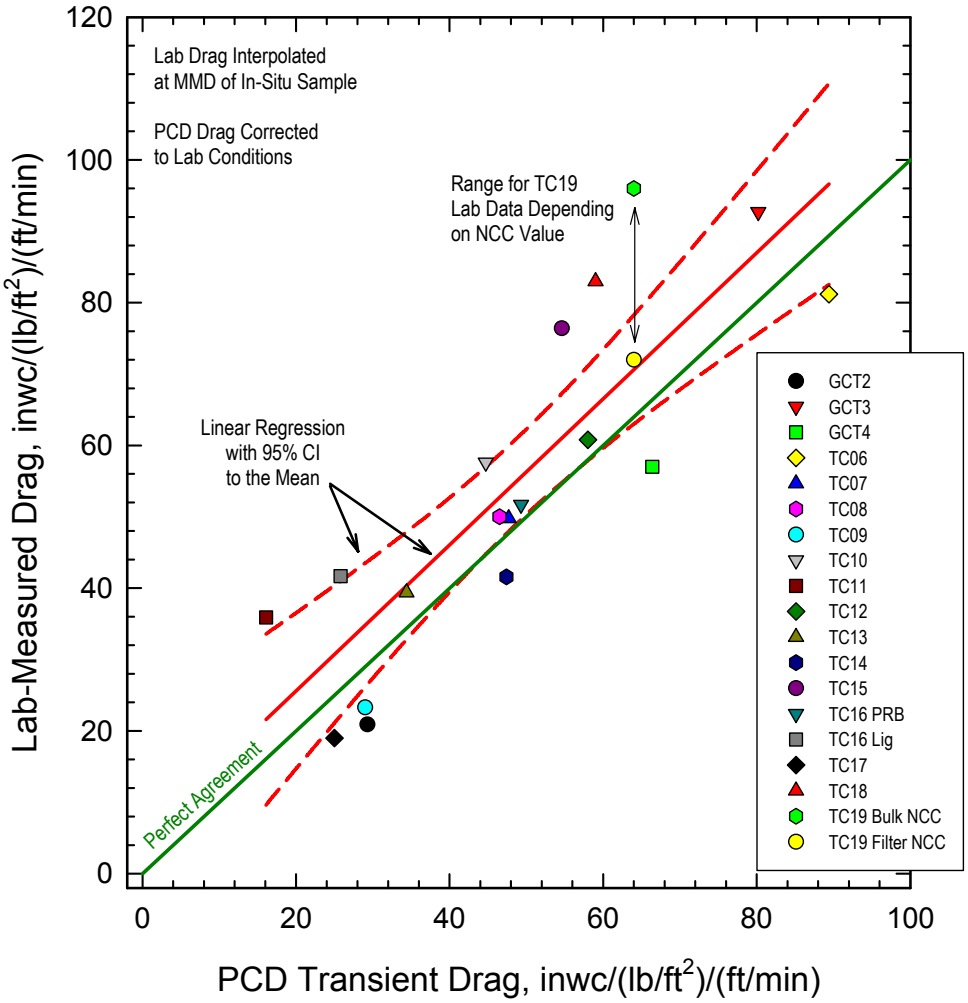

Figure 4-15. Comparison of PCD Transient Drag with Lab Measurements.

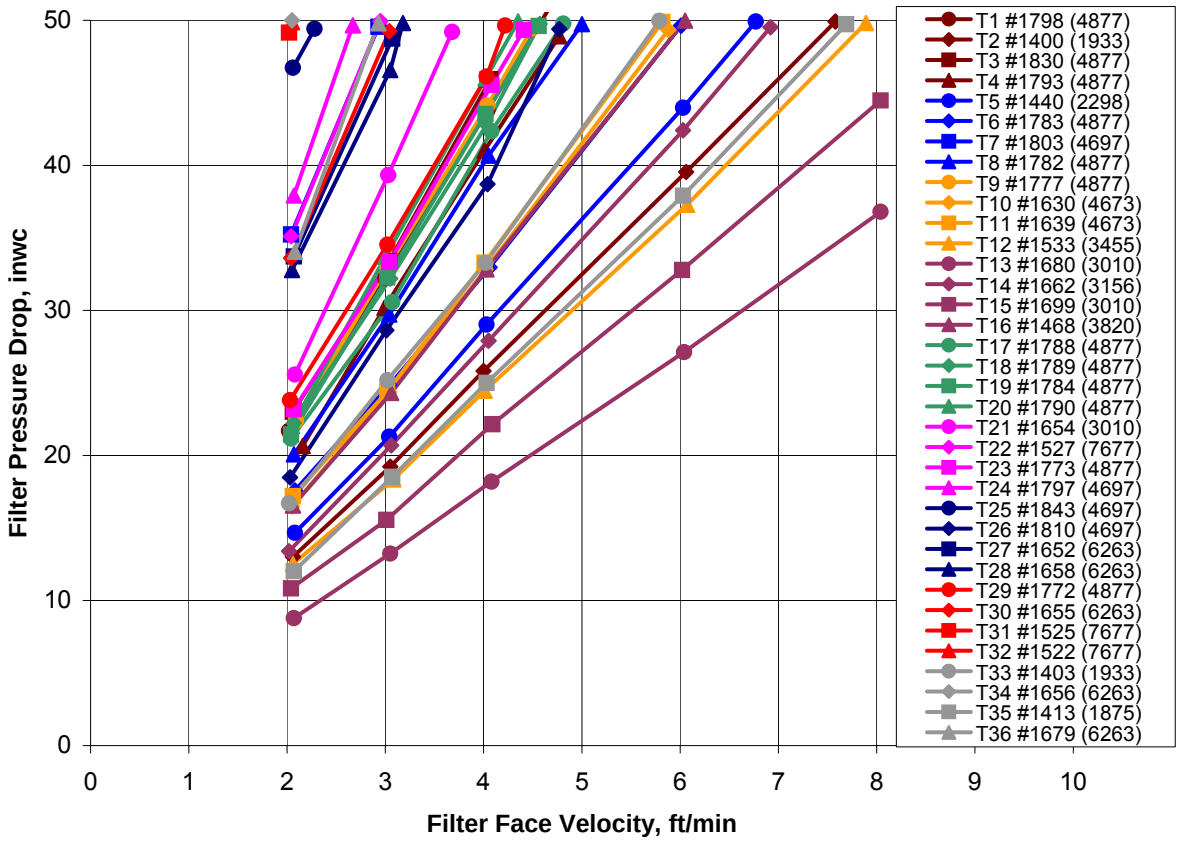

Figure 4-16. Pressure Drop Versus Face Velocity of Top Plenum Filter Elements before Cleaning.

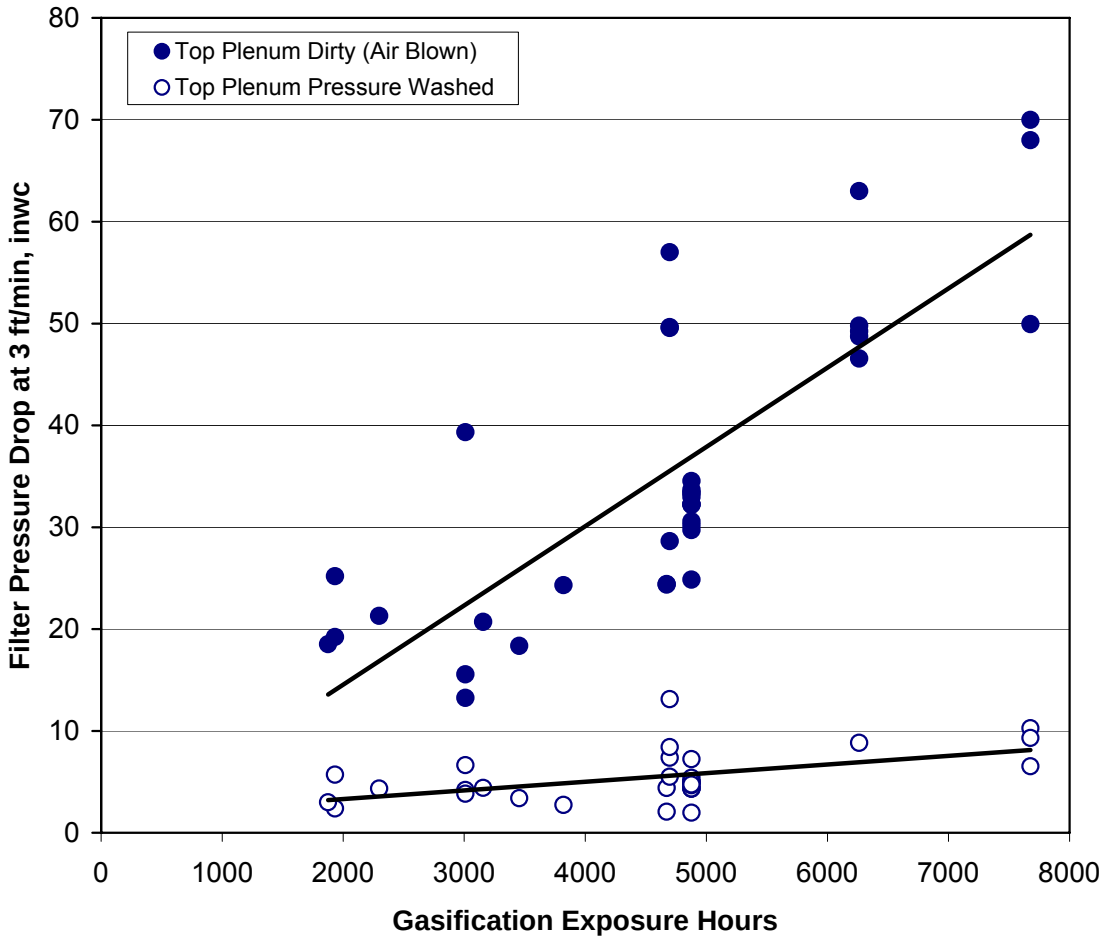

Figure 4-17. Pressure Drop versus Exposure Hours of Top Plenum Filter Elements Before and After Cleaning.

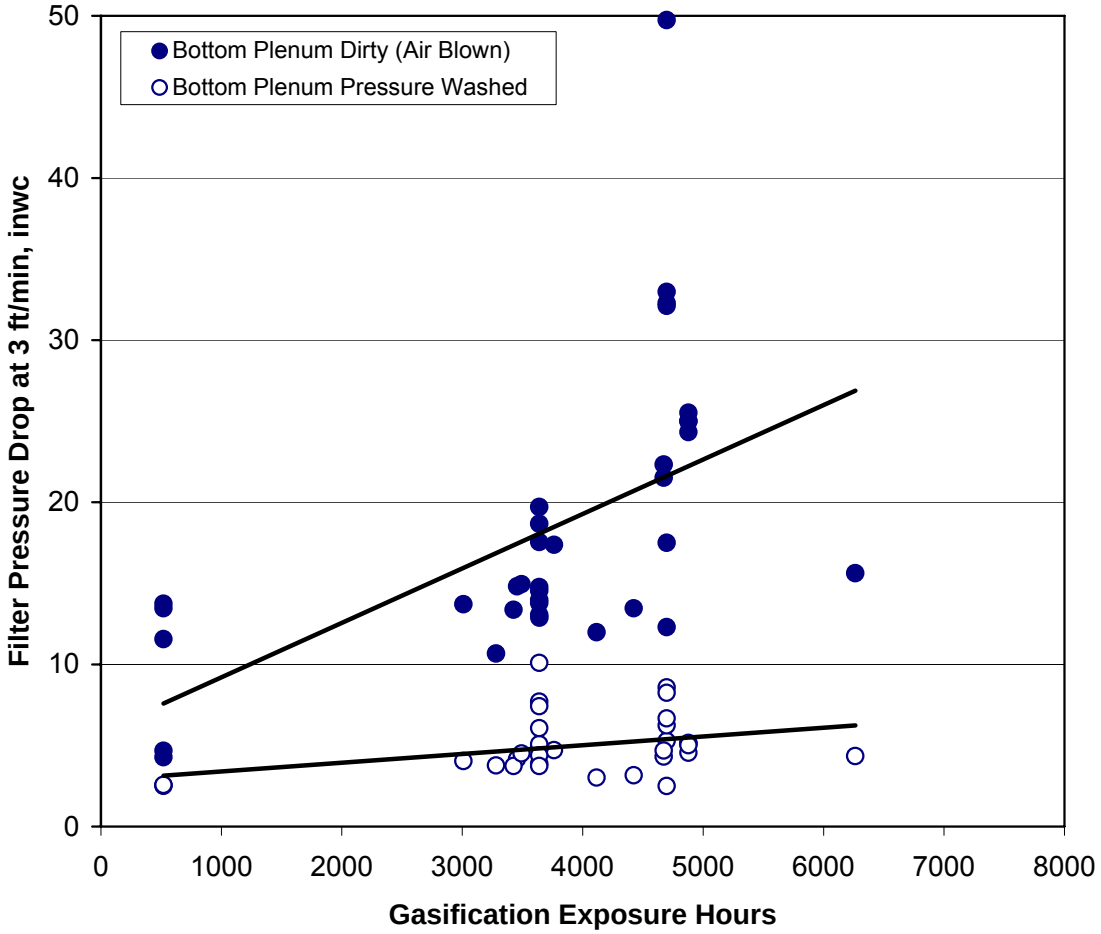

Figure 4-18. Pressure Drop versus Exposure Hours of Bottom Plenum Filter Elements Before and After Cleaning.

Figure 4-19. Photograph of Filter Elements from TC19 Arranged by Age.

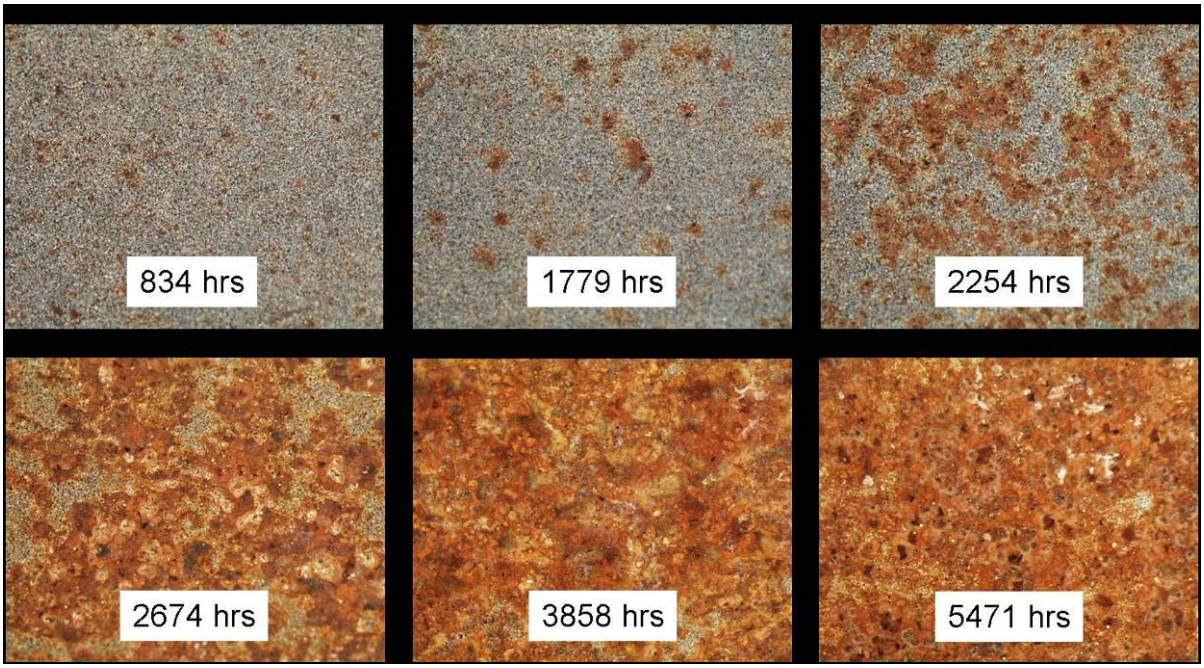

Figure 4-20. Photograph of Iron Aluminide Filter Media Showing Corrosion Progression with Age.

5.0 ADVANCED SYNGAS CLEANUP

5.1 Desulfurization and COS Hydrolysis

Hot syngas desulfurization tests were continued using Sud-Chemie RVS-1 sorbent, which was developed by the DOE's National Energy Technology Laboratory. The RVS-1 sorbent tests were started during TC18 and sorbent was exposed for 76 hours before the test campaign ended. The sorbent was left in the vessel during the outage, and tests continued in TC19. The test lasted for 145 hours until exit sulfur breakthrough (above 50 ppm) was observed. After completing RVS-1 sorbent tests, desulfurization tests with RVSLT-1 sorbent were begun.

Syngas COS hydrolysis tests were also conducted in the hot gas cleanup unit with Sud-Chemie COS hydrolysis catalyst, C53-2-01. Testing was conducted at temperatures between 400 and 500°F and pressures ranging from 170 to 200 psig. The tests lasted for 250 hours, and the COS concentrations at the reactor outlet were near equilibrium.

Table 5-1 shows the nominal sorbent and catalyst properties and operating parameters during desulfurization and COS hydrolysis testing. These tests were conducted in stainless steel vessels with five-inch inner diameters and heights of five feet.

5.2 Ammonia Cracking and Hydrocarbon Reforming

Syngas ammonia cracking and hydrocarbon reforming tests were conducted with a Sud-Chemie nickel-based catalyst at 1,700^{o}F and low pressures. The reactor used for this testing was a two-inch inner diameter, four feet tall vessel. The tests lasted for over 300 hours, and the ammonia concentration was reduced from about 2,250 ppm to less than 10 ppm. Benzene concentrations were reduced from about 800 ppm to about 20 ppm. Other hydrocarbon concentrations measured included ethylene, phenanthrene, and naphthalene, which were typically reduced by 99 percent or more, and acenaphthene, which was reduced by about 89 percent. The nominal catalyst properties and operating parameters are given in Table 5-2.

Table 5-1. Nominal Properties of Sulfur Sorbents and COS Hydrolysis Catalyst and Operating Parameters.

Sorbent/Catalyst	RVS-1	RVSLT-1	C53-2-01
Chemical Composition, weight percent			
Zinc Oxide	40 – 60	50 – 70	----
Calcium Sulfate	15 – 25	15 – 30	----
Calcium Oxide	5 – 10	5 –15	----
Nickel Oxide	5 –15		----
Bentonite	5 –15	5 – 15	----
Silica, Quartz	<5	<5	----
Platinum	----	----	0.08
Physical Properties			
Shape	Spheres	Spheres	Extrusion
Size, mm	3 – 4	3 – 4	3.175
Density, lb/ft^3	60 – 85	60 – 85	30
Bed Mass, lb	16	16	6.5
Bed Height, in	28	28	14.4
Syngas Flow Rate	30	30	30
Pressure, psig	200	180	180
Temperature, ^{o}F	635	570	415
Space Velocity, hr^{-1}	1,950	1,950	1,990
Inlet H_2S and COS, ppm	215	215	215
Inlet COS, ppm	15	15	15

Table 5-2. Nominal Properties of Ammonia Cracking and Hydrocarbon Reforming Catalyst and Operating Parameters.

Catalyst	G-31
Chemical Composition, weight percent	
Nickel Oxide	1 - 25
Aluminum Oxide	75 - 99
Physical Properties	
Shape	Spheres
Size, mm	1
Density, lb/ft^3	90
Bed Mass, lb	0.5
Bed Height, in	4.5
Syngas Flow Rate, SCFH	15 – 20
Pressure, psig	2 – 10
Temperature, ^{o}F	1750
Space Velocity, hr^{-1}	1,950 – 2,600
Ammonia Inlet Concentration, ppm	2,250
Ammonia Outlet Concentration, ppm	5
Benzene Inlet Concentration, ppm	800
Benzene Outlet Concentration, ppm	20

6.0 CONCLUSIONS

During TC19, the PSDF gasifier train accumulated 518 hours of operation using PRB subbituminous coal in air-blown gasification. The major objectives of the test campaign were accomplished. Commissioning of the new CCAD system was completed, and it operated remarkably well in both cooling and depressurizing the gasifier solids. Operation of the new on-line particulate monitor, the Process Particle Counter, presented challenges, but was responsive to testing performed with dust injection. A new on-line PCD failsafe tester was commissioned and operated without problems.

Lessons Learned

The achievement of stable operation provided for testing of process additions and modifications and for quality data acquisition. Lessons learned from TC19 are listed below.

- Due to the numerous bends in the piping to the lower coal feed nozzle, flow could not be maintained. For future testing, coal flow path restrictions will be reduced and/or assisted by booster nitrogen.
- The use of reflux probes allowed syngas samples for gas analysis to be taken upstream of the PCD, improving the analyzer response time. This in turn allowed for quicker response to system upsets/changes.
- Following TC18, the automatic steam purge, which was designed to clean the recycle syngas piping in the event of a trip was temporarily disabled after inspections showed water accumulation in the piping. The inspections following TC19 showed that no tar or crystal accumulation had occurred in the recycle syngas piping despite not having the steam purge. Therefore, the decision was made to permanently disable the automatic steam purge following a trip.
- The regression analysis technique used to compare field and lab PCD dustcake data was modified for TC19, producing much better predictions of pressure drop from dust characteristics. The new analysis technique allowed for accounting of particle size as well as carbon content in predicting dustcake drag.
- The valve-activated failsafe tester proved to be the simplest, most reliable failsafe tester used to date for on-line testing in the PCD. Exposure to unfiltered syngas and thermal cycles did not degrade operation of the ball valve.
- Although failsafe testing with the iron aluminide fuse showed very good collection performance, these failsafe devices have continued to break unexpectedly, not only during installation and removal, but also during operation. Therefore, a more robust failsafe is needed.
- The most significant technical issues related to operation of the Process Particle Counter were condensation and contamination of optical windows with water and organic compounds from the syngas. Efforts will be made to increase the operating temperature to reduce the amount of condensation.
- Significant corrosion of the iron aluminide PCD filter elements was observed along with an increase of pressure drop across the elements with operation time.

More expanded testing of alternatives to the iron aluminide material is planned. Despite the apparent corrosion, the iron aluminide elements continued to demonstrate excellent collection performance.

- Commissioning of the CCAD ash removal system demonstrated the viability of the fundamental design concepts.
- The slip-stream unit proved to be a reliable source for various testing and allowed successful testing of desulfurization, COS hydrolysis, ammonia cracking, and hydrocarbon reforming technologies.

APPENDIX A OPERATING HISTORY

System commissioning of the KBR Transport Reactor train and the first five test campaigns (TCs) were performed in combustion mode. Approximately 5,000 hours of combustion operation were completed from 1996 to 1999. The system was transitioned to gasification operation in late 1999. Four gasification commissioning tests (GCTs), each lasting nominally 250 hours, were completed by early 2001. At the conclusion of TC19, 14 gasification test campaigns were completed, each nominally 250 to 1,500 hours in duration, for a total of about 8,280 hours of coal gasification operation. Powder River Basin subbituminous coal is the most extensively tested fuel, although several bituminous and lignite coals have also been tested. The Transport Gasifier has operated successfully in both air-blown and oxygen-blown modes.

Table A-1 summarizes the gasification testing completed at the conclusion of TC19. The table lists the duration, number of hours on coal, fuel type, and major objectives of each test. More information about the individual test campaigns may be found in the test campaign reports, located on the PSDF website, http://psdf.southernco.com.

Table A-1. Gasification Operating History.

Test	Start Date	Duration (hrs)	Type of Coal	Comments
GCT1	09/1999	233	PRB, Illinois #6, Alabama	First gasification testing
GCT2	04/2000	218	PRB	Stable operations
GCT3	02/2001	184	PRB	Loop seal commissioning
GCT4	03/2001	242	PRB	Final gasification commissioning test
TC06	07/2001	1,025	PRB	First long duration test campaign
TC07	04/2002	442	PRB, Alabama	Lower mixing zone commissioning
TC08	06/2002	365	PRB	First oxygen-blown testing First on-line failsafe testing
TC09	09/2002	309	Hiawatha	New mixing zone steam system
TC10	11/2002	416	PRB	Developmental coal feeder
TC11	04/2003	192	Falkirk Lignite	First lignite testing
TC12	05/2003	733	PRB	Fuel cell testing
TC13	09/2003	501	PRB, Freedom Lignite	Syngas to combustion turbine
TC14	02/2004	214	PRB	Syngas to combustion turbine CFAD commissioning
TC15	04/2004	200	PRB	Improved oxygen feed distribution
TC16	07/2004	835	PRB, Freedom Lignite	Fuel cell testing High pressure O_2-blown operation
TC17	10/2004	313	PRB, Illinois Basin	Bituminous coal testing
TC18	06/2005	1,342	PRB	Recycle gas compressor commissioning
TC19	11/2005	518	PRB	CCAD commissioning

*Note: PRB coal is subbituminous; Illinois #6, Alabama, Hiawatha, and Illinois Basin coals are bituminous coals.

APPENDIX B OPERATING TRENDS

Operating parameters for the major equipment of the gasification process as well as data from several on-line syngas analyzers are shown in Figures B-1 through B-13. These figures display the raw data collected from the Plant Information (PI) system. Initial system start-up began on November 5, CCAD commissioning began on November 6, and coal feed was first started on November 8, 2005. Coal feed was interrupted for a few hours on November 25 due to various problems with the coal feeders and was resumed on November 26, 2005. A planned shutdown was completed on December 1, 2005.

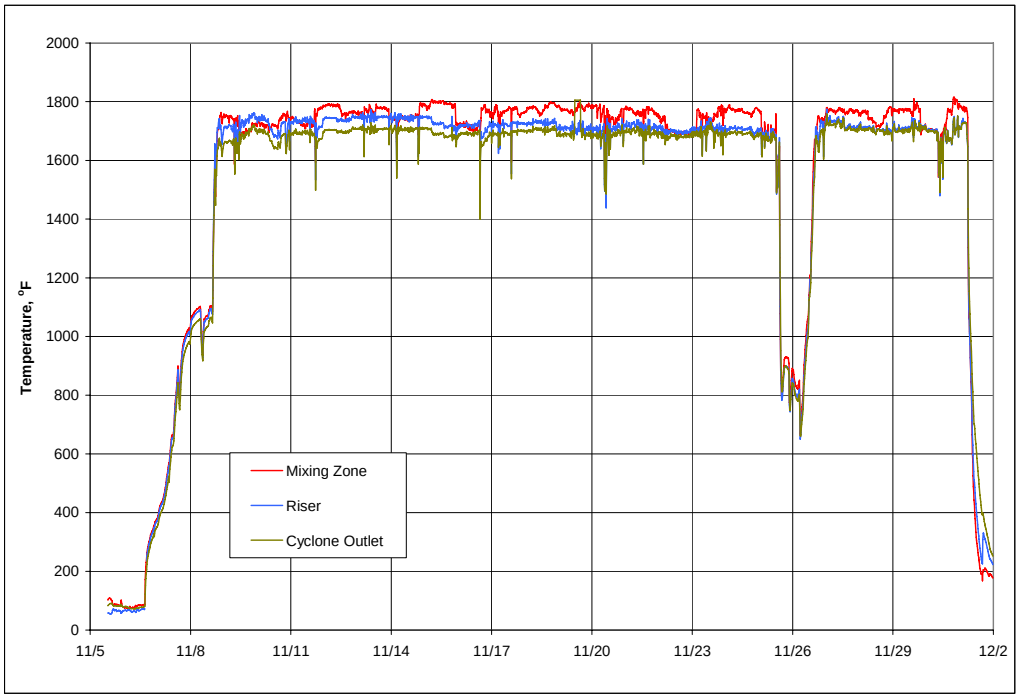

Figure B-1. Gasifier Mixing Zone, Riser, and Outlet Temperatures.

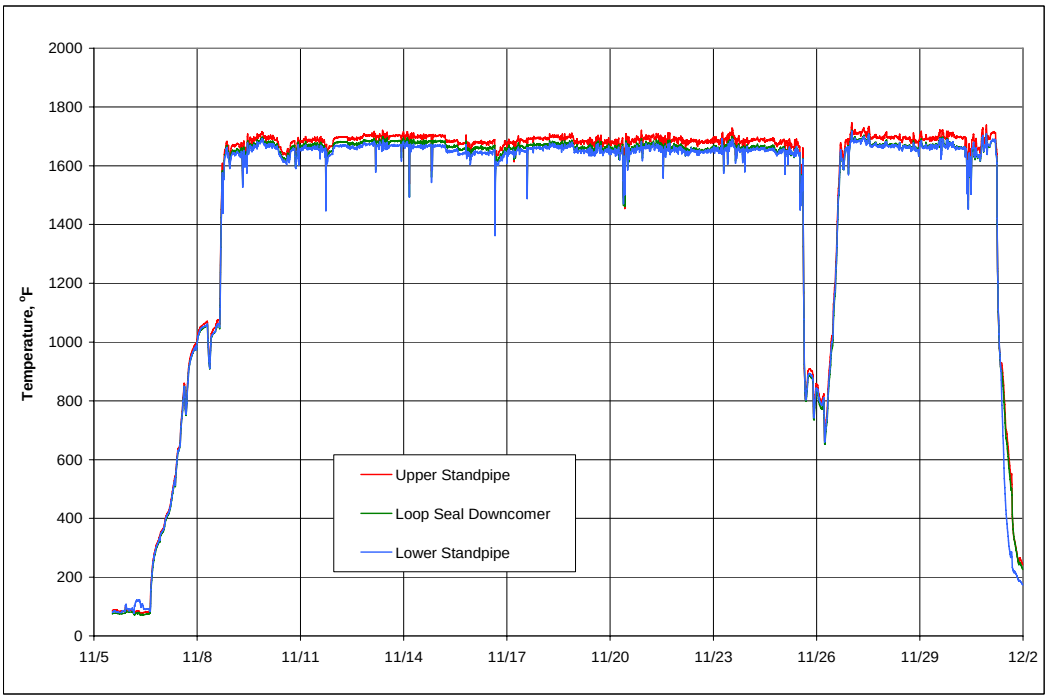

Figure B-2. Standpipe and Loop Seal Temperatures.

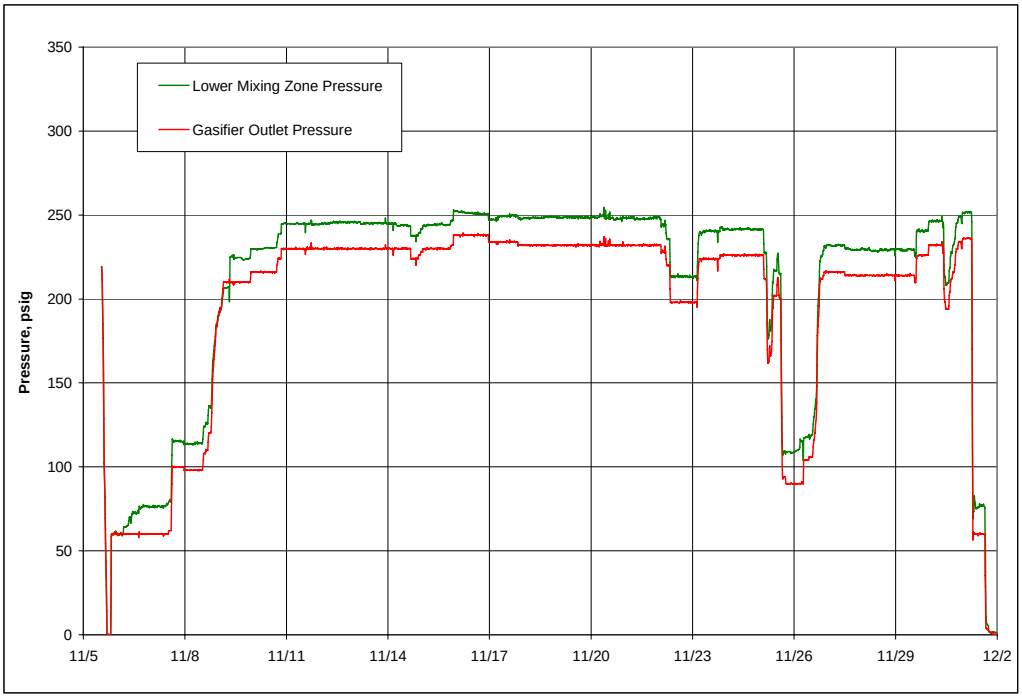

Figure B-3. Gasifier Pressures.

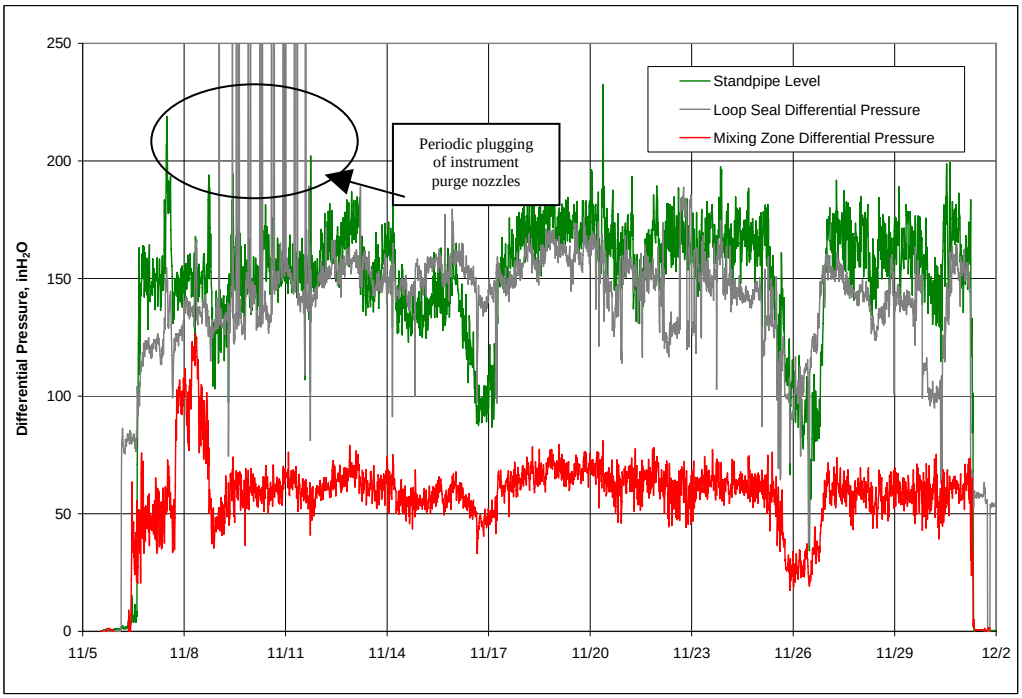

Figure B-4. Gasifier Differential Pressures.

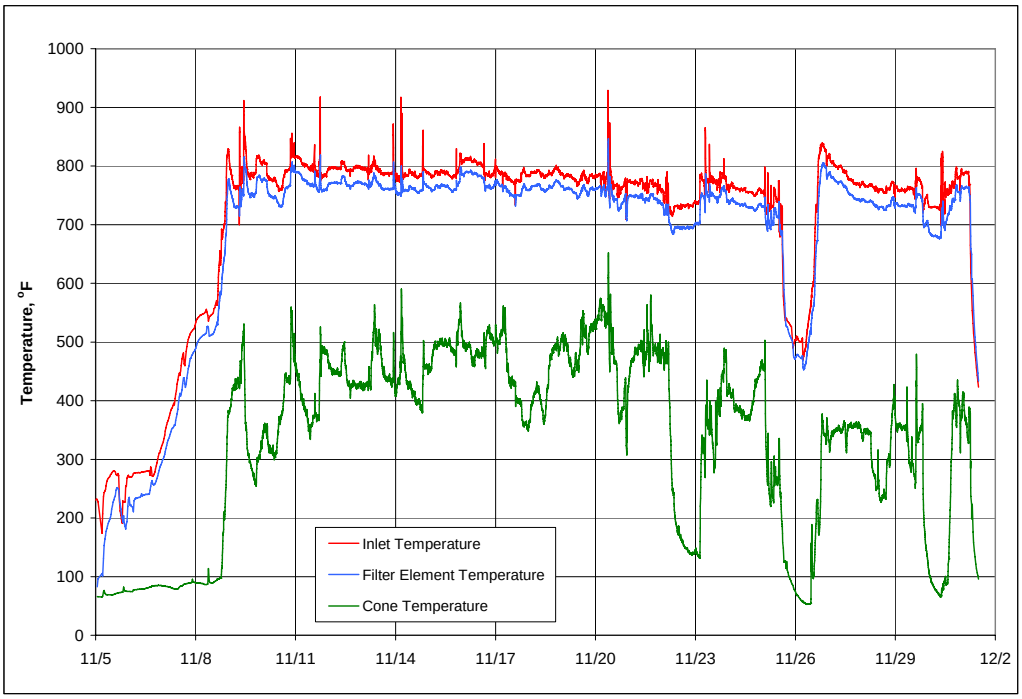

Figure B-5. PCD Temperatures.

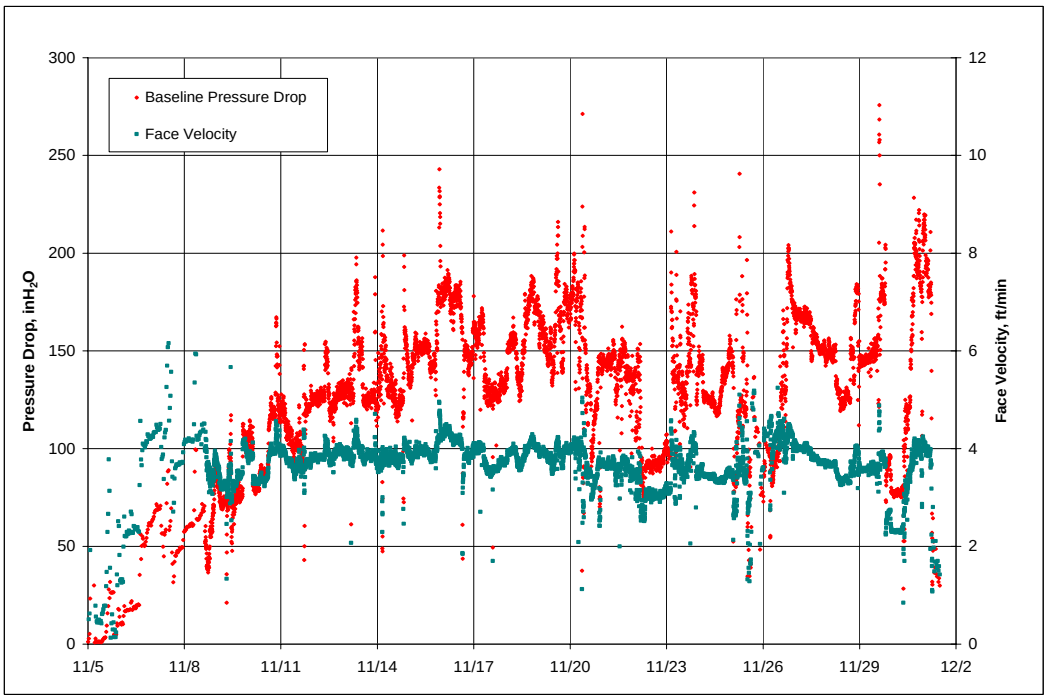

Figure B-6. PCD Baseline Pressure Drop and Face Velocity.

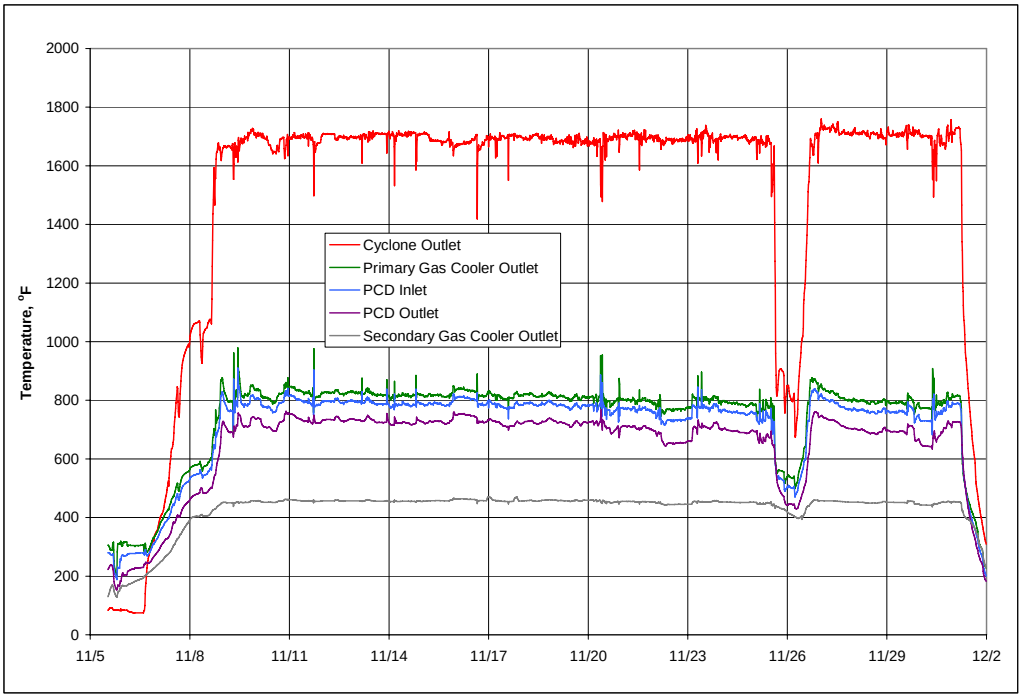

Figure B-7. System Temperature Profile.

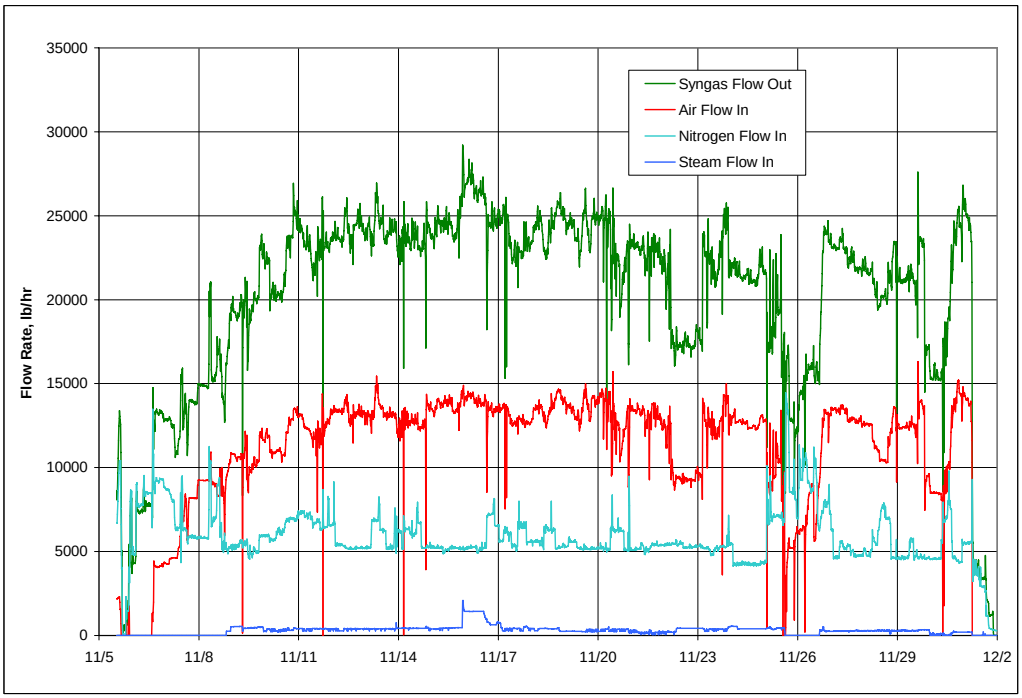

Figure B-8. System Gas Flows.

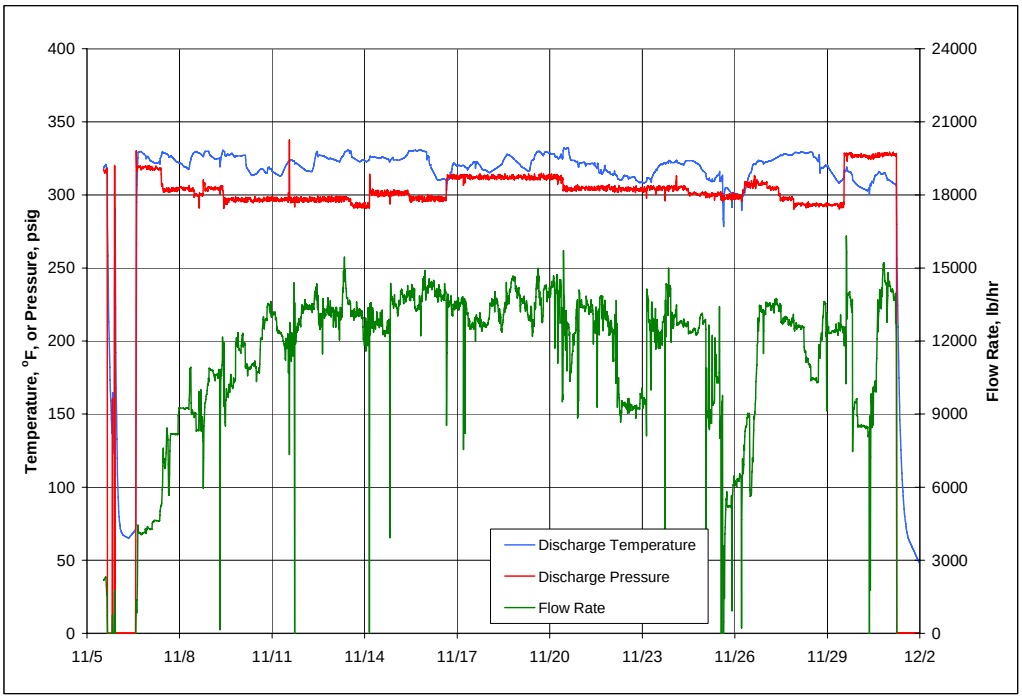

Figure B-9. Main Air Compressor Operation.

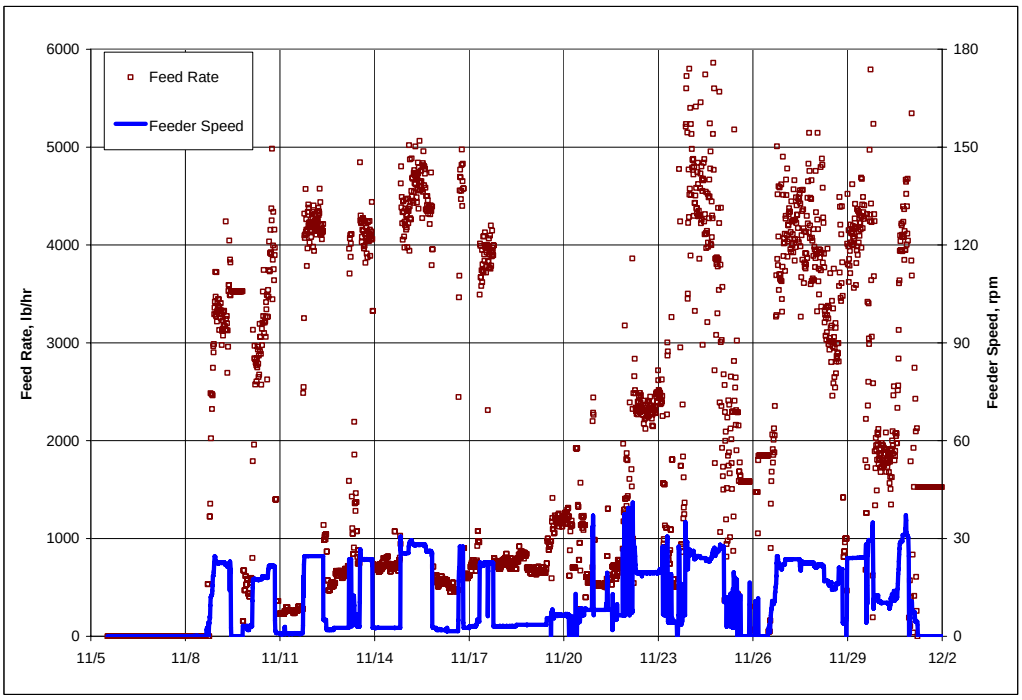

Figure B-10. Original Coal Feeder Operation.

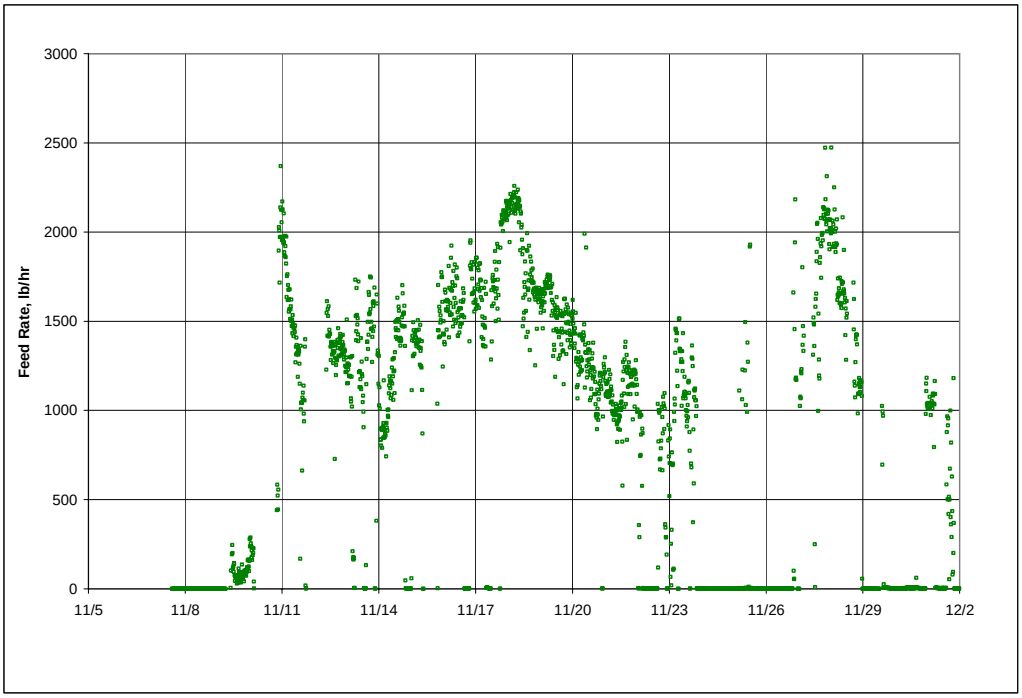

Figure B-11. Developmental Coal Feeder Operation.

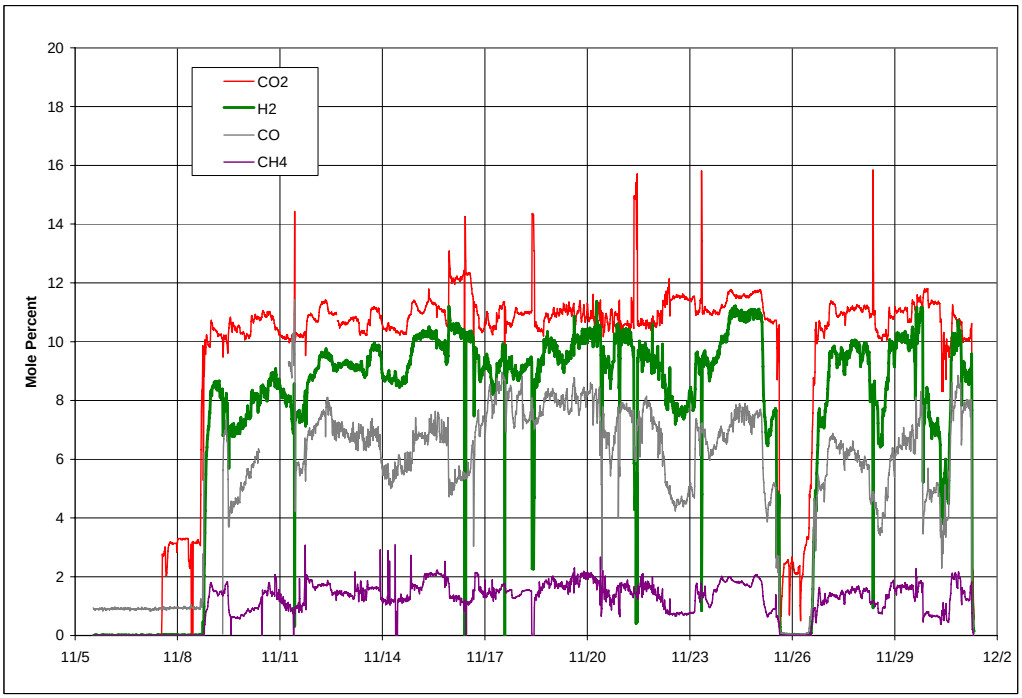

Figure B-12. Syngas Analyzers.

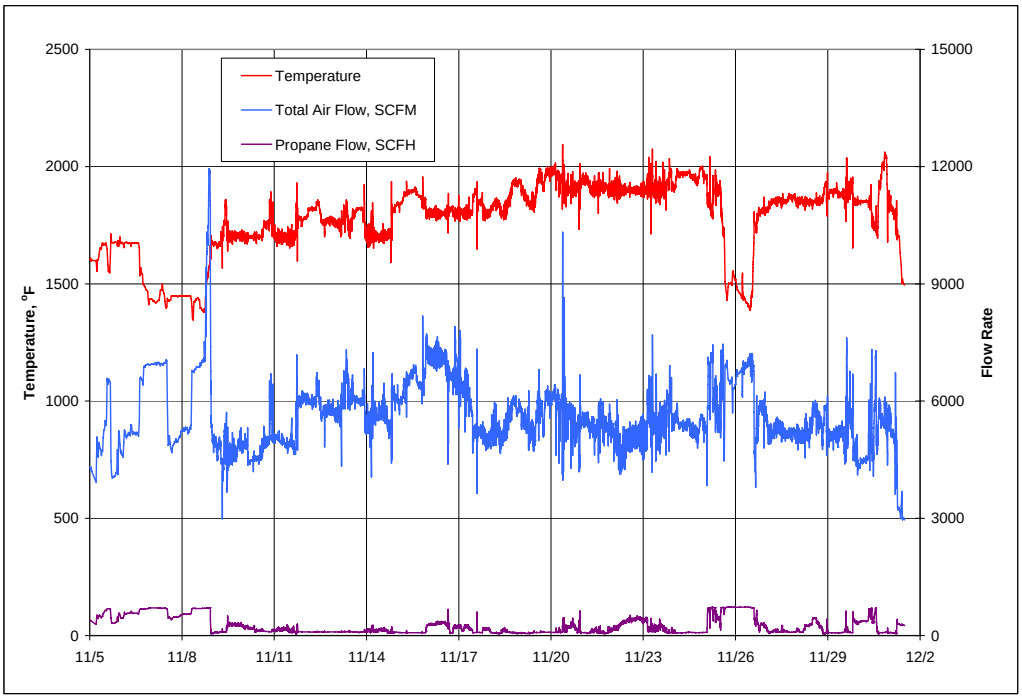

Figure B-13. Atmospheric Syngas Combustor Operation.

APPENDIX C MATERIAL AND ENERGY BALANCES

The material and energy balances showed reasonable accuracy given the diversity of the measurements used for their calculation. A gasifier mass balance for the TC19 steady state operating periods is shown in Figure C-1. The mass balance documents the accuracy of the solids and gas rates at the inlet and outlet of the gasifier. The data generally showed agreement within a ten percent error range.

The overall energy balance for the gasifier is shown in Figure C-2. This balance verifies the accuracy of the gasification efficiencies, and shows agreement within about a 10 percent error range.

The carbon balance documents the accuracy of the carbon conversions, and is shown in Figure C-3. With the exception of data for one operating period, the data fell within a 15 percent error range.

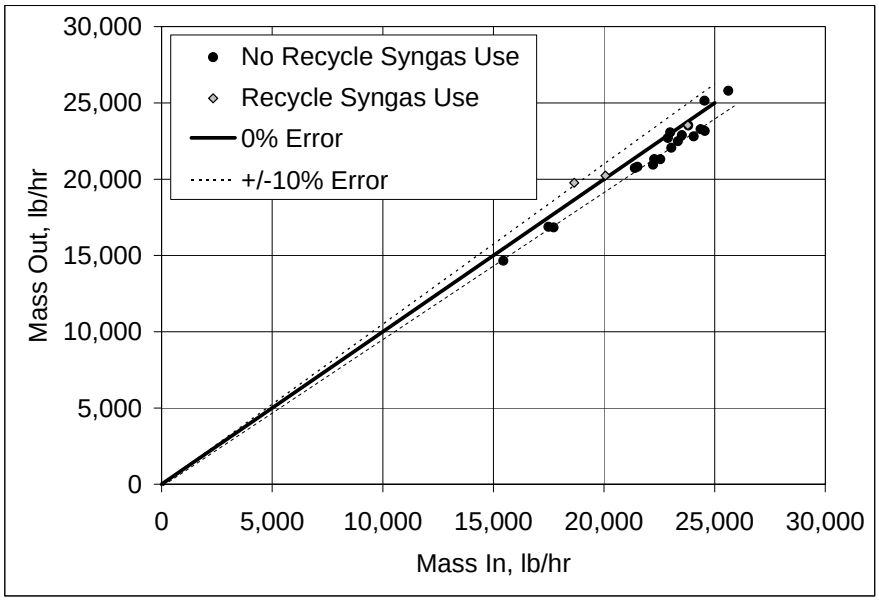

Figure C-1. Mass Balance.

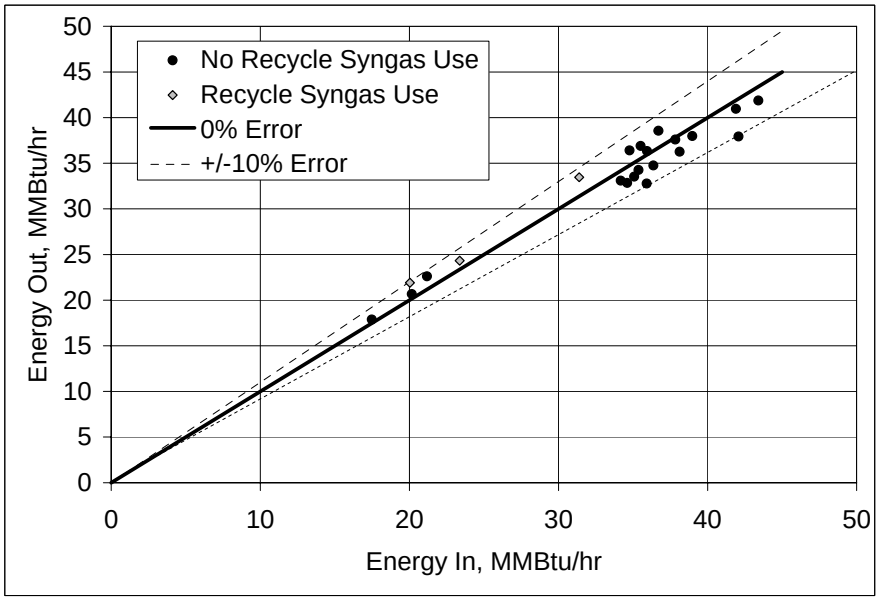

Figure C-2. Energy Balance.

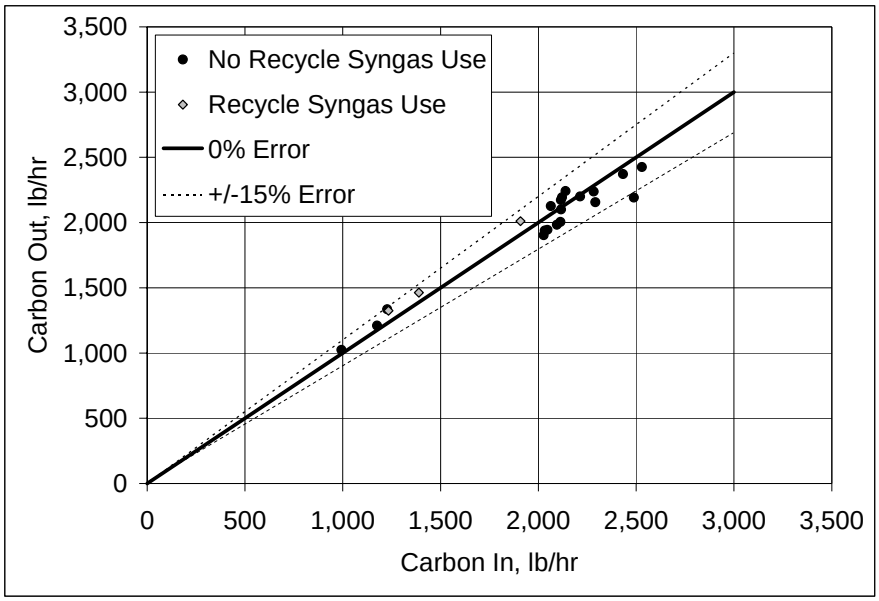

Figure C-3. Carbon Balance.